MAR 22 1957

1959 Vol 29 #1

Volume 27 MARCH, 1957 Number 1

Journal of Sedimentary Petrology

A Publication of the Society of Economic Paleontologists and Mineralogists
a Division of
The American Association of Petroleum Geologists

748 1957-58 VOL 27+2
MAR-DEC
Ind. in back

« CONTENTS »

Brazos River bar: a study in the significance of grain size parameters ... . *Robert L. Folk and William C. Ward* 3

Effects of sphericity, roundness, and velocity on traction transportation of sand grains ..... *William J. Morris* 27

Mineral alteration in rocks of middle Eocene age, Absaroka Range, Wyoming ..... *Richard L. Hay* 32

A fabric and petrologic study of the Pleasantview Sandstone .... *Gene A. Rusnak* 41

Mineralogy of some Pennsylvanian carbonate rocks of Illinois .... *Raymond Siever and Herbert D. Glass* 56

Secondary gypsum of the Sulphur Series, Sicily, and the so-called integration ..... *Leo Ogniben* 64

Differential compaction of Pennsylvanian sediments in relation to sand-shale ratios, Jefferson County, Illinois .... *Joseph C. Mueller and Harold R. Wanless* 80

SOCIETY OF ECONOMIC PALEONTOLOGISTS AND MINERALOGISTS

Program for S.E.P.M. St. Louis Meeting 89

Membership list 91

v1

Journal of Sedimentary Petrology

J. L. HOUGH, EDITOR
University of Illinois
Urbana, Illinois

ASSOCIATE EDITORS

R. E. GRIM
Univerity of Illinois
Urbana, Illinois

W. C. KRUMBEIN
Northwestern University
Evanston, Illinois

R. DANA RUSSELL
Ohio Oil Company
Denver, Colorado

The *Journal of Sedimentary Petrology* is published by the Society of Economic Paleontologists and Mineralogists, a division of The American Association of Petroleum Geologists. Numbers are issued in March, June, September and December.

The subscription price of the *Journal of Sedimentary Petrology* is $6.00 per year prepaid to addresses in the United States.

Single numbers, $2.00 each ($1.50 to members).

Postage is charged extra for all other countries: 40 cents on annual subscriptions (total $6.40).

The *Journal* will furnish reprints at cost. Orders should accompany corrected galley proof.

Communications about *Journal* subscriptions, rates, memberships, change of address, and non-receipt of preceding number should be addressed to Society of Economic Paleontologists and Mineralogists, P.O. Box 979, Tulsa, Oklahoma. Claims for non-receipt of preceding numbers must be sent in within three months of the date of publication in order to be filled gratis.

Communications in regard to manuscripts and purely editorial matters should be addressed to The Editor, *Journal of Sedimentary Petrology*, University of Illinois, Urbana, Illinois.

Annual Membership dues, including the Journal of Paleontology .....$ 8.00
Annual Membership dues, including the Journal of Sedimentary Petrology .. 5.00
Anual Membership dues, including both Journals 13.00

Non-Member Subscriptions to Journal of Paleontology $15.00; Outside U.S. $15.40
Non-Member Subscriptions to Journal of Sedimentary Petrology
$6.00; Outside U.S. $6.40

GEORGE BANTA COMPANY, INC., MENASHA, WISCONSIN
PRINTED IN THE U.S.A.

Journal
of
Sedimentary Petrology

VOLUME 27
MARCH, 1957-DECEMBER, 1957
NOS. 1-4

J. L. HOUGH, EDITOR

PUBLISHED BY THE
SOCIETY OF ECONOMIC PALEONTOLOGISTS AND
MINERALOGISTS
A DIVISION OF
THE AMERICAN ASSOCIATION OF PETROLEUM GEOLOGISTS
Box 979, Tulsa, Oklahoma

Volume 27 MARCH, 1957 Number 1

Journal of Sedimentary Petrology

A Publication of the Society of Economic Paleontologists and Mineralogists
a Division of
The American Association of Petroleum Geologists

CONTENTS

Brazos River bar: a study in the significance of grain size parameters..... *Robert L. Folk and William C. Ward* 3

Effects of sphericity, roundness, and velocity on traction transportation of sand grains..... *William J. Morris* 27

Mineral alteration in rocks of middle Eocene age, Absaroka Range, Wyoming..... *Richard L. Hay* 32

A fabric and petrologic study of the Pleasantview Sandstone..*Gene A. Rusnak* 41

Mineralogy of some Pennsylvanian carbonate rocks of Illinois..... *Raymond Siever and Herbert D. Glass* 56

Secondary gypsum of the Sulphur Series, Sicily, and the so-called integration..... *Leo Ogniben* 64

Differential compaction of Pennsylvanian sediments in relation to sand-shale ratios, Jefferson County, Illinois..... *Joseph C. Mueller and Harold R. Wanless* 80

SOCIETY OF ECONOMIC PALEONTOLOGISTS AND MINERALOGISTS

Program for S.E.P.M. St. Louis Meeting..... 89

Membership list..... 91

NOTICE

Articles submitted for publication to the *Journal of Sedimentary Petrology* should have a prefatory abstract and sufficient postage should be sent by the author to pay the return of the manuscript as it has been found that many articles require more or less revision before publication.

Persons who are not members of the Society of Economic Paleontologists and Mineralogists or are not subscribers to the *Journal of Sedimentary Petrology* but who desire to publish an article in the *Journal,* should have some member of the Society of Economic Paleontologists and Mineralogists or some member of the American Association of Petroleum Geologists sponsor the article. Members of these Societies are given preference in publication.

Among papers to appear in forthcoming issues of the *Journal* are the following:

Sediments of three bays of Baja California: Sebastian Viscaino, San Cristobal, and Todos Santos. By K. O. Emery, D. S. Gorsline, E. Uchupi, and R. D. Terry.

Beach erosion and concentration of heavy mineral sands. By C. Borreswara Rao.

Heavy mineral studies in tills of Ontario and adjacent areas. By A. Dreimanis, G. H. Reavely, R. J. B. Cook, K. S. Knox, and F. J. Moretti.

Differentiation of marine and sub-aerial sedimentary environments by volume percentage of heavy minerals, Mustang Island, Texas. By John S. Bradley.

Fluvial gravel fabric. By John Schlee.

Flume experiments on the production of stratification and cross-stratification. By E. D. McKee.

Studies on bacterial precipitation of carbonates in sea water. By Claude LaLou.

Comparison of the pebbles of the Shinarump and Moss Back Members of the Chinle Formation. By Howard F. Albee.

Authigenic biotite in spheroidal reduction spots, Pierce Canyon Redbeds, Texas and New Mexico. By D. N. Miller, Jr.

Classification of limestones and dolomites on basis of Ca/Mg ratio. by George V. Chilingar.

Structural petrology of the Pico Anticline, Los Angeles County, California. By Lawrence C. Bonham.

A Bahamian faecal-pellet sediment. By Louis S. Kornicker and Edward G. Purdy.

Pennsylvanian sandstones of the Eastern Interior Coal Basin. By Raymond Siever.

JOURNAL OF SEDIMENTARY PETROLOGY, VOL. 27, NO. 1, PP. 3–26
FIGS. 1–19, MARCH, 1957

BRAZOS RIVER BAR: A STUDY IN THE SIGNIFICANCE OF GRAIN SIZE PARAMETERS

ROBERT L. FOLK AND WILLIAM C. WARD
University of Texas, Austin, Texas

ABSTRACT

A bar on the Brazos River near Calvert, Texas, has been analyzed in order to determine the geologic meaning of certain grain size parameters and to study the behavior of the size fractions with transport. The bar consists of a strongly bimodal mixture of pebble gravel and medium to fine sand; there is a lack of material in the range of 0.5 to 2 mm, because the source does not supply particles of this size. The size distributions of the two modes, which were established in the parent deposits, are nearly invariant over the bar because the present environment of deposition only affects the relative proportions of the two modes, not the grain size properties of the modes themselves. Two proportions are most common; the sediment either contains no gravel or else contains about 60% gravel. Three sediment types with characteristic bedding features occur on the bar in constant stratigraphic order, with the coarsest at the base.

Statistical analysis of the data is based on a series of grain size parameters modified from those of Inman (1952) to provide a more detailed coverage of non-normal size curves. Unimodal sediments have nearly normal curves as defined by their skewness and kurtosis. Non-normal kurtosis and skewness values are held to be the identifying characteristics of bimodal sediments even where such modes are not evident in frequency curves. The relative proportions of each mode define a systematic series of changes in numerical properties; mean size, standard deviation and skewness are shown to be linked in a helical trend, which is believed to be applicable to many other sedimentary suites. The equations of the helix may be characteristic of certain environments. Kurtosis values show rhythmic pulsations along the helix and are diagnostic of two-generation sediments.

INTRODUCTION

Two of the most discussed yet most poorly understood topics in this day of quantitative geology are the concepts of grain size and sorting of sediments. Countless values have been published by research workers, recorded in innumerable theses, and secreted in oil company files; yet the meaning of all these figures and their ultimate geological significance (if any) are still quite obscure. One can hardly read a month's publications without encountering plots of sorting versus size or distance; contour maps showing values of grain size parameters; or statements of the alleged increase of sorting with sediment transport. Despite all this effort, few of these papers attempt to explain why or how the parameters are varying. If this vagueness is true of fairly simple ideas such as mean size or sorting, the situation with regard to more complex parameters like skewness or kurtosis is even worse. Little attempt has been made to relate these measures to the mode of deposition or to environmental characteristics, and most published papers simply tabulate these values without any evident attempt to understand or interpret them. One begins to wonder if all these lengthy computations are not wasted effort—do they show us anything of real value, or are they merely a deceptively impressive shell of figures surrounding a vacuum of geologic meaning?

A sand and gravel bar in the Brazos River near Hearne, Texas, was selected as a test case in which to determine, if possible, the geologic significance of such parameters as skewness and kurtosis in a localized environment; it was hoped that the facts learned here might aid in interpreting the meaning of these measures in other suites. A bar rich in gravel was chosen because it offered an opportunity to extend the size-versus-sorting trend into regions of essentially pure gravels. Hough (1942), Griffiths (1951), Inman (1949), Inman and Chamberlain (1955), and others have shown that the best sorting values are attained by medium to fine sands, and that sorting becomes worse as the sediments get either finer or coarser. Would the sorting continue to worsen as the trend was followed into the pure gravels, or would it reverse itself and begin to improve? This bimodal sand-gravel

bar also afforded an opportunity to study the reason for the peculiar, almost universal lack of sedimentary particles in the range of 0.5 to 2 mm (Hough, 1942; Pettijohn, 1949). Depositional mechanism of the gravel and sand modes could be studied separately, their areal distribution and correlation with sedimentary structures could be obtained, and, in short, the complete size characteristics of a typical coarse river bar could be rigidly defined and interrelated so that some comparison might be made with other environments in future work.

LOCATION AND GROSS FEATURES OF THE BAR

The bar lies in a meander bend of the Brazos River about two miles north of Black Bridge, a crossing five miles west of Calvert, Robertson County, in central Texas (fig. 1). Steeply cliffed grassy terraces 10 to 25 feet above normal water level border the river here. Clement B. Thames, Jr. assisted the senior writer in surveying the bar with steel tape and Brunton compass in December, 1953. The deposit measured approximately 1100 feet long, and tapered from 300 feet wide upstream to 150 feet wide at the downstream end. Surface features were tied in to surveyed stake points by pace and compass. At the time of measurement the maximum bar height was 5 feet above river level; when revisited in December, 1955, it had undergone little change in form.

The bar, situated near mid-channel, consists basically of sandy pebble gravel with only a thin veneer of sand blanketing it mostly on the downstream side. The gravel foundation outcrops at the surface as a V-shaped area pointing downstream (fig. 1). The highest elevation is at the point of the "V," and each limb becomes lower upstream; the low area between the limbs of the "V" consists of gravel covered thinly with current-rippled sand. The thickest mass of sand coats the outer flanks of the gravel "V" and tails out downstream, but a few other small gravel patches also occur near that end of the bar. Thus the V-shaped gravel mound, which extends nearly all the way across the river, has controlled the accumulation of sand on its downstream side.

Extremely discoidal, well-rounded pebbles of Cretaceous limestone make up most of the gravel. On the bar surface pebbles are strikingly imbricated, dipping 20 to 30 degrees in the upcurrent direction. In detail, they are oriented in a complex pattern showing the path of water movement the last time the bar was submerged (fig. 1). Water apparently moves into the "trap" formed by the gravel "V," and spreads out over the limbs at a 45 degree angle to the trend of the channel. In the gravelly areas, the surface is covered with a clean lag deposit about one pebble thick resting on a smooth pavement where the gravel is packed tightly with interstitial sand. Where sand forms the surface of the bar, it is mostly current-rippled, but there are some areas of smooth sand and occasional areas thinly coated with a film of mud.

After the surface had been mapped, 27 sampling sites were distributed over the bar in an attempt to lay an approximately equi-spaced net and still sample all surface sediment types in representative proportions. Unless the water table was encountered, a hole 20 inches deep was dug in order to describe the stratigraphic section and sedimentary structures. From each site 2 samples were taken. A spot sample, designated "S," was collected over the interval from 1 inch to 2 inches below the surface and if the sediment was sand, a volume of about 2 cubic inches was procured. If any gravel was present, 8 to 10 cubic inches (all in the same 1″ to 2″ depth interval) was collected. The surface inch of sediment was not sampled, as in many instances it approached a lag deposit and might not be representative of the character of the sediment that eventually becomes buried. At each site a channel sample (designated "C") was also taken by cutting a sampling trench over the entire height of the hole. Special types of sediment, such as clean gravel layers present at some depth in the hole, were occasionally taken and designated by the code "X." These samples were separately treated in the statistical analysis of the results.

In digging sampling pits it soon became evident that the bar was made up of 3 sediment types which bore a constant stratigraphic relationship to each other. The sandy pebble gravels, containing over 30

percent (commonly 45 to 70 percent) gravel, occurred at the bottom of every hole that was dug deep enough, hence underlaid the entire bar in addition to outcropping over a large portion of its surface. These sediments showed a rude horizontal banding expressed by varying gravel content, but little cross-stratification was seen. Within this deposit were occasional sand layers and a few one- or two-inch thick streaks of "pure" openwork gravel (slightly coated with mud filtered down through the overlying sediment). It is interesting to observe the excellent imbrication of pebbles on the bar surface and to contrast it with the relative lack of imbrication of the buried pebbles. Perhaps imbrication takes place not on initial deposition of the pebbles and sand, but only when calmer currents later scour the surface and remove the interstitial sand—i.e. upon erosion of the sediment.

Above the foundation of sandy pebble gravel occurred a distinct layer of slightly gravelly medium sand usually containing a trace to 1 percent of granule-sized particles. This layer, at most 2 feet thick, consisted of sands which appeared to be clean and and well sorted, forming tabular "torrentially" cross-laminated units 2 to 4 inches thick. Cross-laminae dipped about 30 degrees and were rather consistent in direction, swinging in a 50 degree arc on each side of the downcurrent direction.

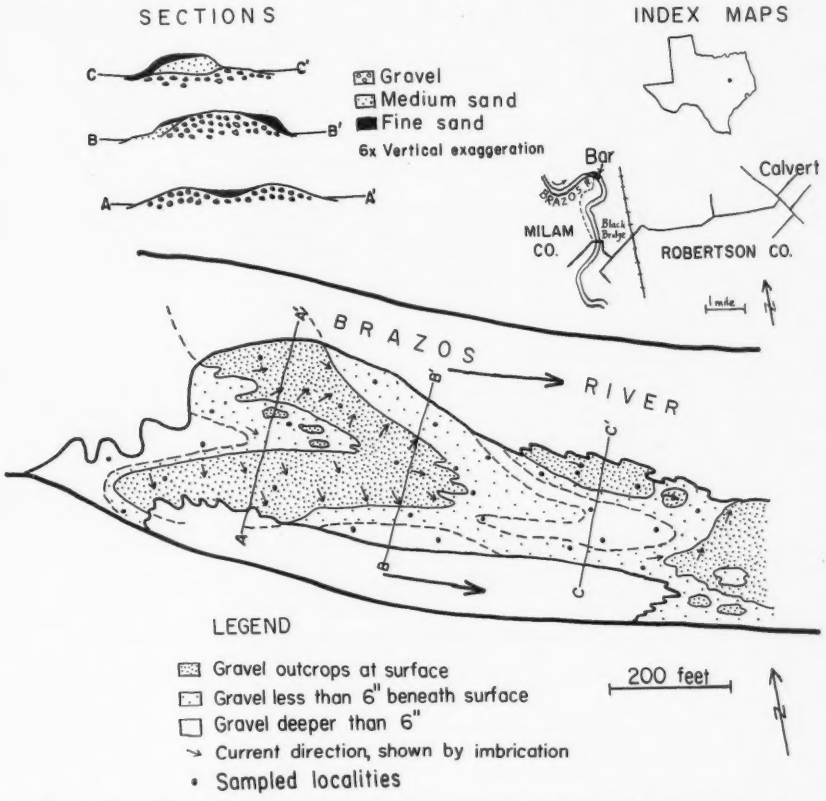

FIG. 1.—General features of the bar. Sandy pebble gravel forms the foundation of the bar, and outcrops as a V-shaped area pointing downstream.

The topmost layer of the bar consisted of fine sands and silty fine sands in a stratum at most 2 to 6 inches thick; occasionally this layer lay directly on the sandy gravel, and the middle layer was missing. This finest sediment type showed very small-scale lenticular cross-lamination with amplitudes of about 1 inch. Laminae were convexo-concave and had random dip direction.

In every hole the same sequence of layering was followed, and the layers were shaply bounded from each other with only rare interfingering. Thus the bar tends to become finer both upward stratigraphically and downstream.

GRAIN SIZE DISTRIBUTION

Laboratory Methods

If the sample consisted entirely of sand, it was split to between 50 and 75 grams, carefully disaggregated using a rubber cork and porcelain mortar, and sieved with Ro-Tap machine for 15 minutes. Eight-inch diameter Tyler screens, spaced at half-phi intervals (Krumbein, 1934), were used. Each fraction was weighed to 0.01 gm, and those amounts smaller than 1 gm were weighed to 0.001 gm. It is necessary to go to such accuracy when probability paper is used in plotting because the tails of the distribution are expanded so greatly. After being weighed, each fraction was examined with binocular microscope, and the percentage of aggregates (if any) was deducted from the raw weight as shown in the sample calculation (table 1). Deduction of aggregates is a critical step that is all too often overlooked in grain size analyses. Failure to do so has a very marked effect on sensitive measures such as skewness and kurtosis, which reflect the normality of the distribution. Few Brazos bar sieve fractions contained more than 5 percent aggregates, and most contained none. The corrected weights were cumulated, and the cumulative percentages were derived from the cumulated weights. This eliminates errors due to rounding off percentages and also insures that the anlysis will end at exactly 100.00 percent, a necessity when using probability graph paper.

TABLE 1.—*Method of computing analyses. The sample illustrated is not from this study but serves to illustrate the method*

Phi Interval	Raw Weight	Percent Aggregates	Corrected Weight	Cumulated Weight	Cumulated Percent
2.0–2.5	1.0	20	0.8	0.8	5.0
2.5–3.0	8.0	10	7.2	8.0	50.0
3.0–3.5	6.0	0	6.0	14.0	87.5
3.5–4.0	2.0	0	2.0	16.0	100.0

If the sediment contained any gravel at all, the entire sample was sieved through a 2 mm (-1ϕ) screen and the total amount of gravel retained on this screen was then sieved at an interval of one phi. The sand passing through the screen was split to a weight of between 50 and 75 grams, and this split was sieved as before. The weight of each sand fraction was then multiplied by the splitting factor (total weight of sand in the entire sample, divided by total weight of sand in the sieved split), and the weights cumulated together with the gravel portion of the analysis.

Cumulative percentages were then plotted against phi diameter on arithmetic probability paper. It is a waste of time to plot analyses on any other type paper (ordinary squared paper for example), as interpolation between data points is much more inaccurate and not reproducible. Values of skewness and kurtosis read off curves drawn on squared paper are worse than meaningless, because they depend almost entirely on the artistry of the draftsman and not on the sample characteristics. All curve parameters were read to the nearest 0.01ϕ, an accuracy which is meaningful when probability paper is used (Folk, 1955).

Bimodal Character of the Sediment

Brazos Bar sediments consist of a strongly bimodal mixture of pebble gravel with medium to fine sand. The gravel mode in most samples ranges between -2.0ϕ and -3.5ϕ (4 to 11 mm), while the sand mode generally lies between 1.2 and 2.8ϕ (0.45 to 0.15 mm) (fig. 4). In nearly all specimens, the minimum of the size distribution falls in the range of -0.5ϕ to $+0.35\phi$ (1.4 to 0.8 mm) (fig. 6). Only a few of the samples collected are unimodal.

As shown in figure 2, the relative proportion of the gravel and sand fractions varies

widely between samples, but there are two preferred values: considering only spot samples (where only one sedimentation unit was collected), most samples contain 0.0 to 0.5 percent gravel, but another large group of samples contain 45 to 70 percent gravel. Between these two most frequent proportions occurs a pronounced gap, and indeed no spot samples collected had gravel contents between 8 and 30 percent. Channel samples show this same characteristic of having either almost no gravel or about 60 percent gravel, but the tendency is subdued. Special samples of clean, openwork gravel layers contained 90 to 95 percent gravel. This frequency distribution of gravel percentages, if it is characteristic of other

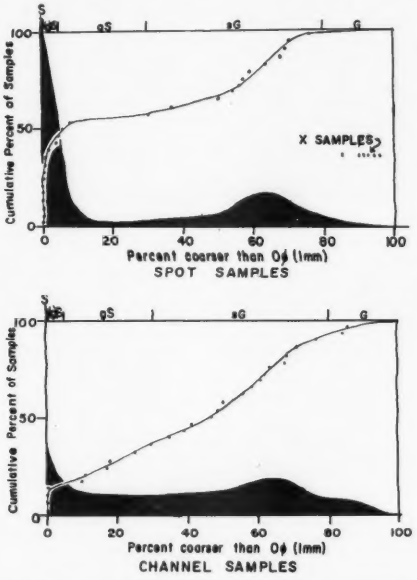

FIG. 2.—Cumulative and frequency curves of the proportion of gravel in each sample; these are constructed by arranging the samples in order of increasing gravel content and plotting them at equi-spaced intervals from 0% to 100%. In both channel and spot samples, there is a tendency for samples to have either 0% or about 60% gravel. Specially-collected layers of lag or openwork gravels contain 85 to 95% gravel (X samples). Textural designations are given at the top: S, sand; (g)S, slightly gravelly sand; gS, gravelly sand; sG, sandy gravel; and G, gravel.

sand and gravel bars, affirms the textural nomenclature proposed by Folk (1954) as the dividing lines between grain size classes occur at minima in the gravel frequency distribution.

In the Lafayette gravels in western Kentucky, Potter (1955) found the most common proportion to be 60 to 80 percent gravel, and Plumley (1948) found an average of 80 percent gravel in Black Hills terrace gravels. They have shown that because of restrictions of packing, a sediment with less than about 70 percent gravel must have had the sand and gravel deposited concurrently, i.e. the sand is not a later infiltration. Therefore, simultaneous deposition of the 2 modes must have occurred in the Brazos Bar, and infiltration of sand was unimportant as shown by the presence of openwork gravel layers.

The variation in percentage of gravel over the area of the bar is shown in figure 3, which is based on values obtained from channel samples only (spot samples show somewhat more fluctuation). Obviously this simulates figure 1 closely; the average gravel content of the top 20 inches of the bar is between 40 and 45 percent.

As will be shown later, the more complex grain size parameters such as mean size, standard deviation, skewness, and kurtosis are all rather close functions of the proportion of gravel in the samples. Consequently, maps showing the areal variation of these parameters are superfluous, and have not been included.

Character of the Gravel Fraction

The size characteristics of the gravel fraction may be analyzed independently of the "diluting" sand by taking the percentage of material coarser than 0ϕ (1 mm), dividing this percentage into 100 percent, and multiplying each of the gravel size grades by the resulting proportionality factor. In this way a cumulative curve for the gravel fraction alone may be plotted on probability paper. For example, if a sediment shows the following cumulative percentages: -4ϕ, 1%; -3ϕ, 7%; -2ϕ, 14%; -1ϕ, 18%; and 0ϕ, 20% all the cumulative percentages are multiplied by 100/20 and the curve is replotted as -4ϕ, 5%; -3ϕ, 35%; -2ϕ, 70%; and -1ϕ, 90%; and 0ϕ,

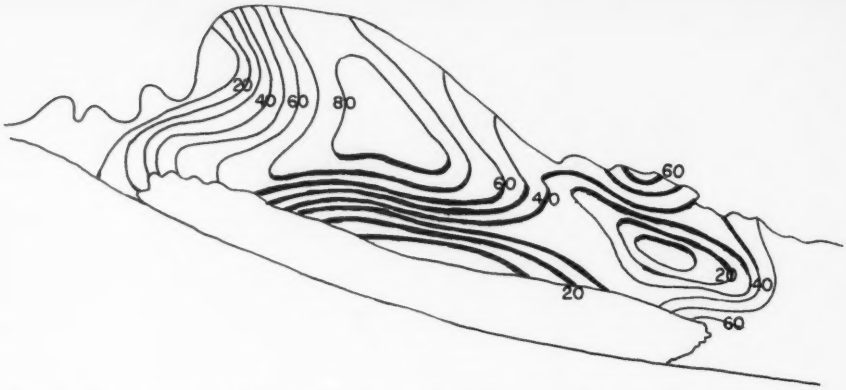

FIG. 3.—Contour diagram of the percent of gravel (material coarser than 0ϕ or 1 mm) in the top 20-inch section of the bar, based on channel samples.

100%. Actually of course, the Wentworth limit of gravel is -1ϕ, but in this particular sediment the significant size break occurs at 0ϕ so that the latter division is used throughout in calculations. Once a cumulative curve is plotted for the gravel fraction considered independently, it is possible to determine the mode, mean or median, standard deviation, skewness, and other critical properties for that fraction alone and to study how they vary in relation to position on the bar, percent gravel, size of the sand mode etc.

If only those samples with more than 10 percent gravel are considered, the grain size and sorting of the gravel fraction is surprisingly constant regardless of the proportion of gravel in the total sample. The average diameter of the gravel mode is -2.6ϕ (fig. 4) and two-thirds of the samples have gravel modes between -2.1ϕ and -3.4ϕ (4.5 to 10 mm). For each sample the sorting or standard deviation (σ_I, see later) of the gravel fraction alone was determined in the hope that it might prove an aid in characterizing river sediments if enough data are collected from other environments. The gravel fraction proved to be moderately to poorly sorted with σ_I averaging 1.1ϕ. Two-thirds of the samples had σ_I between 0.95 and 1.25; hence the sorting value is rather constant from sample to sample. All of the gravel fraction curves were nearly normal with skewness (Sk_I, see later) ranging from .00 to +.15 (equivalent α_ϕ = .00 to +.65). The largest pebbles encountered had intermediate dimensions between 20 and 40 mm. The few samples of lag gravels collected from the surface of the bar and from the one- to two-inch layers of pure openwork gravel within the bar had modal sizes averaging -2.6ϕ with sorting values averaging 0.75ϕ and ranging from 0.5ϕ to 1.1ϕ; these were slightly better sorted than the sandy gravels discussed above. There is no correlation between the grain size of the

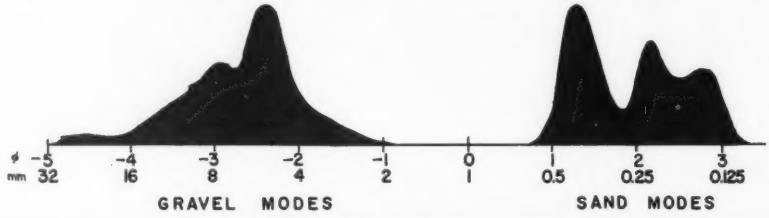

FIG. 4.—Frequency distribution of the sand and gravel modes for all samples.

gravel and sorting of the gravel within the limits of this study.

It is surprising to note that there is little or no correlation ($r = +.05$, negligible) between the diameter of the gravel mode and the percent of gravel in the sample. In other words, a sample with only 5 or 10 percent gravel has pebbles just as coarse as a sample consisting almost entirely of gravel (fig. 5). The fact that the gravel fraction has essentially constant size and sorting and that the pebble size is independent of the proportion of gravel in the sample indicates that the size distribution is chiefly a function of the grain size properties of the gravel supplied by the source in this particular area, and is but little affected by hydraulic factors or strength of the present depositing current. The size distribution of the gravel remains about the same whether the currents are strong (depositing little except gravel) or weak (depositing mostly sand with only a little gravel). Although an areal plot of percentage of gravel on the bar (fig. 3) correlates excellently with bar surface features, specifically the gravel "V," a similar areal plot of the modal size of the gravel showed only a random pattern.

Character of the Sand Fraction

If the sand modes for all samples are compiled into a frequency distribution (fig. 4), it is found that the most common modal diameters are 1.3ϕ, 2.2ϕ, and 2.8ϕ (.41, .22, and .15 mm). In relatively pure sands (containing less than 5 per cent gravel) the mode averages 2.5ϕ and ranges from 2.1ϕ to 3.0ϕ. The sand mode is one full Wentworth grade coarser in samples with 5 to 95 percent gravel, averaging 1.5ϕ and ranging from 1.1ϕ to 2.5ϕ (fig. 5). It is interesting to observe, however, that once the gravel content exceeds 5 percent, there is little or no correlation between the proportion of gravel and the size of the sand.

The average separation of the sand mode

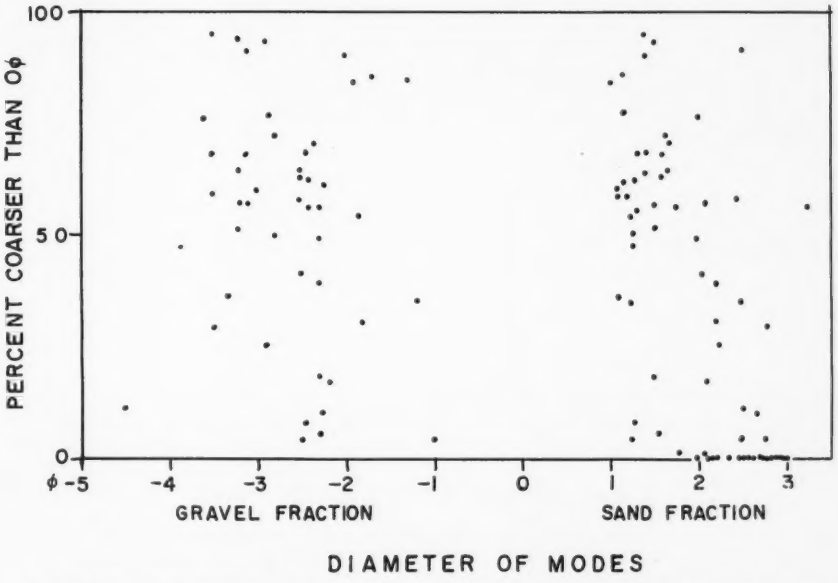

FIG. 5.—Modal diameter of the sand and gravel fractions as a function of the percent of gravel (coarser than 0ϕ) in the sample. Note narrow range of variation of both gravel and sand modes. There is no evident correlation between the amount of gravel and the size of the pebbles. Sands with no gravel have modes averaging 2.5ϕ; sands with 5 to 95% gravel have modes at about 1.5ϕ. This diagram illustrates that the size distribution of the modes themselves is chiefly a function of source area and is but little affected by strength of the depositing currents.

and the gravel mode in an individual sample (fig. 6) is 4.2ϕ, and two-thirds of the samples have separations in the range of 3.6ϕ to 5.1ϕ, or a millimeter ratio varying from about 21:1 to 35:1. Potter found an average separation of 4.4ϕ in the Lafayette Gravels. It is peculiar perhaps that there is no correlation between the size of the gravel mode and the size of the sand mode in the Brazos sediments.

MINERALOGY AND GRAIN SHAPE OF THE TWO MODES

In order to understand the cause of the bimodality, it is necessary to examine the mineralogy of the sand and gravel fractions. If sand grains were being produced by abrasion of the pebbles and some peculiarity of the abrasion process was responsible for the bimodality (such as pebbles of fine-grained granites disaggregating into their individual quartz and feldspar grains to produce the sand), then the sand and gravel should have similar composition. If the two modes were coming from different sources of supply, then their composition should differ.

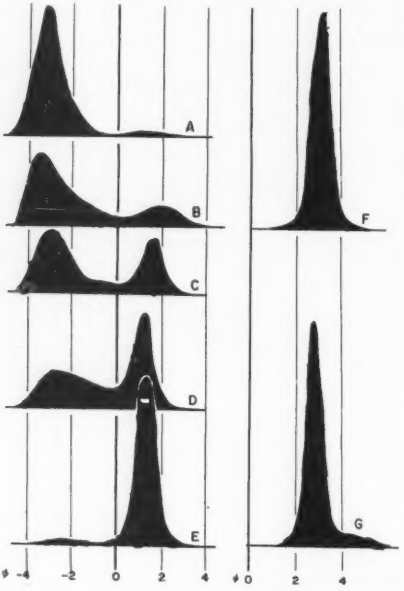

FIG. 6.—Representative frequency curves to cover the full range of variation in Brazos bar sediments. Note the nearly constant grain size of the modes, regardless of the variation in proportion of the modes. Each mode is within itself nearly symmetrical, although the total sample curves show wide variation in skewness and kurtosis. A is an openwork gravel layer; B, C, and D are typical sandy gravels. E is a slightly gravelly sand: F consists of the sand mode alone, and G is a silty sand. A, B, and G are positive-skewed, E and D are negatively skewed, and F and C are nearly symmetrical. A, E, and G are leptokurtic, C and D are platykurtic.

Grain counts were made on three representative samples (fig. 7), and it was evident that the sand fraction was *not* originating through abrasion of the pebbles but was being reworked from older sand and sandstone formations which were not present as pebbles. In order of decreasing abundance the pebbles consisted of (1) very discoidal, well-rounded limestone; (2) subequant, subangular chert; and (3) subequant, round to subround vein quartz. As measured by sieving, limestone was largest with a mode of about -3ϕ (8 mm), virtually diappearing by 1ϕ. Likewise, vein quartz and chert with modes of -2.2ϕ (4.5 mm) almost vanished by 1ϕ. Limestone pebbles presumably were larger because of their low sphericity.

The sand grains were of two very distinct types. Over one-fifth of the grains were superbly rounded, lightly frosted quartz grains of extremely high sphericity, some almost perfect spheres. These quartz grains were probably inherited from Cretaceous supermature orthoquartzitic sands upstream and ranged in size from 0ϕ to 3.5ϕ. The other four-fifths of the sand grains, however, ranged from angular (in the 3ϕ size range) to at best subround (in the 0ϕ grade).

This mixture provides some interesting evidence concerning the classification of Dapples, Krumbein, and Sloss (1953) who have chosen as a measure of sediment maturity the percentage of well-rounded sand grains present in a deposit. This is an unfortunate choice because rounded grains may be so easily inherited (as they are in the Brazos Bar); it is not the most rounded grains but the most *angular* grains that are the true index of the amount of rounding taking place in the site of deposition. In a mixture of well-rounded and angular grains, the well-rounded grains are almost always reworked and have no bearing on the

maturity of the latest sediment. Possibly something like the 16th percentile of the roundness distribution, rather than the mean, would be the best measure of the actual amount of rounding going on.

Chert and quartz show a peculiar reversal in roundness behavior. Above 0ϕ (1 mm) quartz is more rounded apparently because it is tough while the brittle chert pebbles tend to chip or split and remain subangular. Between 0ϕ and 1ϕ, both are of equal roundness, but in grains smaller than 1ϕ (0.5 mm) the chert grains are subangular with slightly though distinctly rounded edges while the quartz fragments are sharp and angular (excepting the readily recognizable inherited grains). Evidence of slight chert rounding was found in grains as small as 2.5ϕ. This seems to indicate that in sand-sized grains chert wears down and rounds faster than quartz because of slightly inferior hardness. A possible confirmation of this is found in the fact that chert grains are rare in supermature (well-rounded and well-sorted) orthoquartzites, while chert is quite common in sandstones of lower textural maturity (Folk, 1954) that have not suffered as much abrasion.

SUMMARY OF MODAL RELATIONSHIPS

If the proportion of gravel be taken as an index of current strength, then the following conclusions can be made:

1. In spot samples, the most common proportions of gravel are 0 percent and 60 percent; the least common proportion is 20 percent. At first, it might appear that this was due to the prevalence of two dominant levels of current strength. Rather, it is believed due to the fact that the sediment is bimodal and the size of the gravel is nearly constant. Thus, once a current is strong enough to move any gravel at all, it will move large quantities of it. If the sediment had a continuous range of particles from sand up to gravel size, then any percentage of gravel would be common; but in the Brazos Bar, there is a range of current strengths for which there are few available particles (-1ϕ to 1ϕ). Consequently the prominent percentages of gravel correspond to current strengths on each side of this gap.

2. On this bar, there is no correlation between current strength and grain size of the gravel. The diameter of the gravel mode appears to be nearly constant about a mean of -2.6ϕ.

3. On this bar, there is little correlation between current strength and the grain size of the sand mode, except that once the gravel content drops below 5 percent the sand is one phi unit finer. The sand mode averages 1.75ϕ.

4. Therefore, on this bar the size characteristics of the sand mode and of the gravel mode are controlled very largely by the source area and are little modified by stream action. The stream only affects the relative proportions of the two modes, not their sorting or grain size; hence its sorting effectiveness is very low. This may indicate that if sediments get finer downstream, it may be chiefly because the amount of gravel becomes less, rather than that its size is changing.

5. The correlation between sedimentary structures and size properties is tabulated below:

Sediment Type	Common Percent Gravel	Size of Sand Mode	Size of Grave Mode	Sedimentary Structures
a. Openwork gravels (rare streaks)	90–95	—	-1.8 to -3.4ϕ	none
b. Sandy gravels (bottom layer of bar)	45–70	1.5ϕ	-2.1 to -3.4ϕ	sub-horizontal banding
c. Slightly gravelly sands (middle layer of bar)	trace —5	2.2ϕ	—	consistent cross-bedding, 3″ amplitude
d. Fine sands (top layer of bar)	0	2.8ϕ	—	random cross-bedding, 1″ amplitude

STATISTISTICAL MEASURES USED IN THE ANALYSIS

In order to compare sedimentary environments with each other quantitatively, it is necessary to adopt precise measures of average size, sorting, and other frequency distribution properties. These properties may be determined either mathematically by the method of moments or graphically by

reading selected percentiles off the cumulative curves (both methods summarized by Krumbein and Pettijohn, 1938). In this study the latter method was used, because it is much quicker and nearly as accurate. Sample-to-sample variation in any given property (say mean size) is so great that it is felt unnecessary to determine any single mean with extreme precision. For example, if one were assigned the task of obtaining the average height of 100 people, he would not have to go about it by measuring each person to the nearest 0.001″.

In a suite of samples as strongly bimodal as those found on the Brazos River Bar, most of the grain size frequency curves are very non-normal. Therefore the commonly-used graphic measures of mean size, sorting and other statistical parameters are inadequate, because they are based on only two or three points read off the cumulative curve; strongly non-normal curves require more detailed coverage in order to render their properties accurately. Consequently the writers have been forced to use a new series of statistical measures corresponding closely to those suggested by Inman (1952), but including more points on the curve. For nearly normal curves the two systems give almost identical results, but for skewed and bimodal curves the system introduced here is superior. In the interests of consistency, the new measures are now used for all size analyses regardless of their modality.

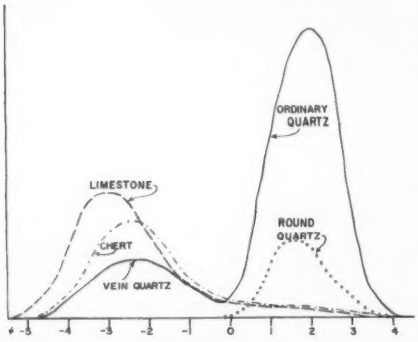

FIG. 7.—Lithologic and mineralogic size-frequency curves, representing a weighted composite of three Brazos bar samples. The sand is not originating by breakdown of the pebbles, but is being reworked from older sand and sandstone deposits. Note nearly symmetrical frequency curves for each constituent taken individually.

Mean Size.—Inman (1952) suggested $(\phi 16+\phi 84)/2$ as a measure of mean size. This serves quite well for nearly normal curves, but fails to reflect accurately the mean size of bimodal and strongly skewed curves. Therefore we have used another measure of the mean, M_z, determined by the formula

$$M_z=\frac{\phi 16+\phi 50+\phi 84}{3}.$$

Here, the $\phi 16$ may be considered roughly as the average size[1] of the coarsest third of the sample, and the $\phi 84$ as the average size of the finest third; the addition of the $\phi 50$ (the average of the middle third) thus completes the picture and gives a better overall representation of the true phi mean. To compare the accuracy of the two graphic systems, ten size analyses were chosen to represent the full range of textures in the Brazos Bar, and the mean size was computed for each sample by the method of moments (Krumbein and Pettijohn, 1938). The deviation of the graphic mean from the moment mean was then determined for both systems. In a range of means from -2.0ϕ to $+3.5\phi$ (in which all curves but two were strongly bimodal), the root mean square (rms) deviation[2] of $M\phi$ (Inman) from the moment mean was 0.25ϕ (maximum observed deviation 0.56ϕ) while the rms deviation of M_z (Folk and Ward) was only 0.12ϕ (maximum observed deviation 0.22ϕ); thus M_z gives twice as accurate an approximation to the moment mean.

Mode.—No good mathematical formula exists for accurate determination of the

[1] More precisely, the *median* of the coarsest third, etc.

[2] The root mean square (rms) deviation is computed by taking the deviations of $M\phi$ (or M_z) from the moment mean, squaring them, summing the squares, dividing the sum of the squares by the number of values, and taking the square root of this quotient. Approximately two-thirds of the individual deviations will then be less than the value of the rms deviation. A simpler but less useful measure is the mean deviation (sum of the deviations divided by the number of deviations, i.e. the average deviation), which is 0.09ϕ for M_z and 0.20ϕ for $M\phi$.

mode. The best approximation is probably that given by Croxton and Cowden (1939, p. 213), but this works well only when the distribution is symmetrical in the region neighboring the mode and fails in skewed curves. The writers have here used a repetitive trial-and-error method, wherein the percentage of sample actually occurring within a size interval of 0.5 phi unit is read directly from the cumulative curve. Readings are taken at successive steps of 0.1ϕ (e.g. first 1.2ϕ to 1.7ϕ, next 1.3ϕ to 1.8ϕ, etc.) until a maximum percentage is reached. The maximum percentage occurring within a half-phi diameter range in any sample has been given the term "modal concentration" and may have some value as an auxiliary measure of the degree of sorting in the region about the mode.

Median.—In the opinion of these writers, the median is a very misleading value and should be abandoned as a measure of average size inasmuch as it is based on only one point of the cumulative curve. For example a sediment consisting of 40 percent pebbles and 60 percent fine sand may have the same median as one with 60 percent fine sand and 40 percent clay.

Standard Deviation.—As a measure of sorting, Inman (1952) followed Krumbein (1938) and Otto (1939) and suggested the phi standard deviation,

$$\sigma_\phi = \frac{\phi 84 - \phi 16}{2},$$

thus using a uniformity measure similar to that employed by statisticians. For many normal curves this measure is adequate; however, it is based only on the central part of the distribution and ignores fully one-third of the sample—specifically, the "tails," which offer some of the most valuable information. Thus a sand with 10 percent pebbles and 10 percent clay may turn out to have a sorting value the same as pure sand. For complex distributions like the Brazos River bar (or, as matter of fact, for many neritic sediments where small amounts of clay are mixed with a dominant sand fraction), this parameter gives misleadingly high sorting values. The remedy is simple: include more of the distribution curve in the sorting measure. Although it would be theoretically best to include everything from the first to the 99th percentiles, Inman (1952) has shown that data are seldom reliable beyond the 5th and 95th percentiles. Hence these percentiles provide a practical end point, and if they are used only one-tenth of the sediment is excluded from the sorting measure. Inasmuch as the spread between the 5th and 95th percentiles includes 3.3 standard deviations, a standard deviation measure based only on the extremes,

$$\sigma_\phi = \frac{\phi 95 - \phi 5}{3.3},$$

could be developed. But neither the $\phi 84 - \phi 16$ measure nor the $\phi 95 - \phi 5$ measure is adequate by itself for complex bimodal sediments, and a superior over-all measure of sorting could be obtained by combining the two and taking their average. This measure, called the Inclusive Graphic Standard Deviation, is found by the formula[3]

$$\sigma_I = \frac{\phi 84 - \phi 16}{4} + \frac{\phi 95 - \phi 5}{6.6}.$$

Again to compare the relative accuracy of the two graphic systems, the standard deviation was computed by the method of moments for the same 10 samples discussed above; these showed a range of σ_I from 0.40ϕ to 2.60ϕ. For σ_ϕ (Inman) the rms deviation was 0.31ϕ, maximum 0.55ϕ; for σ_I (Folk and Ward) the rms deviation was 0.18ϕ, maximum deviation 0.32ϕ. Thus σ_I gives a considerably more accurate approximation to the moment σ.

In discussing sorting, it is convenient to have a verbal scale, particularly so that information may be communicated to nonspecialists. Plotting of hundreds of analyses from many different environments has suggested the following divisional points: σ_I under 0.35, very well sorted; σ_I 0.35–0.50, well sorted; σ_I 0.50–1.00, moderately sorted; σ_I 1.00–2.00, poorly sorted; σ_I 2.00–4.00, very poorly sorted; σ_I over 4.00 extremely poorly sorted. With the exception of the lowest limit the scale is geometric with a

[3] Many analyses of clayey sands and muds never attain the 84th or 95th percentiles. For these we have adopted the convention of extrapolating from the last point determined by pipette or hydrometer to 100% at 14ϕ using a straight-line plot on arithmetic paper. Intercepts are then read off the extrapolated curve.

ratio of 2. The smallest σ_I value so far encountered in our analyses is 0.20, while some sorting values as poor as 8.0 or more have been determined.

It may be argued that any attempt to set verbal limits on sorting values is foolish, because as shown by many (Inman, 1949; Griffiths, 1951), sorting is a rather closely-controlled V-shaped or sinusoidal function of mean size; hence about the only sediments falling in the "well-sorted" category would be the medium and fine sands, and all clays, silts, and most gravels would be poorly sorted to very poorly sorted. The frequent generalization that sorting increases with transport is in many suites simply due to the fact that the mean size of a sediment changes with transport, and the improvement in sorting is dependent only on the decreasing mean size, not the distance. As Inman (1949) suggested, once the sediment attains a minimum σ (best sorting), if it continues to get finer it will "round the turn" on the curve and sorting will worsen with further transport. A truly meaningful verbal scale of sorting will be developed only when the general trend of the size versus sorting relationship is worked out for a great number of environments. One will then be able to say, for example, that his sediment has a σ_I 0.25ϕ lower than the average sediment of that same mean grain size.

Skewness.—Inman suggested two measures of skewness: one,

$$\alpha_\phi = \frac{\phi 84 + \phi 16 - 2\phi 50}{\phi 84 - \phi 16},$$

to determine the asymmetry of the central part of the distribution and the other,

$$\alpha_{2\phi} = \frac{\phi 95 + \phi 5 - 2\phi 50}{\phi 84 - \phi 16},$$

to measure the asymmetry of the extremes. Again, a better measure of *over-all* skewness may be obtained by averaging[4] these two values by the formula, Inclusive Graphic Skewness

$$Sk_I = \frac{\phi 16 + \phi 84 - 2\phi 50}{2(\phi 84 - \phi 16)} + \frac{\phi 5 + \phi 95 - 2\phi 50}{2(\phi 95 - \phi 5)}.$$

Using this measure (as in Inman's original formula) skewness is geometrically independent of sorting, perfectly symmetrical curves have $Sk_I = .00$, and the absolute mathematical limits are -1.00 to $+1.00$; however, very few curves have Sk_I beyond $-.80$ or $+.80$. Positive values of Sk_I indicate that the samples have a "tail" of fines; negative values indicate a tail of coarser grains. Plotting of many grain size analyses has suggested the following verbal limits: Sk_I -1.00 to $-.30$, very negative-skewed; Sk_I $-.30$ to $-.10$, negative-skewed; Sk_I $-.10$ to $+.10$, nearly symmetrical; Sk_I $+.10$ to $+.30$, positive-skewed; and Sk_I $+.30$ to $+.100$, very positive-skewed. Plotting Sk_I against the value of skewness α_3 derived from the method of moments (Krumbein and Pettijohn, 1938) reveals that Sk_I equals approximately 0.23 α_3 and α_3 equals about 4.35 Sk_I.

Kurtosis.—Kurtosis, as used by most sedimentationists, measures the ratio of the sorting in the extremes of the distribution compared with the sorting in the central part and as such is a sensitive and valuable test of the normality of a distribution. Many curves designated as "normal" by the skewness measure turn out to be markedly non-normal when the kurtosis is computed. The Graphic Kurtosis (K_G) used here is given by the formula

$$K_G = \frac{\phi 95 - \phi 5}{2.44(\phi 75 - \phi 25)}.$$

In a normal Gaussian curve, the spread in phi units between the 5th and 95th percentiles should be 2.44 times the spread between the 25th and 75th percentiles. Thus, using the equation here, *normal* curves have $K_G = 1.00$. A curve with $K_G = 2.00$ is leptokurtic or excessively peaked (relatively better sorted in the central area than in the tails), inasmuch as the $\phi 5$ to $\phi 95$ spread is exactly 2.00 times as large as it should be for a given $\phi 25$ to $\phi 75$ interval. If $K_G = 0.70$ (platykurtic or deficiently peaked), the $\phi 5$ to $\phi 95$ spread is only 0.70 of what it should be in a normal curve with the same $\phi 25$

[4] In Inman's original equation (1952, p. 137) the denominator of the second term above was σ or $(\phi 84 - \phi 16)/2$. Using this denominator, it is possible to get skewness of absolute value greater than 1.00 in strongly leptokurtic and asymmetrical curves, and skewness becomes to some extent a geometric function of kurtosis. A geometrically independent measure is retained if we use $(\phi 95 - \phi 5)$ in the denominator.

to $\phi 75$ interval. The advantage of the kurtosis measure introduced here over previous measures lies in its simple relation to the normal curve which has $K_G = 1.00$; also the geometric significance can be easily visualized.

Based on analysis of hundreds of samples, the following verbal limits have been used for the kurtosis measure: K_G under 0.67, very platykurtic; K_G 0.67 − 0.90, platykurtic; K_G 0.90 − 1.11, mesokurtic; K_G 1.11 − 1.50, leptokurtic; K_G 1.50 − 3.00 very leptokurtic; and K_G over 3.00, extremely leptokurtic. In this scale the lower kurtosis limits are the reciprocals of the higher ones. The absolute mathematical minimum for the measure is 0.41, but no samples yet analyzed have had K_G below 0.50. There is no theoretical maximum for the measure, but $K_G = 8.0$ appears to be about the highest value attained in natural sediments.

It is evident that the distribution of K_G is itself strongly non-normal, since natural sediments average around $K_G = 1.00$ with a range from 0.50 to 8.0. Hence for plotting graphs and for statistical analyses the distribution has been approximately normalized by using the transformation $K_G' = K_G/(K_G + 1)$. Normal Gaussian curves then have $K_G' = 0.50$ ($K_G = 1.00$), and the range of K_G' in natural sediments is about 0.33 to 0.90.

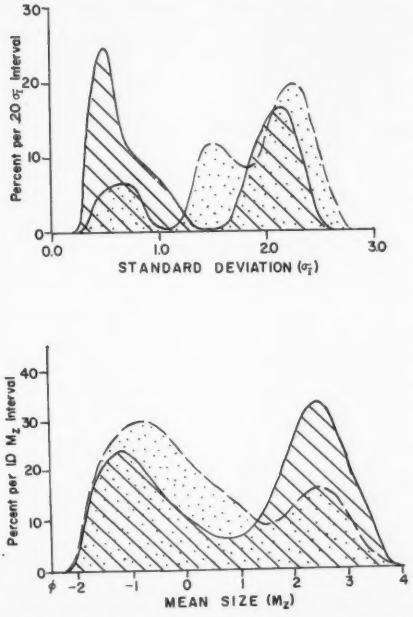

FIG. 8.—Frequency distribution of standard deviation values and mean size values for Brazos bar sediments. Spot samples are shown in a diagonal-line pattern, channel samples by dot pattern. The ordinate gives the percentage of the analyzed samples falling in the given interval (e.g. the curve for standard deviation of channel samples is 11% at $\sigma_1 = 1.5$; this means that 11% of the samples had σ_1 values between 1.4 and 1.6).

FREQUENCY DISTRIBUTION OF PARAMETERS IN THE BRAZOS BAR

It is of considerable theoretical interest to examine the frequency distributions of the values of the 4 size parameters obtained from the Brazos Bar samples, as this may be one of the best ways in which to characterize environments. For example, the 54 channel and spot samples have 54 different skewness values. These questions arise: what is the average skewness of these samples; what is the standard deviation of the skewness values (i.e. how wide a range of skewness is shown by the central two-thirds of the samples); is the skewness distribution unimodal or bimodal; and one may even consider such problems as the skewness of the frequency distribution of skewness values or the kurtosis of the skewness frequency distribution. In this way any size parameter (such as skewness, sorting, etc.) may be treated in exactly the same way as any other numerical parameter obtained for the 54 samples (say porosity, feldspar content, or sphericity), and its frequency distribution may be analyzed in similar fashion.

Mean Size.—Mean size (M_z) ranged from -1.7ϕ to $+3.2\phi$ (3.3 to 0.11 mm) for spot and channel samples (fig. 8), although some of the specially chosen X samples (clean gravel layers) had M_z from -2.5ϕ to -3.3ϕ (5.6 to 10 mm). Spot samples gave an extremely bimodal distribution with a mean M_z of 1.1ϕ and a standard deviation of 1.7ϕ (in other words if the distribution of M_z were normal, about two-thirds of the M_z values would fall between 2.8ϕ and -0.6ϕ). In such a non-normal distribution, however, these values have little significance, and it

is more meaningful to say that the largest clustering of M_z values is between 1.8ϕ and 3.2ϕ, representing the relatively pure fine sands, with a somewhat smaller cluster about -1.5ϕ to 0.0ϕ (sandy gravels). Few spot samples have M_z between 0.5ϕ and 1.5ϕ. Channel samples show a similarly bimodal distribution of M_z, but the maximum concentration is at -1.5ϕ to -1.0ϕ.

Standard Deviation.—Standard deviation (σ_I) values ranged from 0.40ϕ to 2.58ϕ on the Brazos Bar (fig. 8). Spot samples had a mean standard deviation of about 1.2ϕ, but this value is without significance because the distribution of standard deviations is very markedly bimodal. There is a great clustering of σ_I values at 0.40ϕ to 0.50ϕ, representing the well- to moderately-sorted "pure" sands, and an almost equally large group at $\sigma_I = 1.80\phi - 2.30\phi$, representing the poorly to very poorly sorted sandy gravels. No σ_I values between 1.20ϕ and 1.80ϕ occurred.

Channel samples had a mean σ_I value of about 1.8ϕ, but the greatest clustering occurred about a value of 2.0ϕ–2.4ϕ, with another very minor group at 0.40ϕ–0.80ϕ. Again the distribution of values was non-normal. There was little difference in sorting between spot and channel samples, except where the spot samples consisted of sand alone and the channel sample at the same locality contained some gravelly layers deeper in the test pit.

Preliminary work at the University of Texas has shown that most Texas beach sands have σ_I in the range of 0.20–0.40; yet the best sorted Brazos Bar sands, with approximately the same mean grain size as the beach sands, have σ_I ranging from 0.40–0.60ϕ. Hence, the beach sands are almost twice as well sorted. This may be due in part to the method of deposition in the two environments. The Brazos bar sands are deposited as continuous cross-bedded units, in which sediment is rather rapidly dumped down the front of the advancing sand mass as foreset beds. There is little opportunity for sorting, as the sediment, once deposited, is buried rapidly and no gentle reworking takes place. On the contrary, the beach sands tend to be raked back and forth by the continual motion of wave swash, which produces laminae nearly parallel with the slope of the beach. The continuous reworking apparently results in good sorting.

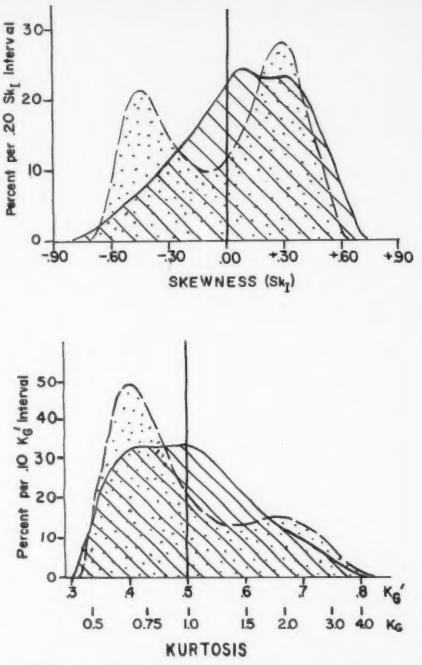

FIG. 9.—Frequency distribution of skewness and kurtosis values from Brazos bar sediments. Spot samples are shown in a diagonal line pattern, channel samples in a dot pattern.

Skewness.—Skewness values ranged widely from $-.68$ to $+.53$ (fig. 9). Spot samples showed a nearly normal distribution of Sk_I grouped about a mean skewness of $+.09$ with a standard deviation of 0.34 (i.e. two-thirds of the samples had skewness values ranging between $-.25$ and $+.42$). Thus most of the samples have a tail to the right, i.e., an excess of fine material for a normal curve.

Channel samples, on the other hand, had distinctly bimodal distribution of skewness values, with a large clustering about $Sk_I = +.20$ to $+.40$ (sandy gravels with a tail in the sand sizes) and another somewhat smaller grouping at $-.30$ to $-.55$ (gravelly sands, dominantly sand with a small tail of gravel). Few skewness values occurred in the range of .00 to $-.20$.

Kurtosis.—In analyzing the data, the transformed value K_G' has been used instead of the actual K_G values. Plotted on

this scale (fig. 9), the distribution of kurtosis values is nearly normal in spot samples with a mean K_G' of 0.49 (corresponding to $K_G = 0.96$) and a standard deviation of 0.12 (two thirds of the K_G' values fall in the range from 0.39–0.62, and corresponding K_G values from 0.64 to 1.63). The range of K_G' was from 0.35 to 0.74 (K_G from 0.54–2.85), and platykurtic and leptokurtic samples occurred with about equal frequency.

Channel samples showed a non-normal distribution of kurtosis with a large clustering about $K_G' = 0.36$–0.47 (platykurtic—$K_G = 0.56$–0.89), and another much smaller grouping at $K_G' = 0.62$–0.70 (leptokurtic, $K_G = 1.63$–2.33).

INTERRELATION OF THE FOUR SIZE PARAMETERS

To understand the geological significance of the four size parameters, it is necessary to plot them against each other in turn as scatter diagrams. In this way their interrelationships are revealed, and a wealth of meaning comes to light. Although in theory the measures are geometrically independent, in actual practice it is usually found that for a given suite of samples the measures are linked by some mathematical relationship. Perhaps the relationships and trends may be clues to the mode of deposition and will add one more criterion for identifying environments by size analyses.

First, all 6 two-variable scatter plots are discussed, and next it is shown that all 4 parameters of the frequency distribution can be combined in a helical trend. The geological significance of this helix is then interpreted, and its application to other sedimentary suites is discussed.

Mean Size versus Standard Deviation.—Generally plots of this type give a great amount of information about an environment (Inman, 1949, p. 64). If a wide range of grain sizes (gravel to clay) is present, scatter bands often form some segment of a broadened M-shaped trend. Often only a V-shaped or inverted V-shaped trend develops if the size range is smaller, and if the range is very small, only one limb of the V may occur. Minima of best sorting coincide with prominent modes in the sediment, and maxima (poorest sorting) correspond to mean sizes midway between modal diameters. In the Brazos bar, an inverted V-shaped trend occurs with a suggestion of a slight upward hook on the right limb (fig. 10). The rare clean gravel layers with M_z about -3ϕ are not too badly sorted with σ_I about 1.0. As the pure and essentially invariant gravel mode becomes mixed with more and more sand, the mean size decreases and the sorting worsens until the highest σ_I values are attained when the sediment consists of subequal proportions of sand and gravel. These samples have a mean size about half-way between that of the sand mode and the gravel mode, i.e. about -1ϕ to 0ϕ and sorting values of 1.75–2.5ϕ.

As the sand mode increases in abundance and the gravel diminishes, the mean size becomes finer and the sorting begins to improve. Finally, in those samples consisting only of the "pure" sand mode, best sorting occurs at a mean size of 2.1ϕ–2.7ϕ with σ_I about 0.40ϕ–0.60ϕ. Having about half as large a standard deviation, the pure sand mode is thus inherently better sorted than the pure gravel mode. This apparently is the result of the type of material supplied by the source area, as the present river deposition has little effect on the sorting of the individual modes.

The suggestion of an upward hook at the right of the diagram is caused by mixture of the dominant sand mode with a small

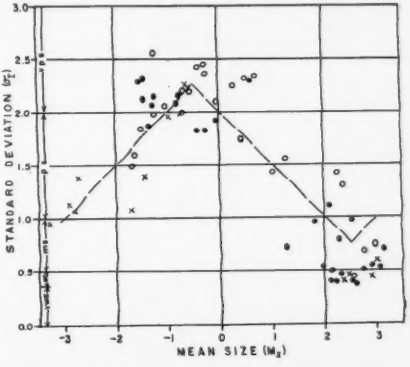

FIG. 10.—Scatter plot of mean size versus standard deviation (sorting). Spot samples shown by filled circles, channel samples by open circles, and special samples by X. Letters along the left margin give verbal limits on sorting: vws, very well sorted; ws, well sorted; ms, moderately sorted; ps, poorly sorted; vps, very poorly sorted. Trend line is discussed in the text.

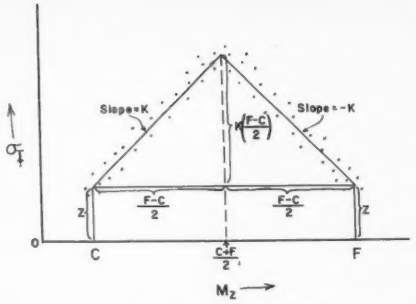

FIG. 11.—Geometry of the general equation for sorting in bimodal sediments, derived in the text. C and F are the phi diameters of the coarse and fine modes, respectively; Z as the σ_I value of the modes when present alone. Poorest sorting occurs at a mean size midway between the sizes of the two modes, i.e., at the position $(C+F)/2$. The trend followed by a series of samples is shown diagramatically by the dots.

amount of a third mode in the silt sizes. This further decreases the mean size and starts to worsen the sorting again, by the same mechanism of adding two modal distributions together. Presumably if enough fine samples had been taken, the plot would have developed another inverted V-shaped trend to the right of the present one, with a maximum σ_I corresponding to a subequal mixture of the sand mode and the silt mode and a minimum σ_I corresponding to the size of the pure silt mode.

As shown later, the true trend is probably a sine curve repeated over several wave lengths, each minimum corresponding to a mode in the suite of sediments being considered. However, an equation nearly as adequate in predicting sorting values may be developed under the assumption that the trend is composed of two intersecting straight-line segments. This equation is $\sigma_I = 2.25\phi - 0.5|M_z + 0.5\phi| \pm 0.4\phi$, where M_z is the mean size of any given sample and σ_I is the corresponding sorting value. The expression $|M_z + 0.5\phi|$ stands for the absolute sum of M_z plus 0.5ϕ taken with sign ignored; i.e. if a given sample has an M_z of -2.0ϕ, the value of the term is $-0.5|-2.0\phi + 0.5\phi| = 0.5|-1.5\phi| = -0.5 \times 1.5\phi = -.75\phi$. The term $\pm 0.4\phi$ is the standard error of estimate and signifies that about two-thirds of the σ_I values will fall within the range of the predicted σ_I value $\pm 0.4\phi$.

This trend line suggests that a general equation for sorting in bimodal sediments can be evolved. The first term of the equation (in the example here, 2.25ϕ) is the value of σ_I at the apex or poorest sorting point of the inverted V trend. The multiplicand of the second term is a constant which is fixed by the slope of the trend lines (assuming that they are of equal slope, sign ignored), and gives the change in σ_I per unit change in M_z (here it is 0.5). In the expression $|M_z + 0.5\phi|$, which in reality is $|M_z - (-0.5\phi)|$, the second term represents the mean size value at which poorest sorting takes place. In most sediments this appears to be at a mean size halfway between the sizes of the two modes. If the slope constant is designated K, the phi diameter of the coarser mode is called C, the phi diameter of the finer mode is called F, and the sorting value of the pure sand mode and pure gravel mode when present separately[5] is Z, then the first term in the generalized equation (corresponding to 2.25 in the specific example here) will be $K(F-C)/2+Z$ (fig. 11). The mean size value at which poorest sorting takes place, being halfway between the two modes, can be represented by their average $(F+C)/2$; therefore the second term in the generalized equation becomes

$$K\left|M_z - \frac{F+C}{2}\right|,$$

and the final equation is

$$(1) \qquad \sigma_I = K\left(\frac{F-C}{2}\right) + Z - K\left|M_z - \frac{F+C}{2}\right|.$$

In sediments deposited under conditions similar to the Brazos River bar where $K = 0.5$ and $Z = 0.75$, the equation reduces to

$$(2) \qquad \sigma_I = \frac{F-C}{4} + 0.75 - 0.5\left|M_z - \frac{F+C}{2}\right|.$$

Geologically, the F and C terms reflect the modal size of the material contributed by the source area or areas; Z represents the individual sorting of these fractions, strongly affected by the character of the source; and K represents the interplay between two factors: (1) distinctness of the modes contributed by the source areas, and (2) efficacy of the transporting agent in doing its own

[5] This equation applies only if the sorting of the coarser mode and the finer mode are nearly equal.

sorting on the material contributed to it. If the modes contributed by the source of supply are only two, are well sorted and essentially invariant, and are of widely differing size, then K will approach 1.0. If there are many indistinct modal distributions contributed by the source or if these modes are in themselves widely variant or poorly sorted, then K may approach 0, and there will be no significant change in sorting with change in size. Secondly, if the environment of final deposition is very ineffective in sorting, K will remain high. If the environment is effective in sorting, then K will be lowered because not only will the modal sediments be well-sorted, but the hybrid sediments consisting of mixtures of modes, instead of having the poor sorting normally associated with these mixtures, will have good sorting and the inverted V trend will be flattened.

Hence K is high, for example, in some lagoonal sediments, because a relatively nonvariant, well-sorted sand mode is produced on the beaches and a non-variant clay mode accumulates in the lagoon. When these two sediments become mixed and deposited in the low-energy environment of the lagoon where no further sorting takes place, then K will remain at a maximum. K should be at a minimum for beach sands fronting a coast with many rivers contributing sediment from different types of source areas. Here sediments entering the area are polymodal, the modes are blurred, and the environment is one in which efficient sorting is going on. Thus sediments of all grain sizes can become well sorted, and there should be little association of sorting with size.

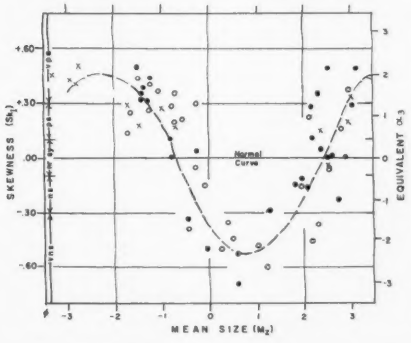

FIG. 12.—Scatter plot of skewness versus mean size. Spot samples shown by filled circles, channel samples by open circles, and special samples by X. The trend is markedly sinusoidal, with nearly equal numbers of positive-skewed and negative-skewed samples. Letters along the left margin give verbal limits for skewness; vns, very negative-skewed; ns, negative-skewed; nr sy, near-symmetrical; ps, positive-skewed; vps, very positive skewed. Equivalent α_3, based on the method of moments, is shown along the right margin.

Mean Size versus Skewness.—In this bimodal sediment, skewness is very closely a function of grain size (fig. 12). The trend is markedly sinusoidal. The pure sand mode when it occurs by itself (at a mean size of about 2.5ϕ) produces a symmetrical size curve, but the addition of increasing quantities of gravel mode[6] imparts negative skewness, which becomes most extreme at a mean size of +0.7ϕ, where the skewness averages −.50 or more. As more gravel is added and the two modes become equal in quantity, the trend reverses itself and sweeps briefly through a region of symmetry (Sk_I = .00 at about $M_z = -0.5\phi$). As the amount of gravel comes to exceed the amount of sand, the size curves become more and more positive-skewed reaching a maximum skewness of +.50 at $M_z = -2.2\phi$. In the pure gravels the skewness decreases, but in the samples collected here Sk_I never attains .00 (theoretically Sk_I should reach .00 again in a pure openwork gravel mode, but these samples always contained 5 percent or more sand which imparted a positive skewness).

In sediments finer than 2.5ϕ, the decrease in size comes about through addition of small quantities of silt mode to the dominant sand mode. This explains the positive skewness values at the right edge of the trend. Thus, to generalize, the pure modal fractions are in themselves nearly symmetrical, but the mixing of the two modes produces negative skewness if the finer mode is most abundant and positive skewness if the coarser mode is most abundant. An equal quantity of the two modes results in a symmetrical curve.

Mean Size versus Kurtosis.—This relationship is complex. The curve shown in figure 13 is theoretical, based on what the trend should look like given the two modes present in the Brazos bar and mixing them in vari-

[6] Sk_I is affected as soon as the gravel content exceeds 5%.

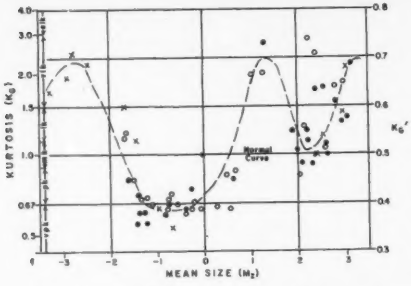

FIG. 13.—Scatter plot of kurtosis versus mean size. Spot samples shown by filled circles, channel samples by open circles, and special samples by X. The trend is complex. Letters along the left margin give verbal limits on kurtosis; vpk, very platykurtic; pk, platykurtic; mk, mesokurtic; lk, leptokurtic; vlk, very leptokurtic; elk, extremely leptokurtic. Points are actually plotted using the transformation K_G' shown along the right margin; equivalent K_G is shown at left.

ous proportions. Not enough samples were collected to cover this theoretical skeleton with the flesh of numerous analyses. Again, the pure sand mode and the pure gravel mode by themselves give nearly normal curves with $K_G = 1.00$. The addition of very small amounts (3 to 10 percent) of another mode means that the sorting in the tails is worsened while the sorting in the central part remains good; hence the curves become strongly leptokurtic with K_G considerably higher than 1.00. Further additions of the new mode give rise to a strongly bimodal sediment, and if the two modes are subequal (in proportions anywhere between 25:75 to 75:25), then the sediment becomes very platykurtic. When the second mode attains 90 percent or more of the sediment, the curve once more becomes leptokurtic, and when the second mode reaches 100 percent, a normal curve with $K_G = 1.00$ should occur again.

This theoretical trend is well illustrated in Brazos bar samples. The largest clustering of values is around $K_G = .60 - .65$ (very platykurtic) at $M_z = -0.8\phi$. These represent the sandy gravels with subequal amounts of the two modes, i.e. 45 to 70 percent gravel. The leptokurtic curves when M_z becomes finer than 2.5ϕ indicate again the addition of a small tail of silt to the sand mode.

Standard Deviation versus Skewness.—It is evident that if standard deviation is a function of mean size, and if skewness is also a function of mean size, then sorting and skewness will bear a mathematical relation to each other. However, the exact nature of their relation was a great surprise: the two variables form a scatter trend in the form of a nearly circular ring (fig. 14)! The reason becomes obvious on a moment's thought, however; symmetrical curves may be obtained either in (1) unimodal samples with good sorting, or (2) equal mixtures of the two modes which have the poorest possible sorting for this suite of samples. The most extreme values of skewness will be shown by samples with one mode dominant and the other subordinate. These show moderate sorting, and the skewness can be either positive or negative. If one starts with the finest Brazos bar samples (the silty sands) and progresses through coarser and coarser samples to the pure gravels, the loci of these points on the scatter plot is a clockwise circular or elliptical path starting at A and going through B to C.

Standard Deviation versus Kurtosis.—Worst sorting is found in the bimodal mixtures with equal amounts of the two modes, and these also have lowest kurtosis (fig. 15). Highest kurtosis is found in those samples with one mode dominant and the other very subordinate; these have moderate sorting. Unimodal sediments produce normal kurtosis and are best sorted. Starting with the fin-

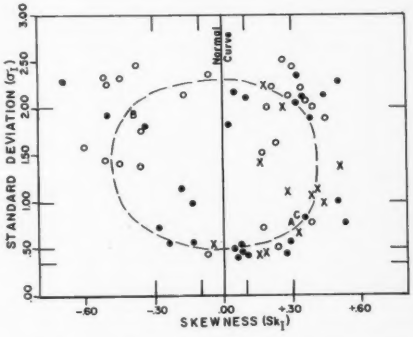

FIG. 14.—Scatter plot of skewness versus standard deviation. The trend is nearly circular. In order of increasing size, samples pass on this diagram clockwise from A through B to C.

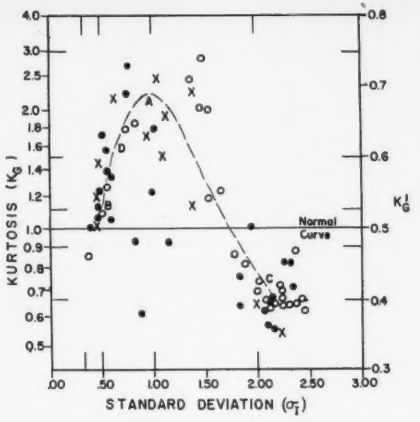

FIG. 15.—Scatter plot of kurtosis versus standard deviation. In order of increasing size, samples follow a regular progression on this diagram, from silty sands (A) to pure sands (B) to slightly gravelly sands (A again), to subequal mixtures of sand and gravel (C). As the gravel content increases, the changes are gone through in reverse, first travelling back to A (gravels with a little sand) and ending at D (nearly pure gravels). A sample of pure gravel would plot approximately at B, just as the samples of pure sand. If one mode is dominant and the other very subordinate, analyses plot at A; if both modes are nearly equal, the analysis plots at C.

est Brazos bar silty sands and going to coarser and coarser sediments, the path progressed on this diagram is a complicated inverted double V, from A through B, A, C, A, and D.

Skewness versus Kurtosis.—Both of these properties depend on the proportions of the two modes present. Thus a regular path is followed on the skewness versus kurtosis diagram as these proportions change and the mean size changes, shown in fig. 16 and 17. Starting with the nearly pure gravel mode[7] (field A), as more and more sand is added the points follow a U-shaped path through the platykurtic regions (modes now equal), then sweep up to reach highly leptokurtic and negatively skewed values in the sands with 7 to 20 percent gravel. As the gravel mode disappears, the path returns to the center point so that the pure sand mode gives a normal curve. But now, as the sediment continues to become finer by the addition of increasing quantities of the silt mode, the path moves again into positively skewed, leptokurtic regions, and if one continued to add silt, the entire cycle would presumably be repeated so that the path of the sand-silt mixtures would follow the path of the gravel-sand mixtures.

[7] A sample of the gravel mode itself would give a nearly normal curve. All gravel samples collected in this study contained a little sand, hence were leptokurtic and positive-skewed.

It will be noted that in the samples studied only very few analyses fall in the range of what would be considered "normal" curves, and the departures from normality are very great. This is because the two main modes on the Brazos bar are far apart and quite distinct. Sediments with two modes closer together or more poorly differentiated would give more nearly "normal" values of skewness and kurtosis, and all the points would be clustered around the center of the diagram. The farther apart the modes, the more extreme the values of skewness and kurtosis.

There is a conspicuous lack of samples that are symmetrical with high kurtosis, i.e. there is a gap in the upper center of the plot although the rest of the diagram is well filled. The reason is obvious. A leptokurtic, symmetrical sample would have to have a steep, well-sorted central mode, and, to re-

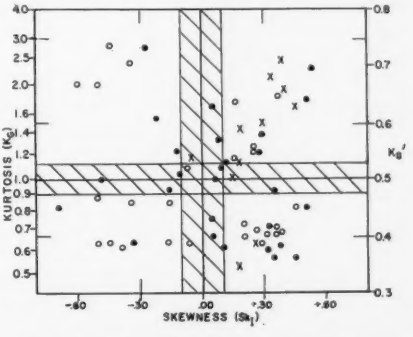

FIG. 16.—Scatter plot of skewness versus kurtosis. Areas here defined as within the range of the normal curve are shown by diagonal-line patterns; only 3 out of the 65 analyzed samples were normal with regard to both skewness and kurtosis. The wide range in skewness and kurtosis values is due to the wide separation between the modes and the ineffective sorting of the depositional environment.

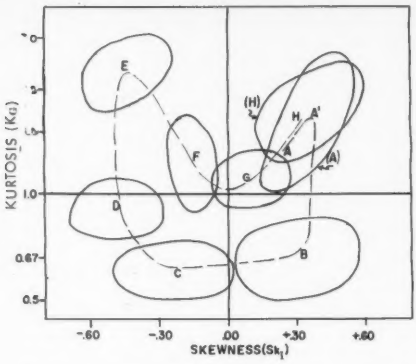

FIG. 17.—Skewness versus kurtosis, a summarization of figure 16 to show fields occupied by sediments of differing modal ratios. The dashed line extending from A through D to H shows the path followed by samples of continually decreasing grain size. Field A is occupied by the nearly pure gravels, with 80 to 95% gravel (perfectly pure gravel would plot as a normal curve). Fields B, C, and D are the sandy gravels containing respectively 55–80%, 37–55%, and 30–37% gravel. Between D and E is an unoccupied area representing the lack of samples with 20 to 30% gravel among the sediments analyzed. Field E, gravelly sand, contains 7–20% gravel, and field F contains 1–7%. G represents the nearly pure sands, with less than 1% gravel and less than 5% silt. Field H includes the silty sands, containing 5–15% silt. Fields H and A overlap because both consist of a dominant coarse mode and subordinate fine mode. If more silt were added, the sediments would follow the same path over a second cycle.

main symmetrical, must have a long "tail" of secondary modes equally balanced on both sides. In short, it must be a trimodal sediment with the middle mode most pronounced. Such sediments are understandably rare; only one Brazos bar sample fell in this area, and it *was* a trimodal mixture of dominant sand with small amounts of gravel and silt. Nearly all leptokurtic curves therefore show extreme skewness, either positive or negative.

Four-dimensional Plot.—In casting about for a way to depict all four parameters of the frequency distribution as one graph, it was discovered that the relation between mean, standard deviation and skewness (if plotted in three dimensions using x, z, and y axes respectively) formed a very close approximation to a helix (fig. 18). The clue that gave it away was the circular form of the standard deviation versus skewness trend, which would be obtained figuratively by looking down the rotational axis of the helix, i.e. looking down the x direction. The sinusoidal plots of mean versus standard deviation and mean versus skewness were simply side and top views of the horizontally-lying helix.

Figure 18 is an accurately plotted isometric projection of this three dimensional trend. The three sides of the "box" enclosing the helix represent two-dimensional projections of the trend, obtained by coplotting each pair of variables in turn. The fourth variable or dimension, kurtosis, is shown as pulsations of shading along the helix and the two-dimensional projections. We have constructed a large three-dimensional model of this trend to aid in visualizing the relationships. From a horizontal sheet of lucite (whose length represents the M_z scale. width the skewness scale) are hung plastic balls, one being placed at the proper coordinates for each sample. Height of the balls is determined by standard deviation. Kurtosis is shown by using balls of ten different colors in spectral order, to represent ten different ranges of kurtosis values.

Again, this helical trend shows how all four parameters of the frequency distribution are related to the relative abundance of the two modes. Best sorting and most "normal" curves occur if the sediment consists entirely of the sand mode. As the proportion of the gravel mode is increased, the size continually increases (moves left in the diagram), sorting continually worsens, and skewness goes to a maximum negative value and then decreases again. Kurtosis also attains a maximum (at a point just before maximum skewness), and then rapidly decreases passing quickly through the "normal" range to reach extreme platykurtic values when the 2 modes are present in equal amounts. As the gravel mode becomes dominant, the sequence of changes is undergone in reverse until, in the pure gravels, better-sorted normal curves again appear. The addition of silt, representing a third mode, starts a new cycle of the helix which is just beginning in the upward hook at the right of the trend.

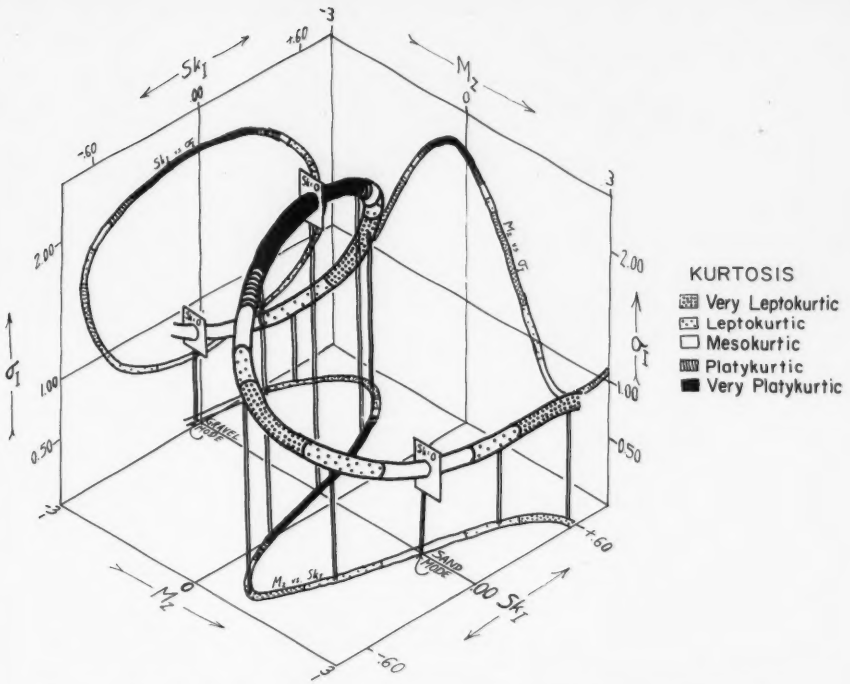

FIG. 18.—Four-variate graph, showing the relation between mean size (M_z), standard deviation (σ_I), skewness (Sk_I), and kurtosis. This is an accurately-plotted isometric projection of the helix which results when mean size, standard deviation and skewness are plotted against each other. Each of the three sides of the box containing the helix represents each pair of variables plotted in turn, hence correspond to two-dimensional projections of the helical trend. Standard deviation, the vertical dimension, is shown also by the height of the "supports" to the helix; points where the helix passes through the .00 skewness plane are shown by small "signboards." Kurtosis is shown by pulsations of shading along the helix and its three projections. The following limits are used: Very Platykurtic, K_G below 0.67; Platykurtic, K_G 0.67–0.90; Mesokurtic, K_G 0.90–1.11; Leptokurtic, K_G 1.11–1.50; and Very Leptokurtic, K_G 1.50–23.90.

The equation for the helix is

$$\begin{cases} \sigma_I = 1.5\phi - 0.75 \sin [60^\circ (M_z - 0.75\phi)] \pm 0.4\phi \\ Sk_I = -0.03\phi - 0.5 \sin [60^\circ (M_z + 0.75\phi)] \pm 0.12\phi \end{cases}$$

where σ_I and Sk_I represent the values for standard deviation and skewness (the dependent variables), M_z is the mean size in phi units, and the last term is the standard error of estimate (two-thirds of the values will fall within the predicted value plus or minus the standard error).

For example, consider a sediment with M_z of $+0.13\phi$. In the standard deviation equation, one finds the sine of 60° $(0.13 - 0.75)$ $= \sin 60^\circ (-0.62) = \sin -37.2^\circ = -0.60$. When the rest of the equation is computed, the predicted value of σ_I is $1.5 - 0.75(-0.60)$ $= 1.5 + 0.45 = 1.95\phi$, and two-thirds of the time the actual σ_I values will lie between 1.55ϕ and 2.35ϕ. In the skewness equation, one finds the sine of $60^\circ(0.13 + 0.75) = \sin 60^\circ(0.88) = \sin 52.8^\circ = 0.79$. The predicted value of Sk_I is then $0.50(0.79) - 0.03 - 0.40 - 0.03 = -0.43$, and two-thirds of the actual values will lie between $-.31$ and $-.55$.

It is possible to work out a general equation for helical trends of this type, wherein the wave length of 360° gives the phi inter-

val between modes (in this example the distance was about 6ϕ, therefore both the equations contained the factor $360°/6 = 60°$, and the skewness and standard deviation sine curves are one-quarter wave length out of phase (in this example $6\phi/4$ or 1.5ϕ, hence one equation contained the factor $M_z + 0.75\phi$ and the other $M_z - 0.75\phi$). The minimum point on the standard deviation sine curve coincides with the modal diameter, and the amplitude on the standard deviation curve is governed by the difference in σ_I between the average worst and the average best sorted samples. Actually it is not quite so simple, because seldom do both modes have equivalent σ_I values, but this type of formula may give a good approximation to the true quantities.

Preliminary work at the University of Texas and examination of previous published results (Inman, 1949) indicates that this helical trend applies in grain size distributions from many other environments. The helix probably goes through several more cycles, with each minimum of best sorting coinciding with a mode in the environment and each maximum coinciding with an inter-modal position, as shown in figure 19. These inter-modal regions can be easily identified by their platykurtic character.

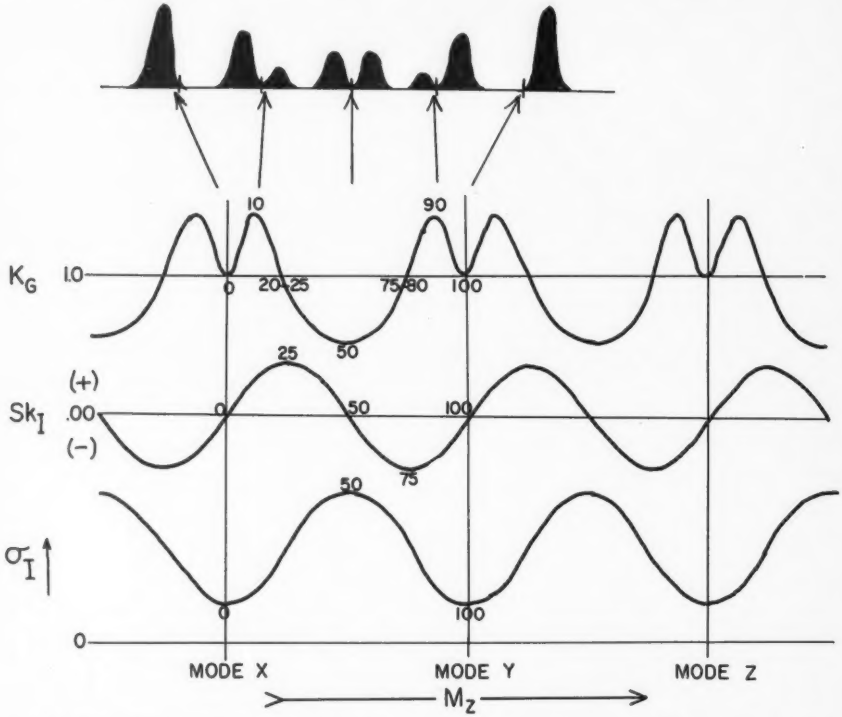

FIG. 19.—Theoretical variation of standard deviation (σ_I), skewness (Sk_I) and Kurtosis (K_G) as a function of mean size (M_Z) in a hypothetical polymodal sediment. Plots of σ_I and Sk_I form sine curves one-quarter wave length out of phase (actually combining to form a helix in three dimensions), while kurtosis forms a complex rhythmic curve. For mixtures of Mode X with Mode Y, the percentages given indicate the proportion of Mode Y present at critical points on each of the curves, provided the measures described herein are used. These percentages hold for the Brazos bar, but probably are slightly different in other environments. Shaded frequency curves at the top of the diagram illustrate the appearance of grain size curves for the critical points designated.

Work in progress indicates that in some neritic environments the modes are sand (or coarse silt) plus clay, also linked by a helix which would add another cycle to the right of the one shown here for the Brazos bar. Many sedimentary environments show only a segment of this helix; to have a complete cycle one needs two distinct and fairly widely separated modes, and within the suite of samples analyzed the pure end members as well as all intermediate mixtures must be present. If, for example, the samples examined consist only of the gradation from sand to clayey sand (say at most 35 percent clay), then only one-third (120°) of a helical cycle will be completed.

Special conditions may alter the form and position of the helix. Work in progress by Todd (1956) on some Eocene sands in Texas shows that these are polymodal sediments in which there usually is a small amount of clay, regardless of the size of the sand. This has the effect of making all the samples positive-skewed and leptokurtic, but here the addition of clay has simply shifted the axis of the helix in the xz plane; instead of being parallel to x with Sk_I equal nearly to .00 (giving nearly equal frequency of positive and negative skewness values), the axis is still in the xz plane but has a Sk_I value of .00 at 1ϕ and +.30 at 3ϕ. Similarly, Miller (1955), found in the Permian Pierce Canyon siltstone of southeast New Mexico a 180° segment of a helical trend but with the axis shifted back into positive Sk_I values because of the constant presence of small "tail" of clay. These positional shifts of the helical axis also exert a strong effect on kurtosis values, tending to shift them into leptokurtic regions.

Will these helical trends show up if other measures of grain size, such as those proposed by Inman, are used? The answer appears to be affirmative, but the trends are not as distinct. The measures proposed here are based on more points, hence are more sensitive and should be expected to give a better trend. For example, addition of a secondary mode affects σ_I and Sk_I if as little as 5 percent occurs, but 16 percent is required to affect Inman's $\sigma\phi$ or $\alpha\phi$. A sample with 30 percent gravel and 70 percent sand has nearly the same mean size as one with 70 percent gravel and 30 percent sand, using Inman's measures, but M_z is considerably more sensitive because the median is included in the calculation.

POSSIBLE GEOLOGICAL SIGNIFICANCE OF SKEWNESS AND KURTOSIS

If one may be permitted to extrapolate from a small study such as this one and enter the seductive field of generalization, it appears that both skewness and kurtosis are vital clues to the bimodality of a distribution, even when the modes are not immediately apparent. For example, these modes may be hidden in an obscure sidewise kick or gentle curvature of the cumulative plot on probability paper, enough to show up as non-normal skewness and kurtosis values, but not enough to show up as a secondary mode on a frequency curve or histogram. Strictly unimodal sediments (like some beach sands) should give normal curves; non-normal values of skewness and kurtosis indicate something "wrong" with the sediment, and indicate a mixing of two or more modal fractions. As an illustration of this principle, many dune sands on the South Texas coast have slight positive skewness and leptokurtosis, caused by the presence of a very minor coarse silt mode in a size finer than the principle mode.

Extreme high or low values of kurtosis imply that part of the sediment achieved its sorting elsewhere in a high-energy environment, and that it was transported essentially with its size characteristics unmodified into another environment where it was mixed with another type of material. The new environment is one of less effective sorting energy so that the two distributions retain their individual characteristics—i.e. the mixed sediment is strongly bimodal. In the Brazos bar, extreme kurtosis values are attained because the bulk of the sand apparently received its sorting in the parent Cretaceous marine sediments, but is now being deposited in the less efficient sorting environment of a river bar, where it is rapidly dumped together with gravel or silt. In neritic sediments, extreme kurtosis values are common because the sand mode achieves good sorting in the high-energy environment of the beach, and then is transported en masse by storms to the neritic environ-

ment, where it becomes mixed with clay and hence is finally deposited in a medium of low sorting efficiency. If the sediments are near the source of the sand, they are characteristically leptokurtic and positive-skewed because the sand is in excess. The more extreme the kurtosis values, the more extreme is the sorting of the modes in their previous environment and the less effective is the sorting in the present environment. Thus one may conclude that kurtosis and skewness are very valuable clues to the "genealogy" of a sediment.

CONCLUSIONS

Once a relationship is established in an ideal case, where the changes are laid out before the observer in their most perfect form, one soon learns to recognize the same relationships in less ideal examples, where the changes are obscure. The obscure examples, hitherto unfathomable, are explained in the light provided by the ideal examples. So it has been with the Brazos bar study. We have studied a simple environment, where the changes follow an orderly helical progression because of the ideally bimodal character. Now, fortified with the knowledge of the ideal trend, we have been able to unravel many once-puzzling relationships in other sedimentary suites of more complex nature and to understand better what is going on in the sedimentary environment. The meaning of skewness and kurtosis has, we feel, been ascertained: they are vitally important distinguishing characteristics of bimodal sediments and enable us to recognize bimodality where it was previously obscure. The changes of skewness, kurtosis, and sorting with sediment transport are probably simple functions of the ratio between the two modes of the sediment. The equations tying these variables together will, we hope, be of some value in distinguishing sedimentary environments. It is not the absolute values of parameters themselves, but their four-dimensional relationships to each other which offer the best hope of further progress.

REFERENCES

CROXTON, F. E., AND COWDEN, D. J., 1939, Applied general statistics. Prentice-Hall, New York, 944 p.

DAPPLES, E. C., KRUMBEIN, W. C., AND SLOSS, L. L., 1953, Petrographic and lithologic attributes of sandstones: Jour. Geology v. 61, p. 291–317.

FOLK, R. L., 1954, The distinction between grain size and mineral composition in sedimentary rock nomenclature: Jour. Geology v. 62, p. 344–359.

———, 1955, Student operator error in determination of roundness, sphericity, and grain size: Jour. Sedimentary Petrology, v. 25, p. 297–301.

GRIFFITHS, J. C., 1951, Size versus sorting in some Caribbean sediments: Jour. Geology v. 59, p. 211–243.

HOUGH, J. L., 1942, Sediments of Cape Cod Bay, Massachusetts: Jour. Sedimentary Petrology v. 12, p. 10–30.

INMAN, D. L., 1949, Sorting of sediments in the light of fluid mechanics: Jour. Sedimentary Petrology, v. 19, p. 51–70.

———, 1952, Measures for describing the size distribution of sediments: Jour. Sedimentary Petrology v. 22, p. 125–145.

INMAN, D. L., AND CHAMBERLAIN, T. K., 1955, Particle-size distribution in nearshore sediments, in Finding ancient shorelines. Society of Economic Paleontologists and Mineralogists Spec. Publ. 3, p. 99–105.

KRUMBEIN, W. C., 1934, Size frequency distribution of sediments: Jour. Sedimentary Petrology, v. 4, p. 65–77.

———, 1938, Size frequency distribution of sediments and the normal phi curve: Jour. Sedimentary Petrology, v. 8, p. 84–90.

KRUMBEIN, W. C., AND PETTIJOHN, F. J., 1938, Manual of sedimentary petrography. D. Appleton-Century, New York, 549 p.

MILLER, D. N., JR., 1955, Petrology of pierce canyon redbeds: Delaware Basin, Texas and New Mexico. Ph.D. Thesis, University of Texas.

OTTO, G. H., 1939, A modified logarithmic probability graph for the interpretation of mechanical analyses of sediments: Jour. Sedimentary Petrology, v. 9, p. 62–75.

PETTIJOHN, F. J., 1949, Sedimentary rocks. Harper and Brothers, New York, 526 p.

PLUMLEY, W. J., 1948, Black Hills terrace gravels: a study in sediment transport: Jour. Geology, v. 56, p. 526–577.

POTTER, P. E., 1955, The petrology and origin of the Lafayette Gravels. Part I; Mineralogy and Petrology: Jour. Geology, v. 63, pp. 1–38.

TODD, T. W., 1956, Comparative petrology of the Carrizo and Newby Sandstones, Bastrop County, Texas, Master's Thesis, University of Texas.

JOURNAL OF SEDIMENTARY PETROLOGY, VOL. 27, NO. 1, PP. 27–31
MARCH, 1957

EFFECTS OF SPHERICITY, ROUNDNESS, AND VELOCITY ON TRACTION TRANSPORTATION OF SAND GRAINS

WILLIAM J. MORRIS
Texas Engineering Experiment Station, College Station, Texas[1]

ABSTRACT

Detrital quartz grains were introduced into a tube under conditions of differing average fluid velocity in order to note quantitatively as well as qualitatively the importance of particle attributes affecting rate of transportation. Difference in rate of transport due to sphericity, roundness, and size were measured and compared by use of arithmetic mean and standard deviation. Results indicate that rate of transportation is influenced by the local turbulence created by individual grains. However, rate of transport of small grains, where local turbulence is minor, is more dependent upon the ability of the particle to roll. The effect of sphericity on rate of transport is complex and is dependent upon rate of fluid flow and degree of sphericity.

INTRODUCTION

The properties of detrital grains that influence the type, duration, and speed of transport are known empirically and have been incorporated into Stokes' Law and the Impact Law concerning the settling velocities of particles. Both formulae show that the primary charaeteristics of a grain which influence its settling velocity (and therefore, conditions of transportation), are size, sphericity, roundness, and specific gravity. The manner of transportation, however, is not only related to particle characteristics but also depends upon the laws of fluid flow governed by velocity, viscosity, and turbulence of the stream or ocean current. It is the combined effects of both particle attributes and fluid characteristics that determine the extent of transportation.

It is the purpose of this experiment to investigate effects of size, sphericity, and roundness, as well as characteristics of the fluid medium on the transportation of detrital grains, and to attempt to correlate the effects of both characteristics on grain movement. Data were recorded on 2400 quartz grains in traction transportation. Although this might seem to be a representative sample, it is only a small fraction of an extremely large and complex population required to describe sedimentary processes satisfactorily. The limitations of the sample necessitate careful consideration before the data can be applied to geologic interpretation. The writer believes, however, that such experimentation is necessary and will, if extended considerably and correlated with field studies, be of benefit in the understanding of the process of sedimentation.

[1] Present address: Occidental College, Los Angeles, California.

METHOD OF STUDY

Detrital quartz grains were introduced individually into a level plexiglass pipe 250 cm long and having an inside diameter of 10 cm. The grains were transported by tap water and the average fluid flow was maintained constant by means of a reservoir tank and valve leading into the tube. The grains were placed in the transportation pipe by means of a smaller plexiglass tube cemented to the larger pipe 35 cm from the water inlet valve. At this distance from the inlet valve turbulence on the grain due to the end effect at the valve can be ignored. For a similar reason, 35 cm were allowed at the opposite end where the grains emerged.

Angular grains were obtained by crushing in a mortar. The well-rounded grains were taken from deposits of Pleistocene fluvial gravels. The angular and well-rounded samples were placed in the Ro-tap for twenty minutes in order to divide them into size grades. The sphericity and roundness of each grain was determined before introduction into the pipe by use of a visual chart (Krumbein & Sloss, 1951, p. 81) for estimating roundness and sphericity.

After the grains were introduced into the pipe, the inlet valve was set to the desired flow setting, the small plexiglass tube through which the grain was introduced was

closed, and a clamp at the open end of the pipe was released. This method allowed an almost instantaneous flow to be reached by the transporting fluid. Each grain was introduced separately and its travel along the pipe was timed by a stop watch and electric timer, and the rate of transport was computed accordingly.

2400 quartz grains with different attributes were run and the results were arranged into class intervals from which standard deviations and arithmetic means were computed.

The velocity of water at any distance from the center of a smooth pipe can be determined, or at least estimated, quite closely. When the flow is laminar, the velocity profile is parabolic where the velocity is a maximum at the center of the pipe, and is zero at the surface. The average velocity, numerically the same as the flow rate, exists at only one point at a determinable distance from the center of the pipe. When the flow is turbulent, the velocity profile is more complicated and is determined empirically. The profile appears to be more "U" shaped than for laminar motion. In turbulent flow the average velocity is, therefore, nearer to the maximum velocity than in the case of laminar flow. Hence, the decrease of velocity in the profile as the walls of the tube are approached is more rapid for turbulent flow. At minute distances from the wall, however, the fluid flow is laminar, whether laminar or turbulent within the rest of the pipe.

It was impossible to transport the grains in conditions of laminar flow in these experiments. Reynolds numbers indicating turbulent flow were involved at even the smallest flow rates usable.

ROUNDNESS EFFECTS

As progressively smaller grains were run, it was found that the smaller the grain, the consistently slower was the rate of transportation. This is because a small grain would be carried along by a markedly lower velocity than a larger grain, since the larger grain projects outward from the wall of the pipe to where the velocity is higher. Although the difference of effective velocities was known to exist for the different grain sizes, it was difficult to reliably calculate them. Consequently only grains of the same size were compared directly with one another.

TABLE 1.—*Standard deviation (σ) and arithmetic mean (M) of 100 grains of angular quartz compared with 100 grains of well-rounded quartz in average fluid velocity of 82.7 cm/sec*

Grain Size	Angular	Well Rounded
1.981 to 1.397 mm	σ 36.36*	34.86
	M 3.14	1.86
1.397 to .991 mm	σ 34.40	33.94
	M 2.79	3.12
.991 to .701 mm	σ 32.18	31.24
	M 3.38	0.28
.701 to .495 mm	σ 29.36	28.52
	M 2.91	2.59
.495 to .351 mm	σ 26.84	26.20
	M 5.19	3.39
.351 to .246 mm	σ 25.26	25.16
	M 2.39	4.21

* M and σ given in cm./sec.

Two types of comparisons were justified and are recorded. The first compares grains of the same size differing in roundness, and the second compares grains of the same size traveling at both higher and lower flow velocities.

Comparison of figures given in tables 1 and 2 shows that the degree of roundness did not appear to affect the rate of transport when the average fluid velocity was constant. The effect at a higher average velocity (82.7 cm/sec) is quite different from that at a lower average velocity (40.2 cm/sec). At an average velocity of 82.7 cm/sec, the angular grains traveled at a faster rate than the rounded grains, and although this difference is not appreciable, the cumulative difference over long distances could be significant. Conversely, at an average velocity of 40.2 cm/sec all of the well-rounded grains appear to travel more rapidly than the angular grains of the same size except for the grains in the .495 to .351 mm diameter grade where the reverse is true. This anomaly is due either to errors in sampling or, perhaps, to the prevalence of a shape in the angular fraction more susceptible to the effects of

turbulence. If in this fraction the angular portion is composed of more equant grains, while those of the rounded fraction are disk-like or bladed, the dominance of the more equant would cause a reversal of trend (tables 1 and 2).

Russell and Taylor (1937) have pointed out that in the Mississippi River between Cairo, Illinois, and the Gulf of Mexico, transported sediments become slightly more angular downstream and that this characteristic is particularly noticeable in the larger sized fraction. Sorting on the basis of shape appeared to be negligible and, at least in part, the decrease in roundness was ascribed to chipping and fracturing of the larger grains. Pettijohn and Lundahl (1943) noted the relationships between roundness and distance of transport and found that there was a definite although fluctuating decrease in roundness with distance of transport, an observation contrary to the experiments formed in abrasion mills. Due to the lack of of coarser materials, little evidence of fracturing was apparent in similar studies of lake sediments. The decrease in roundness, since roundness tends to decrease as sphericity decreases, was ascribed to processes of selective sorting. Although such sorting is quite real, interpretations of the data presented in tables 1 and 2 indicate that additional factors may be present affecting progressive changes of roundness in sedimentary deposits.

TABLE 2.—*Standard deviation* (M) *and arithmetic mean* (σ) *of 100 grains of angular quartz compared to 100 grains of well-rounded quartz in average fluid velocity of 40.2 cm/sec*

Grain Size		Angular	Well Rounded
1.981 to 1.397 mm	σ	6.12	8.66
	M	2.50	3.91
1.397 to .991 mm	σ	5.60	7.26
	M	3.37	3.09
.991 to .701 mm	σ	4.90	6.18
	M	2.55	3.02
.701 to .495 mm	σ	3.78	5.50
	M	3.05	0.58
.495 to .351 mm	σ	3.76	3.50
	M	2.59	0.16
.351 to .246 mm	σ	2.80	3.14
	M	0.42	0.75

At higher velocities the angular grains with their inherent lesser sphericities tend to block the normal flow of the transporting medium. The influence of the less streamlined forms tends to produce eddies in the fluid, presumably leading to increased turbulence in the immediate area surrounding the particle. Due to this increased turbulence, the settling velocity of the grain under stationary conditions is reduced and less resistance to the line of flow results. Well-rounded grains, on the other hand, have a lower local turbulence, so that less resistance is offered to settling, with the effect that movement in the direction of fluid flow is less than that of angular grains.

While this local turbulence produced by the grain is apparent at an average velocity of 82.7 cm/sec, the reverse is true at an average velocity of 40.2 cm/sec. Perhaps at the lower velocity there is a decreased local turbulence effect on even the largest grains. Possibly the ability of a grain to roll freely becomes more important at lower fluid velocities than the effect of local turbulence. Thus, shape becomes the dominant factor in transport. The results suggest that local turbulence is not only an overall effect at high fluid velocities, but that particles of different sizes are also affected differently by local turbulence. The differences in rate of transportation between the larger and smaller size particles (table 1) progressively decreases as the fluid velocity decreases, indicating that the rate of movement of the smaller grains will be more influenced by their ability to roll while the larger ones will be more influenced by local turbulence.

The progressive decrease in particle roundness in the direction of transportation observed in rivers may be due mostly to the effect of local turbulence for the larger grains at higher velocities and the ability to roll for the smaller grains at lower velocities. If these factors actually apply, then the resulting sedimentary deposit would show a decrease in roundness downstream in the larger fraction and an increase in roundness downstream in the smaller fraction.

The effect of change in average fluid veloc-

ity of the transporting medium on the rate of movement of individual grains was not examined fully, but as one series of tests was run at approximately half the average velocities of the other, some tentative conclusions can be drawn. 1600 grains were run at an average velocity of 82.7 cm/sec while the same number was run at an average of 40.2 cm/sec. Half of the grains of each series was angular and the other half well rounded.

Results of the runs show that a decrease in the average fluid velocity decreases the rate of transportation of the individual particles considerably. Examination of tables 1 and 2 reveals that when the velocity was decreased by half, the rate of movement of the grains was only one fifth as great. The competency of the fluid to cause traction movement decreased disproportionally with lowered average fluid velocity.

Further work is needed before the effect of the change in fluid velocity becomes clear. No doubt the effects caused by the velocity variation would be greatly changed if the grains were transported over a rough surface rather than the smooth wall of a pipe.

SPHERICITY EFFECTS

The weighted arithmetic mean was computed for several size grades and degrees of sphericity and includes both well-rounded and angular particles (tables 3 and 4) traveling at average velocities of 82.7 cm/sec and 40.2 cm/sec.

Comparison of the rates of particle transportation shows a marked decrease with the decrease of average fluid velocity and, in addition, inspection of the difference in rates within each size grade shows the influence of the sphericity on the transportation rate for the selected sample. In each case, as expected, the grains having a sphericity greater than 0.8 traveled at maximum velocity as a result of the ability to overcome the friction between the grain and the wall of the pipe. While the action of high sphericity grains appears to be a relatively simple relationship between the grain and the surface of the fluid container, the grains with the least sphericity, 0.4 to 0.6 show a more complex relationship, perhaps dependent upon turbulence effects as well as friction phenomena. Conjecturally, grains of low sphericity should, because of the greater resistance to flow due to friction, travel at a slower speed than the more spherical particles when transported along the wall of the tube. The summary presented in tables 3 and 4 does not entirely support this conclusion. When grains are placed in a fluid flow of 82.7 cm/sec and all grains of the same size are compared, a decrease in rate of transportation is apparent that may be correlated with a decrease of sphericity. This is particularly noticeable in the largest grains traveling in an average fluid velocity of 82.7 cm/sec. Comparison of grains of smaller size, however, shows a more complex relationship as grains of small size having sphericities from 0.4 to 0.6 travel at a faster rate although never reaching a rate as fast as those of maximum sphericity but greater than those grains having sphericities from 0.6 to 0.8. This reversal in trend might be ascribed to a lesser proportion of prolate grains in the 1.981 to .991 mm range and a larger proportion of grains offering more resistance to fluid flow. When the same size particles were run at lower velocities, however (table 4), an increase in rate of transportation was noted for grains of 1.981 to .991 mm diameter, and a tendency towards reduction of rate with reduction of sphericity was noted in the smaller sizes traveling in an average fluid velocity of 40.2 cm/sec. A possible explanation of the differences of the rate of transportation as shown by the sample appears to be dependent upon the number of grains in each size offering resistance to flow together with the turbulence affecting grains of different characteristics. It appears that at maximum average fluid

TABLE 3.—*Weighted average arithmetic mean* (σ) *of quartz grains in fluid velocity of 82.7 cm/sec*

Grain Size	Sphericity	No. of Particles	σ (cm/sec)
1.981 to 1.397 mm	0.8 to 1.0	117	35.59
	0.6 to 0.8	164	35.05
	0.4 to 0.6	75	34.33
1.397 to .991 mm	0.8 to 1.0	83	31.24
	0.6 to 0.8	105	29.93
	0.4 to 0.6	76	30.68
.991 to .246 mm	0.8 to 1.0	126	27.89
	0.6 to 0.8	125	21.11
	0.4 to 0.6	75	24.97

TABLE 4.—*Weighted average arithmetic means (σ) of quartz grains in fluid velocity of 40.2 cm/sec*

Grain Size	Sphericity	No. of Particles	σ (cm/sec)
1.981 to 1.397 mm	0.8 to 1.0	133	8.20
	0.6 to 0.8	167	6.14
	0.4 to 0.6	75	6.95
1.397 to .991 mm	0.8 to 1.0	146	6.35
	0.6 to 0.8	148	4.90
	0.4 to 0.6	86	3.67
.991 to .246 mm	0.8 to 1.0	133	4.03
	0.6 to 0.8	155	3.62
	0.4 to 0.6	72	3.14

flow as well as maximum average size, the shape of grain influences the rate of transportation less than does the greater average turbulence of the transporting fluid. When the fluid velocity is decreased, the effect of difference in amount of turbulence between grains of differing sphericity is increased but is less than at higher rates of fluid flow. Because of this, the effect of shape becomes once again apparent, i.e. the least spherical and the grains of maximum sphericity travel faster than the grains of intermediate sphericity.

If the average fluid velocity is decreased to a minimum (table 4—size .991 to .246 mm) once again there is a decrease in rate of transportation coupled with a decrease in sphericity. Thus, it appears that, at conditions of maximum and minimum fluid velocity, the shape of the grain is less important on rate of transportation than are the effects of such factors as turbulence and friction.

CONCLUSIONS

Considerations of the factors discussed leads to the following tentative conclusions:

1. The complex relationship between particle attributes and fluid laws governing the transporting medium is important in determining the ultimate characteristics of a sedimentary deposit.
2. At relatively high fluid velocities angular grains appear to travel faster than rounded grains, as the angular grains create local turbulence.
3. At relatively low fluid velocities well-rounded grains appear to travel faster than angular grains, as the rounder grains are influenced more by the ability to roll than by the effect of small local turbulence.
4. A proportional decrease in fluid velocity results in a disproportional decrease in the rate of transportation of a detrital grain.
5. Grains traveling in conditions of maximum average and in minimum average fluid flow produce a complex decrease in rate of transportation that can be correlated with decreasing sphericity.
6. Conditions of intermediate rate of flow cause a high rate of transportation for grains having sphericities of 0.8 to 1.0, a lower rate for grains having sphericities of 0.6 to 0.8 and a higher rate of transportation for the grains of least sphericity.

ACKNOWLEDGMENTS

The author wishes to thank those who helped make this work possible. Dr. P. H. Kuenen, in several discussions during the preliminary phases of this experiment, aided the writer by suggesting modifications of equipment as well as furnishing recommendations necessary to secure funds. Dr. Peter Dehlinger of the Department of Geology together with members of the Department of Civil Engineering of the Agricultural and Mechanical College of Texas provided invaluable assistance in the understanding and application of the hydraulic principles involved. Special thanks are due Dr. Dehlinger for his help in reviewing the manuscript.

The experiments were conducted in the Department of Geology, A. and M. College of Texas.

REFERENCES

KRUMBEIN, W. C., AND SLOSS, L. L., 1951, Stratigraphy and sedimentation. W. H. Freeman and Company, San Francisco, California, 497 p.

PETTIJOHN, F. J., AND LUNDAHL, H. C., 1943, Shape and roundness of Lake Erie beach sands from Cedar Point, Ohio: Jour. Sedimentary Petrology, v. 3, p. 92–94.

RUSSELL, R. D., AND TAYLOR, R. E., 1937, Roundness and shape of Mississippi river sands: Jour. Geology, v. 45, p. 225–267.

JOURNAL OF SEDIMENTARY PETROLOGY, VOL. 27, NO. 1, PP. 32–40
FIGS. 1–2, MARCH, 1957

MINERAL ALTERATION IN ROCKS OF MIDDLE EOCENE AGE, ABSAROKA RANGE, WYOMING

RICHARD L. HAY
Louisiana State University, Baton Rouge, Louisiana

ABSTRACT

Alteration of primary igneous minerals was studied in sedimentary volcanic deposits of the middle Eocene Aycross formation, Pitchfork formation, and early basic breccia of the Absaroka Range, Wyoming. Olivine, hypersthene, augite, hornblende, and plagioclase are altered to varying extents in these beds. Chlorite, clay, barite, calcite, and chalcedony are present in pseudomorphs after the primary igneous minerals. The sequence of deposition, shown above from earliest to latest, is indicated by replacement relations in pseudomorphs and by successive coatings and replacements in amygdules. A groundmass of recrystallized clay minerals and authigenic chlorite characterizes the beds in which alteration is most complete. Zeolite and koninckite occur as authigenic minerals in some of the sedimentary deposits. Alteration of igneous minerals to clay was accomplished by weathering in a warm, humid climate after the sediment was deposited; later replacements by barite, calcite, and chalcedony took place after burial. Different degrees of alteration are explained by differences in rate of burial and depth of the water table. This alteration of primary igneous minerals greatly affects the reliability of stratigraphic correlations based upon mineral analyses, and may also lead to misidentification of the original composition of the volcanic material.

INTRODUCTION

Beds of middle Eocene age consisting largely of volcanic material form the lower subdivision of the Absaroka Range, a dissected mass of essentially horizontal volcanic accumulations bordering the Big Horn and Wind River basins of Wyoming on the west and northwest, respectively (fig. 1). These beds of middle Eocene age were studied during 1950 and 1951 in order to solve several stratigraphic problems (Hay, 1956). Mineralogic and petrographic study indicate that the minerals of volcanic origin—particularly olivine, pyroxene, and hornblende—have been widely altered on a scale which greatly affects the reliability of stratigraphic correlations based on mineral composition, and which could easily lead to misidentification of the original composition of the volcanic detritus. This study is largely based on examination of about 60 thin sections and 75 mineral separates. Special thanks are due to Dr. Hisashi Kuno of Tokyo University for assisting the writer to recognize pseudomorph shapes and identify the original composition of altered lavas.

STRATIGRAPHY AND LITHOLOGY

The Pitchfork formation, of middle Eocene age, borders the southwestern part of the Big Horn Basin. This formation is about 1000 feet thick and consists largely of reworked volcanic deposits—sandstones, siltstones, wackes, and conglomerates.[1] Volcanic wackes occur only locally; the other types are widespread. Most of these sediments were deposited in stream channels and floodplains. The Pitchfork formation comprises both andesitic and dacitic facies, but andesitic beds predominate. Dominant colors are light olive gray to pale yellowish brown. Most of the andesite pebbles and cobbles are pyroxene andesite, olivine-pyroxene andesite, and hornblende-pyroxene andesite.

The Pitchfork formation interfingers to the north with the coarse pyroclastic early basic breccia, which borders the Big Horn Basin on the northwest. The early basic breccia consists of andesitic volcanic breccia, tuff-breccia, and conglomerates having a maximum reported thickness of about 5500 feet (Rouse, 1937, pp. 1264–1266). The fresh tuff-breccia is light olive gray to pale yellowish brown. Most of the coarser fragments are pyroxene andesite, olivine-pyroxene andesite, and hornblende-pyroxene

[1] Terminology used is largely that discussed in Hay, 1952, and Williams, Turner, and Gilbert, 1954, p. 150. However, volcanic sandstones in which a groundmass of recrystallized clay and authigenic chlorite is relatively abundant will be termed volcanic wackes (slightly modified after Williams, Turner, and Gilbert, pp. 297–304).

andesite where studied by the writer. Several sheets of tuff-breccia interfingering with beds of the Pitchfork formation in the east-central part of the Absaroka Range contain dacitic volcanic sandstone blocks torn from dacitic beds of the Pitchfork formation during underground mud flow (Hay, 1954, pp. 615–619). The smaller dacitic inclusions and the marginal 1 to 3 feet of the larger blocks are generally cemented by chalcedony.

The middle Eocene Aycross formation at the southern margin of the Absaroka Range is very likely equivalent in age to the Pitchfork formation and early basic breccia (table 1). The Aycross formation consists largely of fluviatile volcanic deposits of both andesitic and dacitic composition. At its type area on North Mesa the Aycross formation is about 1000 feet thick (Love, 1939, p. 66) and consists largely of soft-weathering claystones, volcanic wackes, and conglomerates containing andesitic detritus essentially similar in composition to the andesitic debris of the Pitchfork formation and the early basic breccia. These beds are variegated in shades of green, chocolate, cream, and gray. Laterally equivalent beds to the south and southeast consist largely of massive, cliff-forming dacitic volcanic wackes.

MINERAL ALTERATIONS

Primary igneous minerals of volcanic origin are extensively altered in the beds of middle Eocene age previously discussed. Olivine, hypersthene, augite, hornblende, and plagioclase are the minerals most widely altered. Minerals are altered most completely in the Aycross formation and least altered in the early basic breccia; alteration is intermediate between these two in the Pitchfork formation (table 2).

Pseudomorphs after the primary igneous

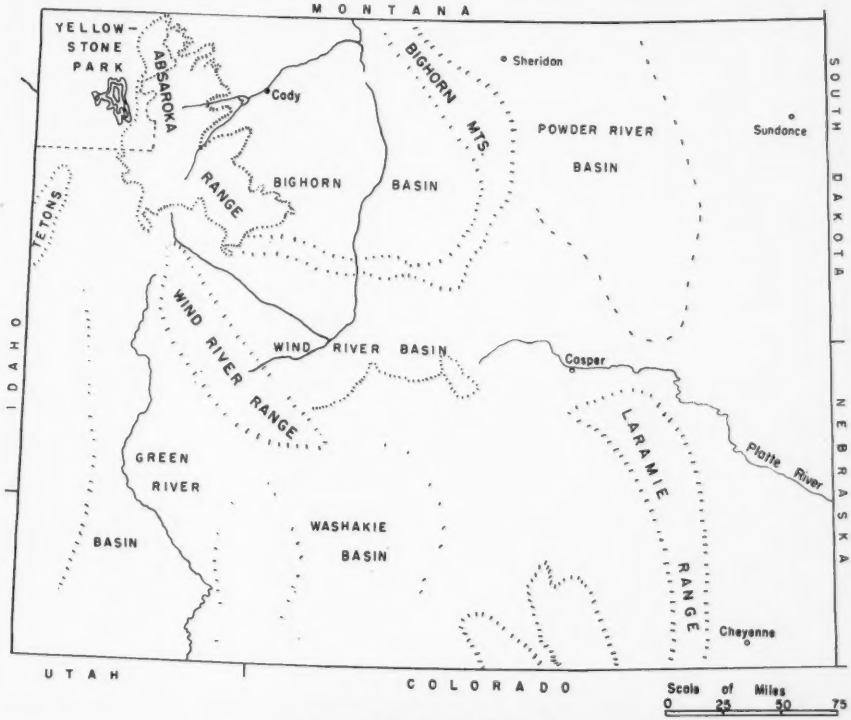

FIG. 1.—Index map of Wyoming.

TABLE 1.—*Correlation chart of beds of Eocene age in Absaroka Range, Wyoming, as adopted by Hay (1956)*

Age	NW corner of Wind River Basin	SW margin of Big Horn Basin	NW margin of Big Horn Basin
Upper Eocene	Tepee Trail formation	Late basic breccia (of Hague, 1899)	Late basic breccia (of Hague, 1899)
Middle Eocene	Aycross formation	Pitchfork formation	Early basic breccia
Lower Eocene	Wind River formation	Willwood and Tatman formations	Willwood formation

minerals include a number of secondary minerals: calcite, chlorite, clay of several types, barite, and chalcedony. Chlorite and clay are direct alteration products of the primary minerals, but barite and chalcedony are largely replacements of earlier alteration products. Calcite replaces both primary igneous minerals and earlier alterations of the igneous minerals. Alterations and replacements are described in more detail below.

Olivine

All of the olivine is altered in the samples studied; its former presence is indicated by pseudomorphs having the distinctive euhedral outline of olivine. Most pseudomorphs consist of chlorite and magnetite, but chalcedony occurs in a small percent, and barite is common in pseudomorphs after olivine in some andesite pebbles from the Aycross formation on North Mesa. Barite occurs at the margin of some pseudomorphs and in the interior of others, apparently as a replacement of chlorite, which forms the remainder of these pseudomorphs.

Pyroxene

Pseudomorphs after pyroxene in andesite pebbles most commonly consist of chlorite, calcite, clay, and chalcedony. Barite is also present in many pebbles and cobbles of the Aycross formation at North Mesa. The sequence in which these minerals were deposited could be determined in the pseudomorphs of several specimens. The sequence is as follows, from earliest to latest:

1. Olive-green chlorite forms the rim and fills fractures in most pseudomorphs.
2. Pale green, colorless, and brown clays form the interior of many pseudomorphs and the rim of some pseudomorphs in which chlorite is absent. The pale green clay appears to grade into the marginal chlorite.
3. Barite replaces much of the clay.
4. Blue-green chlorite is commonly adjacent to barite (fig. 2a) and its distribution suggests that it may have formed during or after deposition of the barite.
5. Calcite extensively replaces the clay and to a lesser extent replaces barite and blue-green chlorite. Calcite is generally the most abundant constituent of the pseudomorphs. Olive-green chlorite is largely unreplaced by calcite, and some early fracture-filling chlorite veinlets in calcite pseudomorphs give the misleading appearance of having formed after the calcite.
6. Chalcedony occurs in a few pseudomorphs, probably replacing clay. Age relationships are not clearly defined, but chalcedony is the latest mineral in amygdules and hence is very likely the latest in pseudomorphs.

Pseudomorphs after detrital pyroxene grains are most commonly calcite and less commonly chlorite and clay, either separately or in the same pseudomorphs. The pseudomorphous clay in volcanic wackes of the Pitchfork formation is commonly orange-brown in color and may be nontronite. Many grains of augite are incompletely altered in volcanic wackes of the Pitchfork formation, and some former single grains consist of small remnants of unaltered augite enclosed by calcite, which is in turn enclosed by nontronite (?)(fig. 2b).

Detrital grains of augite in silicified blocks of dacitic volcanic sandstone show hacksaw terminations and other etching features (fig. 2c). Chalcedony replaces the dissolved augite of some grains (fig. 2c).

Hornblende

Both detrital grains and phenocrysts of hornblende in samples from the Aycross

formation now chiefly consist of pseudomorphous calcite and less commonly clay. Hornblende is partly altered to nontronite (?), chlorite, and calcite in volcanic wackes of the Pitchfork formation. Some of the hornblende in andesite and dacite pebbles of the Pitchfork formation has been altered to magnetite, chlorite, and less commonly chalcedony. The magnetite may be a deuteric alteration product. Some grains of hornblende in silicified blocks of volcanic sandstone display hacksaw and needle-like terminations, and a few others are "shredded" as described below.

Biotite

Most of the altered biotite is split along cleavage planes, the cleavage laminae being separated by chalcedony and less commonly calcite, giving the grains a shredded appearance (fig. 2d). Most of the shredded biotite is unusually green and has abnormally low birefringence, due most likely to chloritic alteration. Biotite is similarly altered in all silicified blocks of dacitic volcanic sandstone examined, and has been observed in several pebbles, a calcareous concretion, and a silicified bed of volcanic sandstone of the Pitchfork formation. A few grains are altered in this fashion in several other beds.

Plagioclase

Plagioclase is extensively altered in many beds, and some grains are completely destroyed. Calcite most commonly replaces plagioclase, but clay and chlorite also occur. The calcite replaces cores, composition zones, fracture margins, and irregular areas of plagioclase and also earlier clay and chlorite alterations. Calcite replacing some plagioclase grains in volcanic sandstones extends into the groundmass of the sediment.

AMYGDULES

Amygdules in andesite pebbles contain the same minerals found in pseudomorphs after primary minerals: chlorite, clay, barite, calcite, and chalcedony. The sequence in which the secondary minerals were deposited is indicated by successive coatings and replacement relations. The sequence in pebbles of the Aycross formation on North Mesa is as follows:

1. Olive-green chlorite forms the outer margin of most amygdules.

2. Pale green, colorless, and brown clays form the interior of many amygdules. The pale green clay commonly grades into the marginal chlorite.

TABLE 2

	Ol	Hyp	Aug	H'blende	Bio	Plag
1. Aycross formation						
a. volcanic wacke	- - -	XXX	XXX	XXX	O-X	XX
b. pebbles & cobbles	XXX	XXX	XXX	XXX	O-X	XX
2. Pitchfork formation						
a. volcanic wacke	- - -	XXX	XX	XX	O	XX
b. volcanic sandstone	- - -	XXX[1]	O	O	O	O-X
c. pebbles & cobbles	XXX	XXX	O	O	O	O-X
3. Early basic breccia						
a. tuff matrix	- - -	O-XX	O	O	O	O
b. lithic fragments	XXX	O-X	O	O	O	O
c. silicified inclusions	- - -	- - -	O-X	O-X	X-XX	O

Table showing the most common degree of alteration of detrital grains and crystals within the larger lithic fragments (e.g. pebbles and cobbles) in beds of middle Eocene age of the Absaroka Range. Alteration of fine lithic debris is not indicated but is generally more extensive than that of detrital grains and coarse lithic fragments. Minerals are indicated as follows: Ol—olivine, Hyp—hypersthene, Aug—augite, H'blende—hornblende, Bio—biotite, and Plag—plagioclase. The following will be used to indicate degree of alteration: O—no alteration, X—slight alteration, XX—moderate to extensive alteration, XXX—complete alteration, and - - - —neither unaltered mineral nor pseudomorphs identified.

[1] Hypersthene is largely unaltered in one sample of coarse conglomeratic volcanic sandstone deposited near a vent (Rose Butte; see Hay, 1954, p. 611, fig. 4).

3. Barite replaces most of the clay in some amygdules. Euhedral blades of barite are intergrown with chlorite in amygdules of one pebble. As chlorite is normally the earliest secondary mineral, the intergrown barite probably replaced chlorite.

4. Calcite replaces the interior clay in most amygdules. Calcite and barite were nowhere found in the same amygdule, but calcite replaces barite in some pseudomorphs, and the calcite in amygdules is probably later than the barite.

Amygdules in andesite pebbles of the Pitchfork formation contain chlorite, clay, calcite, and chalcedony in the following sequence:

1. Green chlorite forms the margin of the amygdules.

2. Pale green and colorless clays form the interior of many amygdules, the pale green clay grading into the marginal chlorite.

3. Calcite forms irregular patches and euhedral rhombs replacing clay.

4. Finely crystalline chalcedony (or quartz) forms the core of some amygdules and fibrous chalcedony extensively replaces clay in other amygdules. Veinlets of chalcedony cutting calcite suggest that the fibrous chalcedony was deposited later than the calcite.

AUTHIGENIC GROUNDMASS MINERALS IN DETRITAL ROCKS

Authigenic chlorite, recrystallized clay minerals, calcite, koninckite, and a zeolite have been found in the sedimentary deposits previously described. Most of the clay is pale brown to yellow in color and has crystallized rather coarsely throughout the groundness and locally forms scaly masses. Birefringence of most of the clays is relatively high, but other optical data are inadequate to determine whether the clays belong to the montmorillonite or illite group, or both. Orange-brown nontronite (?) is abundant in some beds of the Pitchfork formation. In volcanic wackes chlorite forms fibrous, colloform interstitial masses generally enclosed by recrystallized clay minerals. Small flakes of authigenic chlorite are scattered throughout the groundmass of most volcanic sandstones and the tuff matrix of the early basic breccia. Authigenic chlorite is particularly abundant in the blocks of silicified dacitic volcanic sandstone enclosed in tuff-breccia, imparting a greenish gray color to the blocks. Calcite occurs as small irregular masses or patches in the groundmass of both volcanic wackes and volcanic sandstones, forming from less than 1 percent to as much as 20 percent of the rock. Fibrous zeolite is abundant as an interstitial filling in one sample of tuff-breccia and one of andesitic sandstone collected near a volcanic vent in the Rose Butte area of Greybull Valley (Hay, 1954, p. 611, fig. 4). The zeolite is enclosed by a rim of authigenic chlorite and probably filled interstices earlier lined by chlorite. Koninckite, a hydrous phosphate of ferric iron (Larsen and Berman, 1934, p. 54), is present in most heavy-liquid separates of volcanic wacke from the Aycross formation but was not observed in thin sections. Koninckite is friable and was very likely formed in place in these beds.

DATE AND ORIGIN OF ALTERATIONS

The possibility that the minerals were altered by intrastratal solutions after the sediments were consolidated to their present state will first be examined. Bramlette (1941), in a study of Miocene sandstone, has reported that epidote, zoisite, and hornblende are more abundant in calcareous concretions than in non-concretionary samples from the same beds. He suggested that the concretions form a sealed environment in which unstable minerals are protected from the destructive effects of intrastratal solution. Heavy-mineral and magnetic-mineral separates of concretionary samples from the Aycross formation show no visible difference from separates of non-concretionary samples. Thus, the primary igneous minerals in these beds were very likely altered before the concretions were formed. Minerals are most completely altered in claystones and volcanic wackes of the Aycross formation which would normally be the least permeable and hence the least affected by movement of ground water, also suggesting that intrastratal solution was not the cause of most alteration.

The etching of augite and hornblende in silicified blocks of dacitic volcanic sandstone is similar to that resulting from intrastratal solution (Pettijohn, 1949, p. 491, fig. 128),

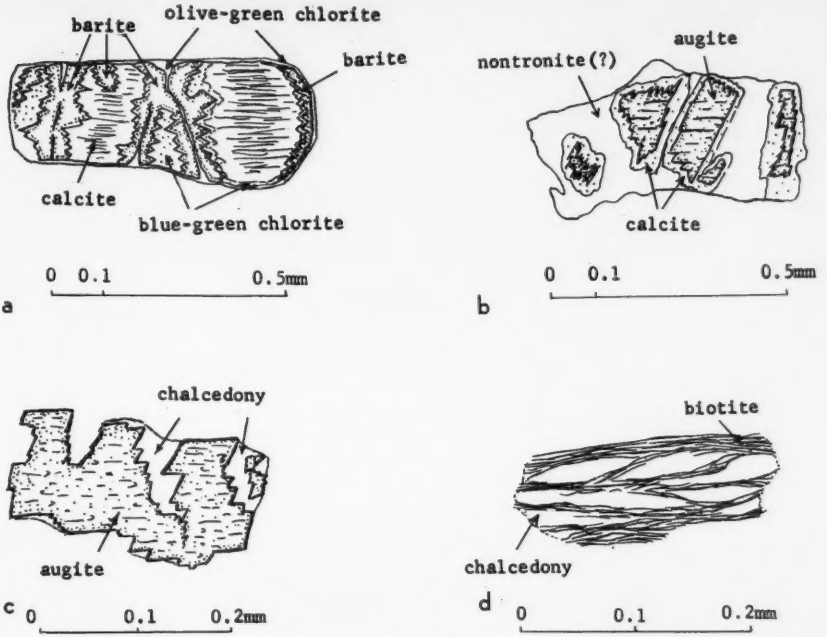

FIG. 2.—Alterations of primary igneous minerals in beds of middle Eocene age, Absaroka Range, Wyoming. a.—Pseudomorph after hypersthene or augite in andesite pebble from the Aycross formation on North Mesa. Barite commonly displays a sawtooth margin in pseudomorphs. b.—Partly altered detrital grain of augite in volcanic wacke of the Pitchfork formation from Greybull Valley. Unaltered remnants of augite enclosed by calcite are in optical continuity. c.—Etched augite grain in a silicified block of dacitic volcanic sandstone enclosed in the early basic breccia in Greybull Valley. d.—Altered detrital biotite grain from the same silicified block as figure 2c above.

and was probably produced in this way. However, the augite and hornblende were etched before or during silicification, as the silicified blocks are now nearly impermeable, and chalcedony replaces much of the dissolved augite and hornblende. The biotite in these blocks was probably altered during silicification by the growth of chalcedony along cleavage lamellae, which shredded the grains and made them more susceptible to chloritization.

The suggestion has previously been made by Love (1939, p. 109) that the volcanic debris in the Aycross formation was altered by weathering in a warm, humid climate similar to that of the coastal states from South Carolina to Louisiana (Berry, 1930, p. 58). Weathering in either or both the source area and depositional site could have altered the minerals; evidence to be discussed below suggests that most alteration took place after the sediment was deposited.

Areas of high relief under a warm, humid climate normally yield a mixture of weathered and unweathered detritus (Krynine, 1950, pp. 157, 158, and 186–189). Volcanic cones are features of relatively high relief, yet fresh volcanic detritus is not extensively intermixed with altered material in beds of middle Eocene age of the Absaroka Range. Rather, the minerals are altered to a different extent in the various sedimentary facies (table 2), suggesting that the alteration was largely accomplished in depositional environments where different conditions altered the sediments to a uniform degree in each environment.

Petrographic evidence also indicates that

the minerals were largely altered after they were deposited. Calcite, chlorite, and clay pseudomorphs after detrital grains could not have been transported from the source area, because erosion and transportation would have destroyed these soft minerals. Former detrital grains of augite enclosed by calcite and mantled in turn by nontronite (?) (fig. 2b) are particularly convincing evidence for post-depositional alteration, for the nontronite (?) and calcite unquestionably replace augite, a fact less easily proved in supposed pseudomorphs where no unaltered mineral remains. Some patches of calcite replacing detrital plagioclase grains in volcanic sandstones extend into the groundmass, indicating that the calcite grew after the plagioclase had been deposited.

Minerals are altered most extensively in argillaceous beds, which were deposited in an environment such as a seasonally well drained flood plain in which decomposition in the subtropic climate was relatively complete. Colors of the Aycross beds, exclusive of green,[2] are found in laterites, and similar deep weathering may have produced colored soils and altered most of the igneous mafic minerals to clay. In conformity with this theory, the Pitchfork beds, characteristically less altered than the Aycross, are dominantly drab shades of pale gray and pale brown, probably little changed from the color of the fresh sediment when deposited. Sedimentary structures and lithologic features indicate that standing water was locally present in the Pitchfork sedimentary environment (Hay, 1956, p. 1882), and the water table may have been at and near the surface, preventing lateritic weathering of most Pitchfork sediments. Alteration is least in the tuff-breccia, which was in all likelihood deposited rapidly and consequently not exposed long to surface weathering.

The later replacements by barite, calcite, and chalcedony probably took place after burial. The sequence in which these mineral types were deposited in the Aycross formation (sulfate-carbonate-silica) and Pitchfork formation (carbonate-silica) is the reverse of their sequence as cements in sandstones described (Waldschmidt, 1941).

One feature worthy of note is the extensive alteration of biotite in silicified rock and in a calcareous concretion; most biotite is unaltered in uncemented beds of similar lithology. Augite and hornblende are etched although otherwise largely unaltered in the silicified rock, thus constituting an exception to the normal stability series in which biotite is more stable than pyroxene at surface conditions (Goldich, 1938, pp. 55, 56).

PHYSIOGRAPHIC SIGNIFICANCE OF ALTERATION

The inferred difference in water table between the Big Horn Basin and the northwest part of the Wind River Basin may reflect an important difference in physiographic setting. Partial continuation of the late early Eocene (=Lost Cabin faunal subdivision) physiography into middle Eocene time may account for the inferred difference in water table. During late early Eocene time the Wind River Basin was an aggradational flood plain drained by a master stream flowing to the east, in contrast to the Big Horn Basin, which was a closed basin containing a large lake (Tourtelot and Thompson, 1948; Hay, 1956, p. 1892). One might reasonably expect a lower water table in a piedmont flood plain drained by a river than in a poorly drained flood plain fringing a lake.[3] That the Wind River Basin was not uniformly well drained in middle Eocene time is suggested by drab-colored middle Eocene beds containing unaltered hypersthene and augite of volcanic origin at the southern margin of the basin (Van Houten, 1954). Pyrite nodules in these beds suggest that reducing (marshy?) conditions prevailed while these sediments were deposited.

Volcanic materials in the early Eocene

[2] Green beds are uncommon—if not altogether absent—in present-day soils, and the green Aycross beds acquired their present color by post-depositional processes.

[3] If present during middle Eocene time, the lake in the Big Horn Basin was smaller than during the late early Eocene (Hay, 1956, p. 1888). During middle Eocene time the major stream probably flowed southeast as well as east across the Wind River Basin, as Absaroka-type andesitic detritus occurs in middle Eocene beds at the southern margin of the Wind River Basin (Van Houten, 1954).

Wind River formation underlying the Aycross formation in the northwest part of the Wind River Basin are much less altered than the Aycross beds (Hay, 1956, p. 1896). Essentially similar physiography has been inferred for both sedimentary environments, and the writer attributes the different degree of alteration to the more rapid deposition of the Wind River sediments. The beds of the latter formation deposited during late early Eocene time (=Lost Cabin faunal unit) alone are commonly thicker than the entire middle Eocene sequence in the Wind River Basin.[4]

SIGNIFICANCE OF MINERAL ALTERATIONS IN STRATIGRAPHIC CORRELATION

Mineral composition of volcanic detritus has been previously used in northwest Wyoming as a basis for stratigraphic correlation of Tertiary beds (e.g. Stow, 1938 and Love, 1950, p. 1482). Minerals in beds of middle Eocene age described here have been altered on an extensive scale, which greatly affects the reliability of correlations based on mineral composition. Correlating on the basis of mineral separates alone is particularly hazardous; thin sections must be studied with care to identify altered primary igneous minerals.

Olivine and pyroxene, most common mafic minerals in basic igneous rocks, are normally more readily altered than biotite, common in acid volcanic rocks (Goldich, 1938, p. 56); hence selective destruction of the olivine and pyroxene, in beds originally containing olivine, pyroxene, and biotite would suggest a misleadingly acid composition unless the pseudomorphs were identified. Plagioclase is rarely entirely altered in any samples examined, and plagioclase composition was found to be much more indicative of the original composition than the content of unaltered mafic minerals. Plagioclase composition affords another advantage over the mafic minerals for determining the original composition of detrital volcanic sediments; it is more sensitive to the chemical composition of the original magma than is the presence of any particular mafic mineral. Acid and basic lavas differ fundamentally in the volume of mafic minerals, but not in the specific occurrence of one mafic mineral such as augite. Hence the presence of unaltered augite in a sedimentary deposit does not necessarily indicate a definite source rock, whereas the common occurrence of labradorite feldspar in the same bed would almost certainly indicate a basic igneous source.

[4] Although the Aycross and Pitchfork formations have approximately the same thickness, present faunal evidence is insufficient to eliminate the possibility that the Pitchfork formation represents only a portion of middle Eocene time —and that the Aycross sediments were deposited more slowly than the Pitchfork, and are more altered for that reason.

REFERENCES

BERRY, E. W., 1930, A flora of Green River age in the Wind River Basin of Wyoming, U. S. Geol. Survey Prof. Paper 165, p. 55–79.

BRAMLETTE, M. N., 1941, The stability of minerals in sandstone: Jour. Sedimentary Petrology, v. 11, p. 32–36.

GOLDICH, S. S., 1938, A study in rock-weathering, Jour. Geology: v. 46, p. 17–58.

HAGUE, A., 1899, Description of the Absaroka Quadrangle: U. S. Geol. Survey G. Atlas, Absaroka Folio, No. 52.

HAY, R. L., 1952, The terminology of fine-grained detrital volcanic rocks: Jour. Sedimentary Petrology, v. 22, p. 119–120.

———, 1954, Structural relationships of tuff-breccia in Absaroka Range, Wyoming: Geol. Soc. America Bull., v. 65, p. 605–620.

———, 1956, Pitchfork formation, detrital facies of early basic breccia, Absaroka Range, Wyoming: Am. Assoc. Petroleum Geologists, Bull., v. 40, p. 1863–1898.

KRYNINE, P. D., 1950, Petrology, stratigraphy, and origin of the Triassic sedimentary rocks of Connecticut: State of Connecticut Geological and Natural History Survey Bull. 73, 274 p.

LARSEN, E. S., and BERMAN, H., 1934, The microscopic determination of the monopaque minerals. U. S. Geol. Surv. Bull. 848, 2d ed., 266 p.

LOVE, J. D., 1939, Geology along the southern margin of the Absaroka Range, Wyoming: Geol. Soc. America Special Paper, no. 20, 134 p.

———, 1950, Petrography as an aid in dating Tertiary volcanic rocks (abstract): Geol. Soc. America Bull., v. 61, p. 1482.

PETTIJOHN, F. J., 1949, Sedimentary rocks. Harper and Bros., New York, 526 p.

ROUSE, J. T., 1937, Genesis and structural relationships of the Absaroka volcanic rocks, Wyoming: Geol. Soc. America Bull., v. 48, p. 1257–1296.

STOW, M. H., 1938, Dating Cretaceous-Eocene tectonic movements in the Big Horn Basin by heavy minerals: Geol. Soc. America Bull., v. 49, p. 731–762.

TOURTELOT, H. A., and THOMPSON, R. M., 1948, Geology of the Boysen area, central Wyoming, U. S. Geol. Survey Map OM 91, Oil and Gas Inv. Ser.

VAN HOUTEN, F. B., 1954, Geology of the Long Creek-Beaver Divide area, Fremont Co., Wyo.: U. S. Geol. Survey Oil and Gas Investigations Map OM 140, 2 sheets.

WALDSCHMIDT, W. A., Cementing materials in sandstones and their probable influence on migration of oil and gas; Am. Assoc. Petroleum Geologists, Bull., v. 25, p. 1839–1879.

WILLIAMS, H., TURNER, F. J., and GILBERT, C. M., 1954, Petrography, an introduction to the study of rocks in thin sections. W. H. Freeman and Co., San Francisco, Calif. 406 p.

JOURNAL OF SEDIMENTARY PETROLOGY, VOL. 27, NO. 1, PP. 41–55
FIGS. 1–8, MARCH, 1957

A FABRIC AND PETROLOGIC STUDY OF THE PLEASANTVIEW SANDSTONE[1]

GENE A. RUSNAK
Scripps Institution of Oceanography, University of California,
La Jolla, California

ABSTRACT

The Pleasantview sandstone is a typical Pennsylvanian cyclothem sandstone in western Illinois exhibiting both channel and non-channel phases. In order to describe the sandstone and to interpret the sediment transport direction and the environmental conditions existing at the time of deposition, an investigation was made of the texture, composition, depositional structure, cross-bedding, and dimensional fabric. Results of this study indicate that the sandstone is a subgraywacke which was deposited in a north and northwest direction. It is concluded that the process which cut the Pleasantview channel was to a large degree independent of the processes which later filled the channel with sediment. No conclusive evidence could be found for the exact nature of the processes operating at the time of channel cutting and filling. However, it is suggested that the environmental conditions of the Pleasantview most closely resemble those conditions existing at present in the Dutch Wadden Sea.

INTRODUCTION

The Pleasantview sandstone occurs in the lower part of the Carbondale between the Colchester (No. 2) and the Springfield (No. 5) coals and represents the basal member of the Summum Cyclothem. This sandstone is typically bluish-gray, fine-grained, micaceous, carbonaceous, and massive to thin-bedded. In the non-channel phase the sandstone is in apparent conformity with the subjacent Purington shale, but in the channel phase the sandstone rests unconformably on the underlying channeled sediments. The thickness of the sandstone ranges from 6–10 feet in the non-channel areas to 100 feet in the deep channels. The stratigraphic section, which includes the Pleasantview, has been previously described in papers by Ekblaw (1930) and Wanless (1931) and is generalized in figure 1.

Although the origin of the cyclothem channels has been ascribed to several possible causes (Wanless, 1950, 1952, 1955; Weller, 1956; Stout, 1931), there has been little work done to determine the direction of current flow within these channels. Ekblaw (1930, 1931) investigated the field relations of the Pleasantview channel system and succeeded in delineating the channel boundaries. From the dendritic pattern obtained, Ekblaw concluded that the currents producing the channels flowed from north to south. The direction of transport of the sandstone fill was not determined at that time, however. The present writer, therefore, attempted to answer the question of transport direction by making a field and petrologic study of the Pleasantview sandstone and channel of Fulton County, Illinois (fig. 2). A secondary objective of this study was the description of the sediment and an attempt at understanding some of the conditions of sedimentation.

[1] Contribution from The Scripps Institution of Oceanography, New Series 907.

GROSS LITHOLOGY

The Pleasantview channel in Fulton County has a width of about $1\frac{1}{4}$ miles and a length of about 22 miles. The depth of this channel and the thickness of the sandstone fill increases from 50 feet at the northern border of Fulton County to 100 feet 22 miles further south where the channel opens out at its mouth. Because the Pleasantview sandstone in the non-channel areas differs from that of the channel areas it is here described separately as "non-channel phase" and "channel phase."

Non-channel phase.—In the non-channel areas the sandstone is fine-grained, bluish-gray, thin-bedded, and contains very little carbonaceous material. This sandstone is in apparent conformity with the underlying Purington shale and exhibits a gradational contact with shale-to-sandstone transition zones ranging in thickness from 6 to 18

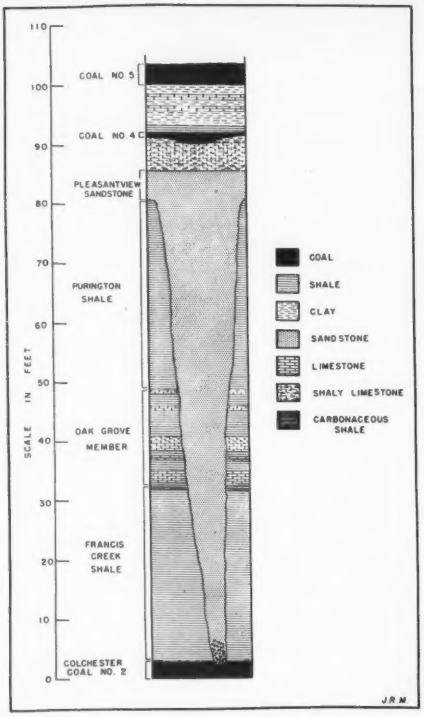

FIG. 1.—Generalized stratigraphic section containing the Pleasantview sandstone (after Ekblaw, 1930 and Wanless, 1931).

inches. Above this contact the sandstone is uniform and evenly bedded. The top of the sandstone is marked by calcareous beds which grade upward into an overlying sandy shale. The total thickness of the non-channel phase ranges from 6 to 10 feet.

Unlike the channel sandstone, the non-channel phase shows some prominent ripple marks. The ripple marks observed by the writer were wave (oscillation) ripple marks rather than current ripple marks. An exceptionally good exposure of these was noted in the NW¼ NE¼ sec. 32, T. 6 N., R. 3 E. of the Havana Quadrangle. The strike of the ripples at this location measured N. 35° E. and thus would indicate a wave oscillation of northwest-southeast. Ekblaw (1930), however, reported current ripples from this same area which indicated a northwest (N. 30° W.) flowing current.

Channel phase.—The Pleasantview sandstone in the channels is also fine-grained, but is very micaceous, and very carbonaceous. The color ranges from bluish-gray to yellowish-gray and locally to black where there is a great abundance of fossil plant material. Although local variations of lithology exist, a generalized description of the channel phase can be made.

The lowermost 15 inches of the sandstone commonly exhibit isolated conglomeratic layers of clay ironstone, limestone, and shale pebbles (long dimensions lying parallel to the bedding planes) which appear to be derived from the underlying sediments. Above this conglomeratic zone is a sandstone, 3 to 5 feet thick, containing many fossil wood fragments carbonized to form coaly streaks. These two basal units are not everywhere present and are often represented only by thin-bedded carbonaceous shales.

The sediments of the next higher zone consist of very thick massive and lenticular sandstones alternating with sandy carbonaceous shales. The bedding planes of this unit are marked by abundant, large mica flakes and plant remains. Although poorly displayed because of inadequate exposures, the massive sandstone commonly contains highly variable cross-bedding. Where cross-bedding was observed, the dip inclinations and dip directions were measured and summarized as in table 1. Normals to these cross-bedding planes are graphically shown in figure 3 and the average dip direction for each sample site is shown in figure 2.

The uppermost 20 feet of the channel sandstone is very shaly and contains much carbonaceous material, thin coaly streaks, and lenses of massive calcareous and stone concretions. This unit grades upward into the shaley and calcareous zone marking the top of the Pleasantview.

Whereas the contacts of the sandstone and the underlying shale appear gradational in the areas far removed from the channels, the contacts at the channel borders are sharp and distinct. Here, the undersurface of the sandstone disclosed markings, resembling minute ripple marks, similar to those described as "groove casts" by Shrock

(1948, p. 163–165) and attributed to subaqueous scour by Rich (1950). These markings are discontinuous and patchy and have an average crest-to-crest width of 6 mm and an average crest height of 2 mm. Groove casts appear to be associated with gentle wall slopes. With steep wall slopes, however, a lobate form of cast is more common (fig. 4). Rich (1950) calls such lobate forms "flow rolls" and describes them also as scour marks. Along the eastern border of the channel, the orientation of both groove and lobe casts is down the channel walls and to the southwest. Hence, if scour formed these marks, the scour was directed down towards the channel from northeast to southwest along the eastern border. This would agree, in general, with the erosion gradient as evidenced by the southward increase in channel depth.

The channel fill has distinctive depositional structures. Along the sides of the channel the sandstone bedding is characteristically parallel to the slope of the channel walls. Thus, the sandstone dips into the channels and is in angular contact with the essentially horizontal underlying channel-cut sediments. In the central portions of the channel, the sandstone beds assume a horizontal attitude. Hence, there is a strong suggestion that this channel was filled from outside the channel rather than by aggradation within channel flowing streams. The channel-flanking sandstone beds are not peculiar to

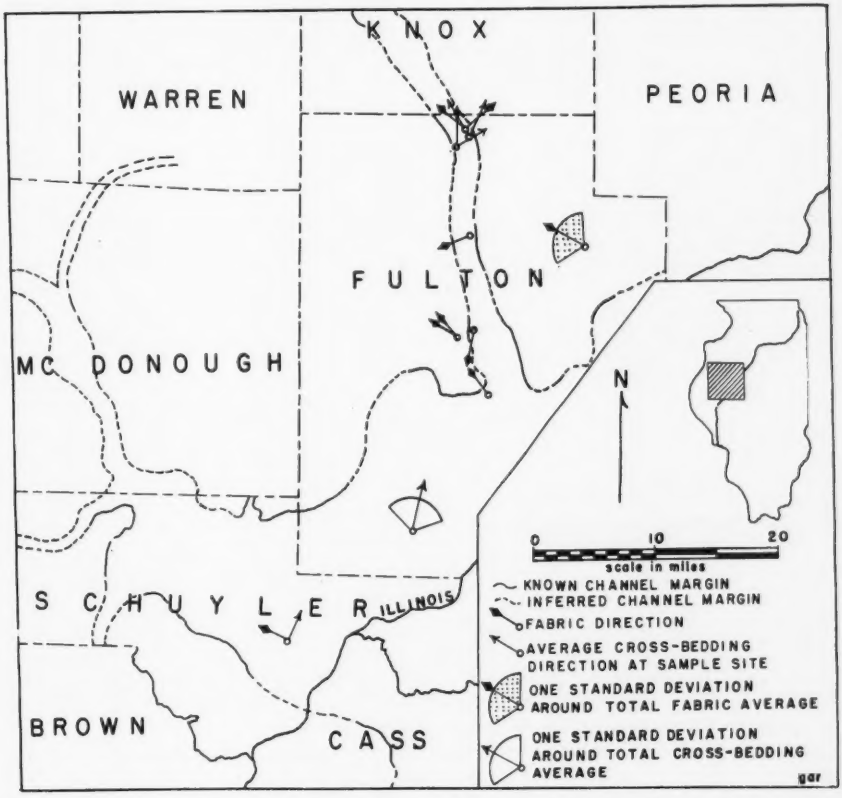

FIG. 2.—Distribution of samples of fabric and cross-bedding directions (Channels after Ekblaw, 1930).

TABLE 1.—*Observed cross-bedding dip direction and inclination*

Location	Direction	Inclination
SE ¼ NW ¼ sec. 31, T. 2 N., R. 1 E. Schuyler County	1	12
	45	10
	69	22
	70	15
	78	8
	96	28
	110	6
	280	12
	285	13
	335	19
	352	26
	355	5
	357	25
NE ¼ SW ¼ sec. 17, T. 8 N., R. 3 E. Fulton County	5	25
	325	22
	340	15
	340	28
SW ¼ NE ¼ sec. 19, T. 8 N., R. 3 E. Fulton County	15	22
	130	17
	331	4
SW ¼ NE ¼ sec. 20, T. 8 N., R. 3 E. Fulton County	40	22

this single channel but have been reported from other Pleasantview channels by Ekblaw (1930, 1931). More recently, van Straaten (1951, 1952) has described similar relations from the sediments in the tidal-cut channels of the Dutch Wadden Sea and makes a distinction between vertical sedimentation (resulting in horizontal beds) and lateral sedimentation (resulting in inclined beds). Although the Dutch Wadden Sea area has this and other similarities to the Pleasantview, differences do exist. Further discussion of the differences and parallels between these two areas is made in the concluding section of this paper.

Near the western margin of the channel in the SW ¼, NE¼, SW ¼ sec. 19, T. 8 N., R. 3 E., Canton Quadrangle, three contorted and disconnected sandstone lenses are imbedded in what is apparently reworked Purington shale (fig. 5). These lenses lie one foot below the gradational contact of the channel sand and the shale. The internal structure of these lenses resembles nappe structure (fig. 6), with overturning and crumpling, and the streamline shape of the lens outlines suggests the lenses were lodged into the enclosing shale *en masse* and in a semifluid state as a sand slide or flow. The horizontal bedding of the surrounding shale does not appear to be disturbed in any way that would suggest mass slumping. Therefore, it might be concluded that, here at least, the shale must have been a very fluid mud at the time the lenses were incorporated. The direction of lens implacement appears to be to the south and may indicate that when the unstable sands started to flow they followed the local gradient of the channel. Other indications of unstable sediments are also present.

Within the shaly members of the channel fill in the NW ¼ SE ¼ sec. 19, T. 8 N., R. 3 E., Canton Quadrangle, two small "slump" folds were observed. One of these folds was noted near the base of the channel and the other was observed near the top of the channel. Neither of these slump folds exceeds 6 feet from limb-to-limb and 3 feet from base to crest (fig. 7). The asymmetry of the folds indicates that the fold at the base of the channel slumped toward the west and the fold near the top of the channel slumped toward the south. Although this deformation might have occurred at a much later time (possibly during Pleistocene glaciation), the horizontal beds above and below the folds show no apparent disturbance and hence strongly indicate that the folds are contemporaneous with the deposit.

Good exposures of the Pleasantview are rather limited because of overburden and strip mining activity. However, a complete cross-section of this Pleasantview channel, showing all the previously mentioned salient features, can be seen in a series of outcrops along Coal Creek in the Canton Quadrangle near the northern border of Fulton County.

METHODS

Because the study was made primarily to determine the direction of sediment transport, the sampling was made for the most part from the channel sandstone deposits. Samples were collected both vertically and laterally along the channel in an effort to evaluate possible textural and compositional variations. Moreover, several areas were sampled which were not bounded by the channel in order to assess variations outside the channel proper. In all, a total of 37 hand specimens was collected for study. Macroscopic examination of these hand specimens

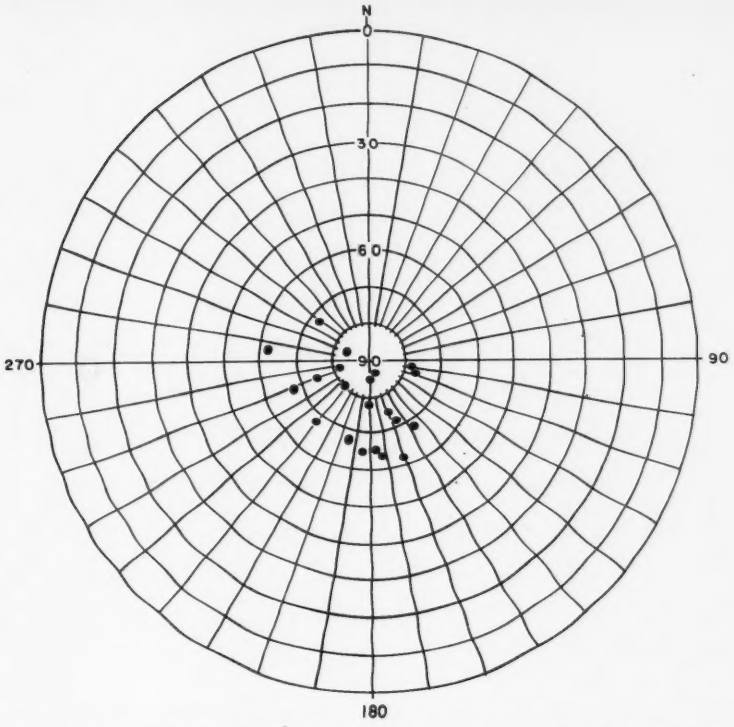

FIG. 3.—Directions of normals to the cross-bedding. Predominant direction to the north. Plotted on the lower hemisphere.

did not reveal any apparent variation in sandstone texture. Hence, to save time in the analyses, only a small number of representative samples was selected for complete textural and compositional study.

At the time of collection, all hand specimens were marked with their orientation in the field. These oriented samples enabled the writer to obtain oriented thin sections cut normal and parallel to the bedding planes. Thin sections cut normal to the bedding were used specifically for microscope and integrating stage analysis of the mineralogical composition (Krumbein and Pettijohn, 1938). The thin sections cut parallel to the bedding were used only for "dimensional fabric" study and a full discussion of this method of analysis is given later in this paper.

The samples selected for size analysis were disaggregated by crushing and then dispersed in a solution of N/100 sodium oxalate. After dispersion, the size fractions greater than 1/16 mm were sieved and the finer material was run through pipette analysis. A small fraction of the clay-sized material was set aside and later run through X-ray analysis by the writer for identification of the minerals constituents.

Heavy minerals were identified from the $\frac{1}{8}$-to-1/16 mm-size fractions and counted until the total mineral count included at least 250 non-opaque grains per sample. Apatite was excluded from this analysis because it is believed that the rigorous method of clarification by boiling in dilute HCl tended to destroy this mineral much more rapidly than any others. Barite, although present, is not considered valid for correlation purposes (because it may be authigenic)

FIG. 4.—Flow rolls occurring at the base of the Pleasantview sandstone on the steep slopes of the channel wall.

and was also excluded. In the final results, all mineral species were expressed as percent of the total heavy-mineral count.

COMPOSITION AND TEXTURE

The results of the analyses of composition and texture, shown in table 2 and figure 8, clearly indicate that the Pleasantview sandstone is a subgraywacke. The dominant detrital components are quartz, rock fragments, and the fine-grained matrix of silt and clay. Feldspar and mica are present in minor amounts only. Texturally the Pleasantview sandstone is uniform and well sorted, with about 70 percent of the material in the very-fine sand size. The uniformity of the size frequency distributions of the several samples analyzed is demonstrated by the range between cumulative curves of figure 8.

In thin sections the detrital quartz grains commonly exhibit euhedral overgrowths of secondary or authigenic quartz. Where the original grain boundaries could be distinguished from these overgrowths by dusty inclusions, the detrital quartz roundness could be estimated by the visual roundness chart of Krumbein (1941). Average roundness was 0.3 with a range from 0.1 to 0.5. Feldspar showed a slightly higher roundness with an average of 0.5.

Very minor constituents of the sandstone are glauconite and the heavy minerals. Glauconite, in amounts less than one percent, was noted in nearly all thin sections. However, because the mineral is only found in these very small quantities, no particular significance is attached to its presence, although it might indicate marine conditions if it is not reworked material.

The heavy minerals of the Pleasantview consist mostly of opaques and the very stable non-opaques. The opaques are represented by leucoxene 31%, black opaques (ilmenite-magnetite) 3% and pyrite 5%. The non-opaque minerals include 41% zir-

con, 7% rutile, 6% garnet, 4% tourmaline, 2% chlorite, and less than 1% sphene.

The sandstone matrix material consists of clay and silt sized mineral grains, carbonate, and secondary silica cement. The clay sized minerals were identified by X-ray and consist of illite, kaolinite, quartz, chlorite, and sericite in order of decreasing abundance. The carbonates of the matrix consist of siderite and calcite. Siderite is apparently the dominant carbonate in the lower and middle members of the sandstone and calcite is the dominant carbonate in the upper members. It is of interest to note that when calcite makes up a high percentage of the constituents, as in sample A-16 of Table 2, the sandstone has the appearance of a "washed" graywacke; i.e., a graywacke which appears to have the fine-grained matrix winnowed out. However, the extensive replacement of detrital constituents by the calcite cement might indicate that the "washing" was accomplished, wholly or in part, by the replacement of the finer materials.

The order of cementation in the Pleasantview is evidenced by the calcite-filled pore spaces where calcite has partially replaced some of the detritals and is itself replaced by euhedral rhombes of siderite. Both calcite and siderite are subsequently replaced by euhedral overgrowths of secondary quartz on the detrital quartz grains. Hence, it is apparent that the initial binding agent was silt and clay and was followed, in turn, by calcite, siderite, and silica cements.

DIMENSIONAL FABRIC

The use of dimensional fabric analysis in sedimentary petrology is relatively new and until recently has been primarily concerned with pebble orientation. Dapples and Rominger (1945), however, made an experimental study of the orientation of inequidimensional sand-size particles and have

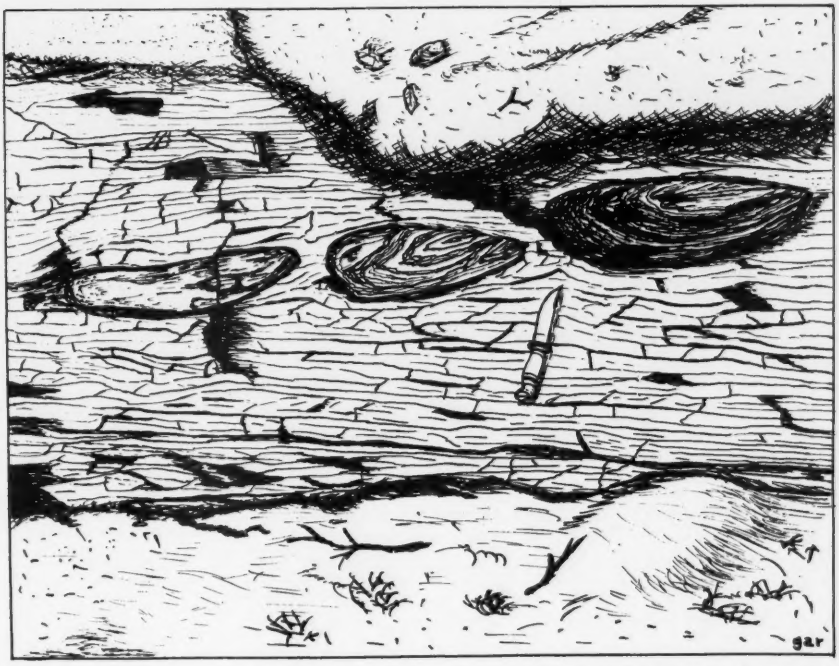

FIG. 5.—Highly contorted sandstone lenses emplaced in reworked Purington shale. The base of the Pleasantview sandstone is visible in the upper left hand corner. Drawn to scale from a photograph. The outcrop is sloping towards the reader.

FIG. 6.—Cross-section of a sandstone lense cut to show the internal structure. The angle of the sandstone lense approximates the angle of emplacement in the field. The blunt end points to the south. A six inch rule is used for scale.

shown that the long axes tend to align themselves parallel to the direction of flow of the transporting medium. These authors made several statistical studies of water, wind, and gravitational-influenced orientation and demonstrated that preferred orientation is best developed in water transport. Moreover, Dapples and Rominger found that those sand grains having a "tear-drop" shape tended to orient themselves with the blunt end upstream and into the current. Hence, the results of their experimental study indicated that the mean value of the long-axis orientation distribution gave a preferred azimuth orientation parallel to the current and the pointed ends of the "tear-drop" shapes gave the direction of flow along this resultant azimuth.

More recently, Schwarzacher (1951) also investigated the existence of sand-grain orientation under experimental conditions and concluded that the long axes aligned themselves parallel to the current just as Dapples and Rominger had previously described. The significant finding of Schwarzacher's experiments, however, was that the sand grains displayed imbrication in the same way that pebbles do in a stream bed. As a supplement to the experimental study, an example of both long-axis preferred orientation and imbrication was demonstrated by Schwarzacher in his analysis of a sandstone sample.

These earlier studies of sand-grain orientation thus demonstrated the possible applicability of sand-grain fabrics for determining transport directions in sandstones. With this purpose in mind, the present writer applied the above methods of analysis to determine the transport direction in the Pleasantview sandstone.

Methods of grain orientation analysis.—Thin sections cut parallel to the bedding planes were used for the analysis of dimensional orientation. These thin sections were placed in a microprojector and the sand-grain images were projected onto a sheet of cross-section paper.[2] The long axes of the least projection rectangles and the pointed ends of the tear-drop shapes were then determined from the grain images.[3] Tear-drop shaped grains were drawn as arrows indicating the direction of the pointed ends and

[2] Polaroids inserted into the microprojector helped to distinguish grain boundaries and greatly expedited the analysis.

[3] A full treatment of this method of drawing long axes and pointed ends has been previously described by Dapples and Rominger (1945). The long axis of the least projection rectangle has been defined by them as the axis which lies parallel to the two parallel lines which can be drawn tangent to a grain with a minimum of separation.

acicular or lath-shaped grains, which did not have a tear-drop shape, were drawn simply as direction lines. By plotting all the quartz grains projected (with the obvious exception of equidimensional grains), bias in the analysis was kept at a minimum; i.e., no particular grain shapes were given undue weight. After 300 or more grains were plotted in this manner, the directions of the long axes were measured and counted on a tally sheet arranged in 20° group intervals from 0° to 360°. A statistical test based on Chi-square and vector summation was then applied to each distribution to obtain the direction of preferred orientation (Tukey, 1954; see also the appendix at the end of this paper).

The statistical test of orientation was performed on a 180° distribution by placing all diametrically opposed long axes in the same group interval from 0° to 180°. The test was then carried out and a preferred-direction line of orientation determined, if one existed. In some cases the sample distribution proved to be insufficiently different from a uniform distribution (i.e., a distribution with an equal number of observations in each group interval) and had to be discarded. During the test, the acceptance level of orientation was arbitrarily chosen at the 90th percentile of significance (i.e., there is a chance of being wrong 10 percent of the time).

After a preferred-direction line of orientation (or azimuth) was determined for a sample, the number of grains pointing in the two opposite directions of this line was counted for the entire sample. If 60 percent or more of the grains pointed in one direction of the preferred line, this direction was chosen as the direction of transport (Dapples and Rominger, 1945). In one case, it was found that the number of grains pointing in either direction was about equal and therefore transport direction was not defined by this criterion. To overcome this difficulty the

FIG. 7.—Small scale slump anticline in the shaly member of the Pleasantview. Knife is used for scale.

TABLE 2.—*Mineralogical composition of the Pleasantview sandstone*

	Components	Specimen Number[1]									
		A17	A16	A18	A14	A15	A25	A12	A22	A51	A10
Detrital	Quartz										
	strain-free	25.3	21.0	33.4	18.3	25.5	33.2	24.3	28.1	28.5	20.0
	strained	15.7	9.0	16.7	11.7	21.0	13.8	19.2	17.2	10.5	18.0
	Rock Fragments										
	quartzite	7.0	4.7	5.3	4.3	9.5	8.2	4.8	7.6	4.0	6.0
	chert	3.0	2.8	4.3	3.5	4.5	4.3	2.3	1.0	3.2	3.0
	argillite	0.7	1.3	3.6	3.2	5.3	6.0	1.9	7.1	3.3	1.0
	phyllite	0.6	0.3	3.0	1.3	6.2	6.0	2.6	2.9	1.0	1.9
	Feldspar										
	Na-feldspar	1.0	1.6	2.3	1.5	2.0	2.3	1.3	4.7	2.2	2.1
	K-feldspar	1.2	1.0	2.3	1.5	1.5	1.7	1.0	1.9	2.0	1.9
	Mica	1.8	1.9	4.7	4.7	2.0	5.0	5.2	6.2	3.5	5.3
Secondary or Interstitial	Carbonates										
	siderite	4.0	6.2	3.7	22.0	3.5	2.3	3.6	8.0	11.3	7.0
	calcite	13.0	42.2	0.0	0.0	0.0	1.0	4.5	0.0	1.0	2.1
	Quartz	5.3	0.7	3.0	2.2	2.1	2.4	3.6	1.0	2.7	1.0
	Clay-Silt	21.4	7.3	17.7	25.8	16.9	13.8	25.7	14.3	26.8	30.9

[1] *Sample Location:* A17, middle non-channel; A16, upper non-channel; A18, basal channel; A14, A15, A25, lower channel; A12, A22, A51, middle channel; A10, upper channel.

writer cut a thin section perpendicular to the bedding plane and parallel to the preferred direction line. A plot of grains from this section was then made to determine whether imbrication, such as that found by Schwarzacher, existed. The results of this plot demonstrated that the sand grains were imbricated. The direction of imbrication was then chosen as the direction of transport for the sample. It thus appears that imbrication direction may be a more reliable method of determining transport direction along an azimuth than are pointed ends.[4]

Results of transport direction analyses.—Eleven samples, taken from channel and non-channel areas, were analyzed for dimensional orientation direction. Of these, 9 proved to be statistically significant with a definite preferred orientation. The resultant directions of the significantly oriented samples have been indicated by the arrows in figure 2. The preferred directions, from one sample to another, appear to be as variable as the cross-bedding directions.

The vector mean direction (Krumbein, 1939) of the 6 samples analyzed from within the channel is 320°; and, for the 2 samples from the non-channel area is 310°. The one sample analysis from Schuyler County has a preferred orientation of 318°. Thus, it would appear that the transport direction of the sediment was to the northwest.

Cross-bedding, on the other hand, shows a vector mean direction (from 8 measures) of 0° for the channel in Fulton County and a direction of 24° (from 13 measures) for Schuyler County. These results would indicate a transport direction to the north; a difference in direction of about 60° from that obtained by grain orientation study. Although it is hazardous to speculate on such a small number of direction measures, one might consider the possibility that two factors influenced the transportation of the sediment. That is, the grain fabric of the uncross-bedded members might represent weak currents such as coastal currents and cross-bedding might represent stronger currents such as tidal currents.

Speculations might also be made for

[4] Experimental work carried out by the writer after this study was completed substantiated the criteria of imbricate and long-axis direction as the direction of transport. The data on the reliability of these measures will soon be ready for publication.

fluvial transport conditions, but it would be difficult to explain the observations since the direction of transport exhibited by both fabric and cross-bedding is diametrically opposed to the apparent erosion gradient of the channel (as previously discussed). For example, grouping of both fabric and cross-bedding directions (a total of 30 direction elements) results in a vector mean direction of 357° with a standard deviation of ±67°. That is, the sediment transport direction indicates the sediment was deposited towards the north whereas the channel gradient indicates that the channel was cut to the south. It seems, therefore, that the process of channel filling was to a large degree independent of the process or processes which cut the channel.

COMPARISON WITH THE DUTCH WADDEN SEA

The Dutch Wadden Sea is an area of broad tidal flats incised by channels of tidal current origin (van Veen, 1950, van Straaten, 1949). The tidal channels are bordered by areas of relatively continuous sedimentation of tidal sands, plant material, and marine organisms (van Straaten, 1952) and the channels themselves are presently being filled with sands swept in from the tidal flats and the North Sea. The result of this sedimentation is described by van Straaten (1951) as vertical sedimentation (resulting in horizontal beds on the tidal flats) and lateral sedimentation (resulting in inclined beds flanking the channel walls). Although the deposits in the channels are mainly sand, thick deposits of mud are also present (van Straaten, 1952). Some of the characteristic features of the channel deposits are the occurrences of slump structures, cross-bedding, and local basal conglomerates (derived from the eroded walls, mainly shells, van Straaten, 1950b, 1951). The cross-bedding (van Straaten, 1950a) may be directed up channel in areas subjected mainly to flood tides and may be directed down channel in those areas dominated by ebb tides (both kinds can also be present in one channel).

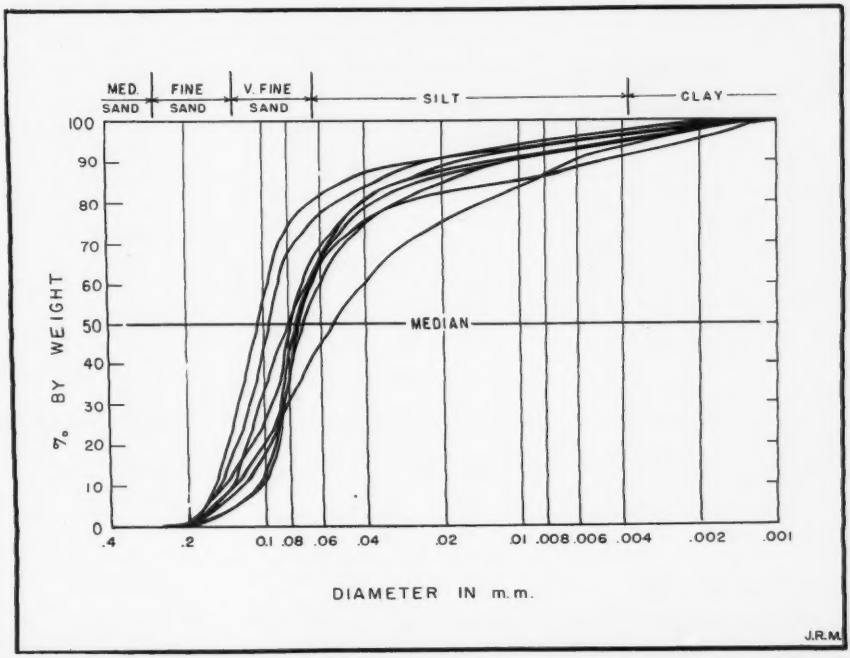

FIG. 8.—Cumulative size frequency distributions of 8 selected Pleasantview sandstone samples.

With the exception of marine organisms all of the examples above, or modifications thereof, are present in the sediments of the Pleasantview. Hence, the environment of the present Wadden Sea is believed to be very near the possible, if not probable, kind of environment which existed during Pleasantview sedimentation.

SUMMARY AND CONCLUSIONS

The study of the Pleasantview sandstone, and the channel which it fills in Fulton County, Illinois, was undertaken in order to describe (1) some of the properties of the sandstone, (2) its depositional transport direction, and (3) the environmental conditions under which it was deposited. It is felt by the writer that the first two objectives of this study have been fulfilled, but the answer to the third is still somewhat tenuous.

The results of the analyses of texture and composition place the Pleasantview sandstone in the subgraywacke classification of Pettijohn (1949). The quartz, rock fragments, and heavy-mineral varieties indicate that the source area of this sediment was made up of a series of rock types ranging from igneous to high and low metamorphics and to pre-existing sediments. Quartz varieties show that igneous and metamorphic rocks (the ultimate source) contributed almost equally to the sediment. However, the fact that only chert, the very stable heavy minerals, and a small amount of feldspar is present indicates that the detritus is of high maturity (Pettijohn, 1949); i.e., the detritus has gone through several cycles of sedimentation. It seems reasonable, therefore, to conclude that the Pleasantview sandstone was largely derived from pre-existing sediments. This conclusion is in agreement with the recent studies made by Siever and Potter (1956) of Pennsylvanian sediments in the Eastern Interior Basin.

The field relations suggest that the Pleasantview can be conveniently described as two-phased; the non-channel phase, and the channel phase. The non-channel phase is thin-bedded, ripple marked, and in apparent conformity with the underlying shales, while the channel phase is massive to thin-bedded, cross-bedded, shaly, and is unconformable with the underlying beds in the channel. Along the channel borders, the sandstone dips into the channel, but in the central portion of the channel the sandstone is essentially horizontal. These relationships, along with the evidences of slump structures and scour markings, are considered by the writer as indications that the Pleasantview sandstone was deposited when both the channel and non-channel areas were submerged. The non-channel areas represent conditions of relatively continuous sedimentation and the channels represent areas of contemporaneous erosion and later filling.

Directional properties which could be measured in the Pleasantview include the following: (1) channel gradient, (2) scour marks, (3) slump and slide structures, (4) ripple marks, (5) cross-bedding, and (6) preferred orientation of sand grains. The results of these measures can best be summarized by a short table as in table 3.

The first three directional properties of table 3 are related to the erosional gradient and reflect the local gradient direction. The last three directional properties reflect the sediment transport direction. From the table, it seems that the directed process which cut the channel was independent of the processes which later filled the channel with sediment because the resultant directions are diametrically opposed. In the writer's opinion the observations can best be explained by considering the channel first to have been cut by tidal current action and later to have been filled with sediments through the action of both coastal (longshore) and tidal currents. Examples from the Dutch Wadden Sea demonstrate that this suggestion is not unreasonable.

ACKNOWLEDGEMENTS

The writer wishes to express his appreciation to Dr. F. J. Pettijohn for his many thoughtful and stimulating comments and advice. Thanks are extended to Dr. H. R. Wanless for his generous and invaluable aid in pointing out many critical sample sites and for his critical discussions of the problem with the writer. Acknowledgements are also due Drs. J. M. Weller, H. A. Lowenstam, Leland Horberg, P. E. Potter, R. Siever, R. L. Miller, F. P. Shepard, and Mr. P. W. Vitanage and Mr. J. R. Curray for the helpful comments, criticisms, and suggestions. Mr. J. R. Moriarty's help in preparing several of the illustrations is also appreciated. Thanks are also extended to

TABLE 3.—*Results of directional-properties measures*

Measure	Resultant Direction	Kind and Number of Measurements
Channel Gradient	South	Increasing depth of channel and thickness of channel fill
Scour marks	Down the channel wall and south	2 outcrops (qualitative orientation of casts)
Slump and slide structures	South (?)	3 structures (direction of asymmetry)
Ripple marks	Northwest-Southeast and Northwest	1 outcrop and 1 reported measure from Ekblaw (1930) (strike and asymmetry)
Cross-bedding	North	21 (foreset dip directions)
Sand grain orientation	Northwest	9 (preferred long-axis directions)

Dr. John W. Tukey for permission to publish a summary of the statistical test of significance of orientation which he designed. The writer takes sole responsibility for any mistakes or omissions in the paper and in the opinions set forth. The major part of this paper represents work carried out by the writer in the spring of 1952 while at the University of Chicago.

APPENDIX

The Tukey (1954) Chi-square test of significance for orientation data from a 180° distribution is based on the departures of the observed data from a distribution which is completely uniform; i.e., from a distribution having an equal number of observations in each class interval.[5] If the distribution were completely uniform, the expected number of observations in each class interval would be the total number of observations divided by the number of class intervals. This expected number in each class interval has been called the "contemplated" by Tukey. The measure of deviations from an expected uniform distribution is given by the following:

$$x = \frac{\text{observed} - \text{contemplated}}{\sqrt{\text{contemplated}}}$$

where x is the frequency deviation measure in each class interval. Vector summation over all class intervals results in the following:

$$C = \frac{\sum x \cos 2\theta}{\sqrt{\sum \cos^2 2\theta}} \quad \text{and} \quad S = \frac{\sum x \sin 2\theta}{\sqrt{\sum \sin^2 2\theta}}$$

where θ is the mid-point of each class interval and the resultant squared is given by $C^2 + S^2 = \chi^2$. This value of Chi-square, χ^2, is then compared with the tables given in standard statistics books for two degrees of freedom. If there is significant departure from uniformity at a chosen level of significance, the preferred direction of orientation is derived from the relation

$$\tan 2\theta = \frac{S}{C}.$$

Where θ plus the mid-point value of the first class interval is then the preferred orientation direction.

Example—Using the data from one of the orientation analyses (grouped in 20° intervals from 0° to 180°); where N, the total number of observations is 590 or contemplated is $590/9 = 65.6$; and, in tabular form we have the following:

Class Interval in Degrees	θ	Observed	Observed-Contemplated	x	cos 2θ	sin 2θ
0–20	0	60	−5.6	−0.69	1.00	.00
20–40	20	60	−5.6	−0.69	.75	.64
40–60	40	90	24.4	3.01	.17	.98
60–80	60	74	8.4	1.04	−.50	.87
80–100	80	71	5.4	0.67	−.94	.34
100–120	100	60	−5.6	−0.69	−.94	−.34
120–140	120	64	−1.6	−0.20	−.50	−.87
140–160	140	60	−5.6	−0.69	.17	−.98
160–180	160	51	−14.6	−1.80	.76	−.64

[5] As has been pointed out to the writer by Dr. H. J. Pincus (personal communication), "uniform" and "random" are not synonymous.

From this table we can obtain the values of C and S by following the previously outlined procedure.

$$C=-1.22 \qquad S=2.78$$

Squaring these values and adding we have the resultant squared which is, in our case equal to the Chi-square value of 9.21. Referring to the Chi-square tables in Dixon and Massey (1951, p. 308) for 2 degrees of freedom at the 90th percentile of significance we find that our value is well above the tabled value 4.61. Therefore, we conclude that there is sufficient evidence our population did not arise from a uniform distribution; i.e., the distribution is not isotropic.

To determine the preferred direction of orientation we have simply to determine

$$\tan 2\theta=\frac{S}{C}=-2.28$$

and distinguish between the two roots by the requirement that the signs of S and C be those of sin 2θ and cos 2θ respectively, from which we obtain the preferred angle

$$\theta=\frac{180°-67°}{2}=57°.$$

However, since θ is the mid-point of our class interval, we have 10° for the mid-point of our first observed interval. Hence, we have to add this to our preferred angle with the result that the preferred direction of orientation for our distribution is 67°. Because we did not make a distinction between diametrically opposed directions, the preferred direction could also be 247°. As it turns out, the sand grains are imbricated to the northeast in this sample and therefore we choose 247° as the vector direction; i.e., the direction of sand transport.

REFERENCES

DAPPLES, E. C., AND ROMINGER, J. F., 1945, Orientation analysis of fine-grained clastic sediments: Jour. Geology, v. 53, p. 246–261.

DIXON, W. J., AND MASSEY, F. J., 1951, Introduction to statistical analysis. McGraw-Hill Book Co., New York, 370 p.

EKBLAW, S. E., 1930, The stratigraphic relations of the Pleasantview Sandstone in western Illinois: Unpublished Master's Thesis, University of Illinois.

———, 1931, Channel deposits of the Pleasantview Sandstone in western Illinois: Illinois Acad. Sci. Trans. 23, p. 391–399.

KRUMBEIN, W. C., 1939, Preferred orientation of pebbles in sedimentary deposits: Jour. Geology, v. 47, p. 673–706.

———, 1941, Measurement and geological significance of shape and roundness of sedimentary particles: Jour. Sedimentary Petrology, v. 11, p. 64–72.

KRUMBEIN, W. C., AND PETTIJOHN, F. J., 1938, Manual of sedimentary petrography, Appleton-Century, New York, 549 p.

PETTIJOHN, F. J., 1949, Sedimentary rocks. Harper and Brothers, New York, 526 p.

RICH, J. L., 1950, Flow marking, grooving, and intra-stratal crumpling as criteria for recognition of slope deposits, with illustrations from Silurian rocks of Wales: Am. Assoc. Petroleum Geologists Bull., v. 34, p. 717–641.

SCHWARZACHER, W., 1951, Grain orientation in sands and sandstones: Jour. Sedimentary Petrology, v. 21, p. 162–172.

SHROCK, R. R., 1948, Sequence in layered rocks. McGraw-Hill Book Co., New York, 507 p.

SIEVER, R., AND POTTER, E., 1956, Sources of basal Pennsylvanian sediments in the Eastern Interior Basin: part 2, sedimentary petrology: Jour. Geology, v. 64, p. 317–335.

STOUT, E., 1931, Pennsylvanian cycles in Ohio: Illinois Geol. Survey Bull., v. 60, p. 195–216.

STRAATEN, L. M. J. U. VAN, 1949, Quelques particularités du relief sous-marin de la Mer des Wadden (Hollande): Comptes Rendus du Congrès de Sedimentation et Quaternaire in France, p. 139–145.

———, 1950a, Giant ripples in tidal channels: Tidjschr. Kon. Nederl. Aardr. Gen., v. 67, p. 76–81.

———, 1950b, Environment of formation and facies of the Wadden Sea sediments. Tijdschr. Kon. Nederl. Aardr. Gen., v. 67, p. 94–108.

———, 1951, Texture and genesis of Dutch Wadden Sea sediments: Proc. 3rd Int. Congress Sedimentology Netherlands, 5–12, July, 1951, p. 225–244.

———, 1952, Biogene textures and the formation of shell beds in the Dutch Wadden Sea: Konikl Nederl. Akademie van Wetenschappen, Amsterdam, Series B, v. 55, p. 500–516.

TUKEY, J. W., 1954, Chi-square test of orientation, comment no. 1A, Earth Sciences Panel Review Group, CSPS—ASA, unpublished communication.

VEEN, J. VAN, 1950, Eb-en vloedshaar-systemen in de Nederlandse getijwateren (with an English summary): Tijdschr. Kon. Nederl. Aardr. Gen., v. 67, p. 43–65.

WANLESS, H. R., 1931, Pennsylvanian cycles in western Illinois: Illinois Geol. Survey Bull., v. 60, p. 179–193.

———, 1950, Late Paleozoic cycles of sedimentation in the United States: International Geological Congress "Report of the Eighteenth Session, Great Britain 1948," part IV, p. 17–28.

———, 1952, Studies of field relations of coal beds: Nova Scotia Research Foundation, Second Conference on the Origin and Constitution of Coal, p. 148–175.

———, 1955, Pennsylvanian rocks of Eastern Interior Basin. Am. Assoc. Petroleum Geologists Bull.. v. 39, p. 1753–1820.

WELLER, J. M., 1956, Diastrophic control of late Paleozoic cyclothems: Am. Assoc. Petroleum Geologists Bull., v. 40, p. 17–50.

JOURNAL OF SEDIMENTARY PETROLOGY, VOL. 27, NO. 1, PP. 56–63
FIGS. 1–3, MARCH, 1957

MINERALOGY OF SOME PENNSYLVANIAN CARBONATE ROCKS OF ILLINOIS[1]

RAYMOND SIEVER AND HERBERT D. GLASS
Illinois Geological Survey, Urbana, Illinois

ABSTRACT

The results of a reconnaissance study of 58 samples of Pennsylvanian carbonate beds, collected over a wide range of areas within the state and the whole stratigraphic section, reveal that significant quantities of ferroan-dolomite are present. Methods of analysis were: (1) X-ray diffraction patterns for estimation of relative abundance of calcite and dolomite structures, (2) differential thermal analysis for identification of ferroan-dolomite, and (3) thin section petrology for characterization of textures and relationships between carbonate minerals in the rocks. Some representatives of all limestone beds below the Trivoli limestone (mid-McLeansboro group) contain ferroan-dolomite; higher limestones are almost completely calcitic. The limestones in the lower part of the McLeansboro group, particularly the Bankston Fork, consistently show some high ferroan-dolomite percentages. There is no apparent correlation of dolomite content with basin or shelf occurrence, or surficial weathering. Study of thin sections shows that dolomite rhombs are secondary and are most abundant in association with certain rock textures. Suggestions are made for further study on problems of mineralogy and genesis of limestone and dolomite beds.

INTRODUCTION

This paper presents the results of a reconnaissance study of the carbonate mineralogy of some of the limestone beds of the Pennsylvanian system in Illinois. The study was undertaken to see if there is any readily apparent relationship of carbonate mineralogy to age, stratigraphic occurrence, or texture. The study also adds to the store of basic chemical and mineralogical data that are essential to understanding the origin of the carbonate rocks.

Most published descriptions of Pennsylvanian limestones in the Eastern Interior Basin include only gross details; generally most descriptive effort has been put into categorizing large-scale textural and bedding features, with little emphasis on mineralogical composition or microscopic textures. This is understandable because it is difficult to differentiate in the field the various species of the complex mineralogical group of carbonates. Some chemical analyses of carbonate rocks of Illinois are available (Krey and Lamar, 1925, p. 311–33; Lamar and Thompson, 1956, p. 7–15), but the use of such analyses is limited by a general lack of published data on mineralogical composition. For these reasons we concentrated on relatively rapid laboratory methods that gave usable semiquantitative results: X-ray diffraction, differential thermal analysis (DTA), and, for comparison of optical determinations with DTA and X-ray results, thin-section petrology.

[1] Published by permission of the Chief, Illinois State Geological Survey.

SAMPLING AND MINERALOGICAL DETERMINATION

Because this study is a brief survey, no attempt was made to systematically sample all Pennsylvanian carbonate beds in all areas of the state. Rather, the attempt was made to get "representative" samples of a number of beds in various stratigraphic positions and of some common gross lithologies. The majority of the 58 samples analyzed are of limestone beds in the upper part of the Carbondale group and the lower part of the McLeansboro group, that part of the Pennsylvanian section which contains many of the stratigraphically important limestones (fig. 1). Only stratigraphic units of some lateral extent were included. Not included were the mineralogies of concretions, nodules, or the numerous other forms of carbonate in the rocks. Samples come from both outcrop sections and subsurface diamond drill cores. The choice between outcrop and core samples was largely determined by availability, although both types of samples were collected for some of

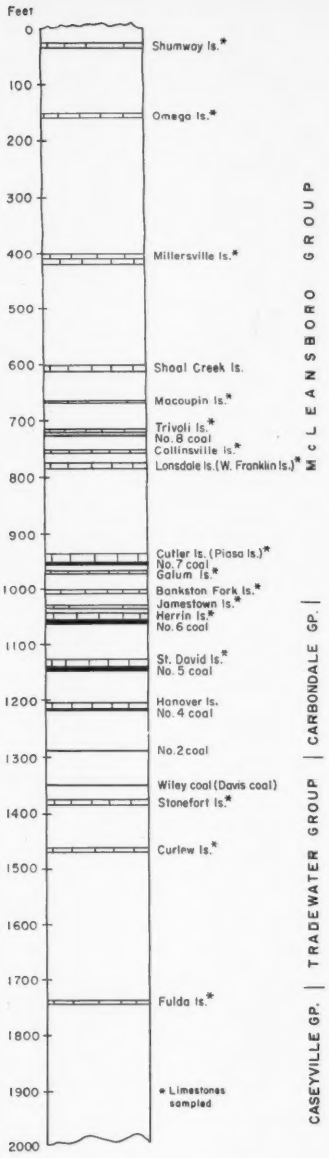

FIG. 1.—Generalized section of Pennsylvanian strata in Illinois showing limestone beds sampled.

the beds. Because of the character of the sampling, the results cannot be easily treated by statistical methods, nor can our results be taken as completely representative of all Pennsylvanian carbonate rocks.

In this investigation, DTA was used for identification of carbonate minerals (see Beck, 1950; Kulp, Kent, and Kerr, 1951; Graf, 1952). Typical curves for some common carbonates are shown in figure 2. Characteristic for calcite is the single endothermic peak at about 960° C. Dolomite (low-iron) can be recognized by two endothermic peaks; the lower temperature peak, at about 780° C is about two-thirds of the amplitude of the higher temperature peak, which is at about the same temperature as the single peak of calcite. Only one sample contained this type of low-iron dolomite; all the others contained mixtures of calcite and ferroan-dolomite.

Ferroan-dolomite[2] can be identified by a sharp, narrow endothermic peak at about 780° C, immediately followed at a slightly higher temperature by a narrow exothermic peak; this is followed by a short broad endothermic peak at about 790–810° C, succeeded in turn by the large endothermic peak at about 930° C. In ferroan-dolomite free of calcite, the 930° peak is lesser in amplitude than the 780° peak. DTA curves that show greater amplitude and higher temperature of the 930° peak indicate mixtures of calcite and ferroan-dolomite (fig. 3). The DTA curve was used for identification of ferroan-dolomite but not for estimation of the amount of Fe substituted for Mg. Probably the lower threshold of the amount of Fe substituted for Mg needed to produce the ferroan-dolomite type of DTA curve described above is $2\frac{1}{2}$ mole percent.

X-ray diffraction patterns were run on all of the samples as a check on identification from DTA curves, particularly for calcite-

[2] There is no general agreement on the compositional variation and terminology of the iron-rich dolomites. We use the general term ferroan-dolomite to include all those iron-rich carbonates that have the same crystal structure as dolomite, aside from any slight changes in the lattice parameters resulting from the substitution of varying amounts of Fe for Mg. For a brief summary of this problem see Graf and Lamar, 1955, p. 665.

dolomite structure differentiation, and for somewhat more reliable semiquantitative estimates of relative abundances of the calcite and dolomite crystal structures. Semiquantitative estimation from X-ray patterns was based on the relative intensities of the (112) lines of calcite and dolomite (rhombohedral structure cell). The scattering intensities of these lines for calcite and ferroan-dolomite are very nearly equal and thus, for practical purposes, quantitative estimates were based on a 1:1 relationship. Without careful and detailed study of slight line shifts and intensity changes caused by solid solution of iron in the dolomite lattice, the X-ray patterns could not be used for identification or estimation of the composition of the ferroan-dolomite. All estimates of ferroan-dolomite abundance were determined with a precision of 1 part in 10. The methods used would not justify more refined estimates.

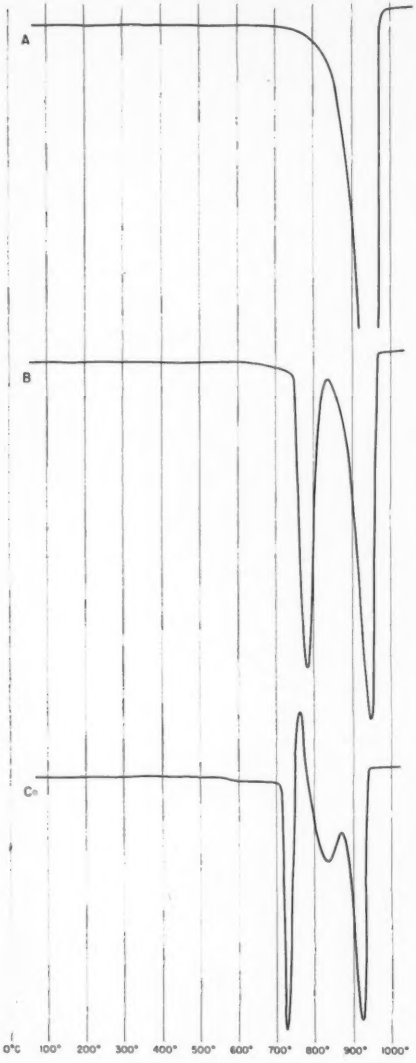

FIG. 2.—Differential thermal curves of common carbonates: A. Calcite. B. Dolomite (low-iron). C. Ferroan-dolomite.

PETROLOGY

Thin sections were studied mainly to evaluate the distribution and occurrence of the various carbonate minerals in the rock. For most samples it was possible to make a rough estimate of relative amounts of different carbonates present; these estimates checked with the DTA and X-ray estimates made later. It was not possible, from thin sections, to estimate the amount of Fe substituted for Mg in the ferroan-dolomite. For this reason, in the petrologic discussion we shall refer to "dolomitization" and "dolomite" rhombs, although we know from the DTA curves that the mineral is ferroan-dolomite; we use the term ferroan-dolomite very broadly to include all Fe-Mg carbonates with dolomite structure.

The information best obtained from thin sections but not given by DTA and X-rays related to dolomitization textures, which led to conclusions concerning the secondary origin of dolomite (in these particular rocks). Petrology also was useful for observing the general texture of the rock, recrystallization effects, the chronology of sequences of carbonates that show replacement phenomena, the nature of fossil materials, and the distribution of non-carbonate materials (quartz, clay minerals).

Almost all the thin sections studied show that carbonate minerals occur in a mixture of three general types of texture: (1) a finely crystalline matrix, (2) medium to coarsely crystalline irregular regions, and 3) shell materials. The finely crystalline or micro-crystalline matrix is brownish and most

sections show rudimentary to well-developed lamination. The individual crystals of carbonate that make up the matrix range from 10 microns down to sizes below the resolution power of the microscope (<1 micron); in the majority of the thin sections, most of the tiny crystals range from 2–5 microns. Although the carbonate is argillaceous in some samples, in most it is relatively pure carbonate. Presumably this fine matrix is crystallized original "lime mud."

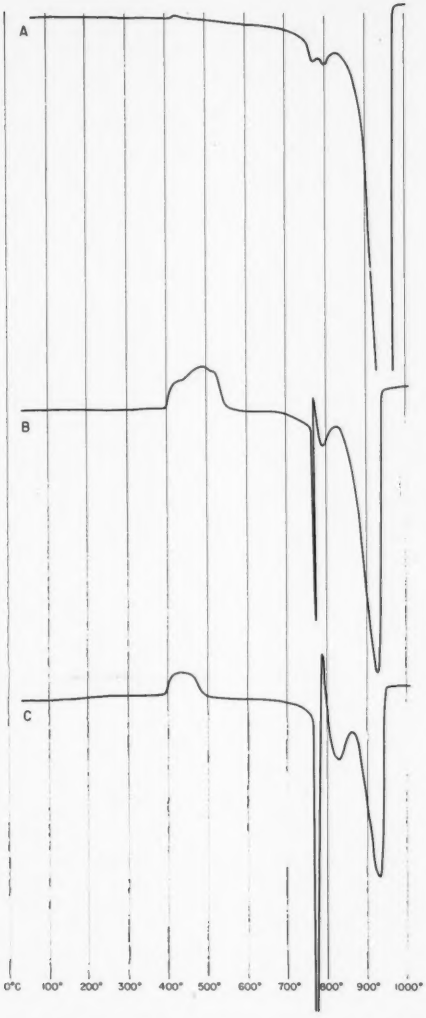

FIG. 3.—Differential thermal curves of mixtures of calcite and ferroan-dolomite. A. 1–2 parts in ten ferroan-dolomite. B. 4–5 parts in ten ferroan-dolomite. C. 8–9 parts in ten ferroan-dolomite.

Distributed more or less randomly through the matrix are patchy, irregular regions of clear, medium to coarsely crystalline carbonate. In these the individual crystals, ranging in size from 40–100 microns, are intergrown in a mosaic. There is no evidence that the carbonate in these areas is detrital and it is assumed that the patches are the result of recrystallization or replacement of the original matrix.

Calcareous hard parts of many different kinds of organisms are present in all of the rocks, except for one underclay limestone. Dominant are brachiopods, pelecypods, gastropods, corals, bryozoa, and in some sections, fusulinids. The degree of preservation ranges from completely intact large brachiopod shells to shell debris so fragmented and disarticulated that identification is almost impossible.

In general, the range of disarticulation and fragmentation is not great in any given sample, but almost every section, including those with the best preservation, contains some slightly fragmented fossil material. The shells are composed of two different types of material. Most are composed of a medium or coarsely crystalline calcite mosaic. Other shells, a significant proportion in some samples, show original biogenic textures of finely fibrous calcite. In some shells the fibers are interlaced in a fine structure with one set of fibers parallel and one set perpendicular to the long axis of the shell It is not clear why there has been a selective recrystallization of some shells in these rocks. The shell fillings of molluscs and other forms are variable in composition, ranging from fine matrix material to coarsely recrystallized mosaics of clear crystals. In many shells the fillings are argillaceous and may contain some concentration of silt (fine-grained quartz).

Although few of the samples studied are true calcarenites (Pettijohn, 1949, pp. 300–307, pl. 24), almost all of them contain some evidence that direct precipitation of carbonate, whether by biochemical or inorganic means, was not responsible for all

of the material in the rock. Although the fine matrix does not show any evidence of detrital origin, it is possible that it is organically derived debris so very finely comminuted that it cannot be identified as such. Most of the rocks studied lie intermediate between two end members, calcarenites and completely autochthonous precipitates, indicating that, while biochemical precipitation of carbonate proceeded more or less uniformly, the precipitated material was diluted by carbonate, silty, and argillaceous detrital material deposited by current action. Of the detrital fraction, probably only the quartz silt and some of the clay had been transported very far.

Most of the noncarbonate material in these rocks is very fine-grained quartz silt. The particles rarely are larger than 15 microns and, in most sections, average about 5 microns. The grains are individual and isolated, "floating" in the carbonate matrix. Many of the grains have been extensively replaced by carbonate; no authigenic quartz overgrowths were seen. None of the sections studied showed any abundance of this silt; the average was only about one percent of the rock.

Some thin sections show small quantities of chert or microcrystalline quartz. Pyrite occurs in several samples as isolated cubes, 1 or 2 microns wide, or as slightly larger clusters in which individual cubical outlines are lost. Organic matter is present in a few samples in very minor amounts, usually distributed along thin laminae in the fine-grained matrix.

In almost every sample for which the X-ray and DTA analysis indicated some ferroan-dolomite, the mineral was revealed in thin section by the presence of rhombs growing in surrounding calcite. The only exceptions were two samples with a uniform microcrystalline matrix. In these, the individual crystals of carbonate and any rhombs that may be present are too small for adequate resolution under the microscope. The lack of dolomite rhombs in the fine-grained matrix is more or less characteristic of all of the samples; in only a few sections could any dolomite rhombs be seen in the matrix. The matrix rhombs are larger than the average crystal size of the matrix calcite, but much smaller than the size of rhombs in coarser crystalline areas.

Shell materials do not show any dolomitization, but the interior fills of many shells have been extensively dolomitized. In general, the fine-grained matrix filling some shells is not dolomitized. In some thin sections the interiors of many of the fusulinid shells are filled with a mosaic of dolomite rhombs. In other sections the interiors of mollusc shells seem to be the main loci of dolomitization.

There is a definite correlation of dolomitization with the irregular areas of coarsely crystalline calcite. In several samples dolomite rhombs are restricted to such areas. Here also, as in the matrix rhombs, the dolomite rhombs are slightly larger than calcite crystals in the same area. In some samples that show extensive dolomitization, entire areas are a mosaic of intergrown coarsely crystalline rhombs. Perhaps the presence of rhombs in coarsely crystalline areas and their absence in the fine-grained matrix is the result of partial recrystallization, which allowed Fe and Mg originally contained in the matrix to separate from it to form rhombs of iron-rich dolomite.

No siderite was noted in thin section. It was difficult to distinguish, under the microscope, between ferroan-dolomite and low-iron dolomite. Indirect evidence is present in a number of weathered outcrop samples in which cracks and cleavage planes are tinged reddish-brown, presumably the result of hydrolysis and oxidation of iron-rich dolomite. The DTA curve of each such sample confirmed the presence of ferroan-dolomite.

A general chronology of post-depositional alterations of the rocks can be deduced from study of thin sections. We consider that the brown matrix is the crystallized "lime mud" or original precipitate, which includes in it many different kinds of shell materials, silt, and clay. Following the original deposition came the recrystallization of original shell materials into large, clear calcite crystals. Perhaps at the same time some parts of the matrix were replaced or recrystallized to form larger crystals of clear calcite. Subsequently, some parts of the rock, notably the shell fillings and coarser crystalline areas in the matrix, were partially or completely dolomitized.

Some thin sections show cross-cutting veinlets and fracture fillings of clear calcite which formed after the dolomitization. In individual sections chronologies of different types of carbonate formation may be much more complex, but most of them fit into the pattern described above.

DTA AND X-RAY RESULTS

Table 1 gives the results of DTA and X-ray analysis of the samples studied. Determinations on many of the samples were checked by duplicate runs. Multiple determinations of some sample numbers shown in the table refer to samples of the different gross lithologies exhibited in hand specimens. Because only one sample (L-17) was composed of low-iron dolomite, and all of the other samples that contained dolomite show it to have a significant iron con-

TABLE 1.—*Relative abundance of calcite and ferroan-dolomite in Illinois limestones*

Sample	Stratigraphic position	Location				Calcite: Ferroan-dolomite (Parts in ten)		Remarks
		Sec.	T.	R.	County in Ill.			
L-26	Shumway	13	6N	5E,	Effingham	10	0	
255	Omega	25	10N	4E,	Shelby	10	0	
247	Millersville	34	12N	1W,	Christian	10	0	
263	Millersville	28	12N	1W,	Christian	10	0	
269*	Millersville	34	12N	1W,	Christian	10	0	
L-25	Millersville	21	18N	13W,	Vermilion	10	0	
557*	Macoupin	31	19N	13W,	Vermilion	10	0	
562*	Trivoli	25	14N	10W,	Edgar	10	0	
L-27	Collinsville	28	2N	8W,	St. Clair	7	3	
L-2	Lonsdale	17†	18N	2W,	Logan	10	0	Dark gray
L-2	Lonsdale	17†	18N	2W,	Logan	10	0	Light brownish gray
568*	Lonsdale	28	8N	5E,	Fulton	10	0	Carbonate "pebbles" in limestone conglomerate
568	Lonsdale	28	8N	5E,	Fulton	0	10	Brown cement in limestone conglomerate
529	West Franklin	13	6S	11W,	Vanderburgh (Ind.)	10	0	
L-1	West Franklin	32†	14N	10W,	Edgar	9	1	Outside of core
L-1	West Franklin	32†	14N	10W,	Edgar	9	1	Inside of core
268*	Piasa	25	8N	10W,	Jersey	7	3	
L-3	Piasa	22†	2N	8W,	St. Clair	10	0	
L-28	Piasa	28	2N	8W,	St. Clair	10	0	
L-4	Cutler	22†	8S	3E,	Williamson	5	5	
L-5	Cutler	25†	8S	3E,	Williamson	4	6	
L-6*	Cutler	22†	4S	5W,	Randolph	6	4	
502*	Cutler	5	2S	7W,	St. Clair	10	0	Gray
502	Cutler	5	2S	7W,	St. Clair	10	0	Brown
L-7	Cutler	11†	4S	1E,	Jefferson	9	1	
L-32	Cutler	27	8S	3E,	Williamson	6	4	
L-23	Cutler	33	1S	7W,	St. Clair	10	0	
L-24	Cutler	33	1S	7W,	St. Clair	10	0	
L-8*	Underclay ls. below Coal No. 7	30†	14N	10W,	Edgar	6	4	Outside of core, light brown
L-8	Underclay ls. below Coal No. 7	30	14N	10W,	Edgar	3	7	Medium brown, near center of core
L-8	Underclay ls. below Coal No. 7	30	14N	10W,	Edgar	1	9	Center of core argillaceous, dark brown
503*	Galum	5	2S	7W,	St. Clair	4	6	
L-9	Bankston Fork	22†	4S	5W,	Randolph	6	4	
L-10	Bankston Fork	20†	10N	6W,	Macoupin	5	5	
L-11	Bankston Fork	10†	9S	7E,	Gallatin	8	2	Dark brown
L-11	Bankston Fork	10	9S	7E,	Gallatin	6	4	Light brown
L-12	Bankston Fork	22†	8S	3E,	Williamson	6	4	
L-13	Bankston Fork	25†	8S	3E,	Williamson	3	7	
8*	Bankston Fork	14†	4S	1E,	Jefferson	½	9½	
4-47*	Bankston Fork	18†	7S	10E,	White	4	6	
L-31	Bankston Fork	27	8S	3E,	Williamson	8	2	
L-30	Jamestown	27	8S	3E,	Williamson	10	0	
L-29	Herrin	27	8S	3E,	Williamson	8	2	
L-14	Herrin	22†	4S	5W,	Randolph	10	0	
L-15	Herrin	15†	8S	3E,	Williamson	9½	½	
L-16*	Herrin	14†	8S	6E,	Saline	6	4	
L-17*	Underclay ls. below No. 6 Coal	30†	9N	1E,	Fayette	0	10	Relatively pure dolomite—no iron
L-18	Underclay ls. below No. 6 Coal	25†	8S	3E,	Williamson	10	0	Medium gray
L-18	Underclay ls. below No. 6 Coal	25†	8S	3E,	Williamson	9	1	Light gray, argillaceous
L-19	Underclay ls. below No. 6 Coal	22†	2N	8W,	St. Clair	10	0	
L-20	Underclay ls. below No. 6 Coal	22†	4S	5W,	Randolph	9	1	
L-22*	Underclay ls. below No. 6 Coal	28†	5S	2E,	Franklin	8	2	
L-21*	St. David	6†	9S	5E,	Saline	6	4	
317	St. David	12†	8S	3E,	Williamson	4	6	
614*	Covel limestone conglomerate	29	17N	10W,	Vermillion (Ind.)			Limestone conglomerate Complex mixture of several types of carbonate
313*	Stonefort	12†	8S	3E,	Williamson	6	4	
312*	Curlew	29	10S	4E,	Williamson	10	0	
88	Fulda				Spencer (Ind.)	9½	½	

* Thin section.
† Diamond drill core sample.

tent, only two columns are shown in the table, indicating the relative abundances of calcite and ferroan-dolomite.

The first and most obvious conclusion from the results is that many different carbonate beds contain an abundance of ferroan-dolomite and a wide range of mixtures of ferroan-dolomite and calcite. Almost all of the beds sampled had previously been described by field workers, on the basis of gross lithologic examination, as more or less pure (calcitic) limestones. The widespread occurrence in these rocks of carbonate minerals other than calcite indicates that field descriptions should be followed up by mineralogical determinations in the laboratory in order to avoid erroneous estimates of mineralogy.

Some correlation of mineralogy with stratigraphic position is apparent from table 1. All samples of beds younger than the Trivoli limestone are almost completely calcitic. The amount of ferroan-dolomite is highly variable in samples of older beds, but some samples of almost every one of the older beds contain noncalcitic carbonates. One limestone, the Bankston Fork, contains significant amounts of ferroan-dolomite in every one of nine samples. This can be contrasted with the composition of the next higher limestone in the section, the Cutler. Four of the nine samples of the Cutler are completely calcitic. The other five samples contain 1–6 parts in ten of ferroan-dolomite.

The reason for the high ferroan-dolomite content of the Bankston Fork is not apparent. The position of the Bankston Fork is somewhat unusual in that it is a marine limestone, which grades upward into a calcareous underclay below the Bankston coal, in contrast to the more common occurrence of marine limestones in the Pennsylvanian as a caprock to a coal bed, in many places separated from the coal by gray and black shale beds (Weller, 1930). Thus, in terms of the normal cyclical succession of Pennsylvanian beds, the Bankston Fork occupies the position of a "freshwater" or "underclay" limestone. Other underclay limestones do not seem to be as uniformly dolomitized as the Bankston Fork but there are not enough analyses of samples of this type of lithology to generalize.

Several beds were sampled from both outcrop and subsurface. There seem to be no significant differences in ferroan-dolomite content that might be ascribed to surficial weathering on the one hand or to effects of infiltration of groundwater on the other.

Positions of samples in relation to structurally deep parts of the Illinois Basin and the marginal shelf areas to the southwest and northwest do not seem to correlate with dolomite abundance. One possible exception is the Cutler limestone and its equivalent, the Piasa; five samples of the Cutler bed in St. Clair County, on the western shelf area, show no ferroan-dolomite, but to the south in Randolph County and in the deep part of the basin to the east, all of five samples show some ferroan-dolomite. Further study of the Cutler bed might reveal dolomitization facies related to basin or shelf position. We have not investigated possible correlation of dolomite content with local structural features which might be related and so cannot evaluate this factor.

Thus, the analyses of the samples studied suggest that the only significant correlation of dolomitization in these rocks is with stratigraphic position. If there is no coincidence of stratigraphic position with other geologic factors (structural, geomorphic, hydrologic), dolomitization may be related to some factors involved in the original sedimentation and composition of the rocks that were operative during the middle part of the Pennsylvanian period.

The fact that petrologic evidence indicates that dolomite is secondary is not necessarily incompatible with this idea. The original composition may have been such (perhaps a significant porportion of magnesian calcite) that a particular facies was more susceptible to penecontemporaneous or later dolomitization. Whether the original sedimentational factors were primarily biological (presence of shell-forming organisms that included Mg in the skeletal materials) or whether such factors were inorganic geochemical (special conditions of pH, Eh, or trace elements that resulted in precipitation of Mg-rich carbonates) is not within the scope of this brief report. Such conclusions would have to be based on much more detailed stratigraphic and faunal analyses of the carbonate beds.

Although occasional dolomites in different

areas and in many other parts of the geologic column contain iron, the Pennsylvanian limestones in Illinois are characterized by rather frequent occurrences of iron-rich dolomites. It is probably not coincidence that this type of dolomite is associated with Pennsylvanian rocks that contain abundant iron-rich minerals in a variety of modes of occurrence: siderite and clay ironstone concretions, siderite cement in some sandstones, siderite veinlets and spherules in shales and siltstones, etc. Although such occurrences are not unique in Pennsylvanian rocks, their abundance and variety make the Pennsylvanian section in this part of the country unusual in this respect.

Perhaps the abundance and variety of forms of iron in this group of rocks is related to the climactic growth of a land flora and the great lateral extent of peat swamps that existed at many times during the period. Swamp and peat waters are rich in organic matter (humic acids, partially decomposed woody remains, etc.) and contain relatively high percentages of dissolved and colloidally suspended ferrous iron (Waksman, 1936, pp. 301–2) and it is probable that, during Pennsylvanian time, a significant amount of iron was contributed from these sources. In this connection, it is noteworthy that the middle part of the Pennsylvanian section, which contains limestones that consistently show some ferroan-dolomite content, is also that part of the section that contains most of the thick and persistent coal beds. Whether the iron was contributed to the sediments at the time of deposition or was introduced later by circulating groundwaters must remain a moot point until much more reliable mineralogical and petrologic evidence is at hand.

In conclusion, it is clear that much more detailed study of the mineralogy and petrology of this group of carbonate rocks is needed before there can be a formulation of some reasonably unified theory of origin that will account for their normal characteristics, much less the abnormal features that many of them display. Considering the variety of textures, it would be desirable to investigate the character and variability of a single carbonate bed; individual beds could be sampled so that contrasts might be revealed between basin and shelf areas; and carbonate mineralogy and texture might be correlated with argillaceous and silt content, local structural conditions, gross lithology, and faunal facies.

The fauna is in itself worthy of intensive study to see if certain types of fossils, and type of fossil preservation, may be related to mineralogy and texture. A more purely petrologic problem lies in the realm of diagenetic alteration of the rocks, which are so subject to recrystallization and replacement. Is there a more or less "universal" general chronology of diagenetic events in these limestones, or can such sequences characterize only limited areas and specific beds? In these and other problems, mineralogical analyses and interpretations will have to be based on the increasing knowledge of the geochemistry and crystal chemistry of the carbonate minerals that has become available in recent years.

REFERENCES

BECK, C. W., 1950, Differential thermal analysis curves of carbonate minerals: Am. Mineralogist, v. 35, p. 985–1013.

GRAF, D. L., 1952, Preliminary report on the variations in differential thermal curves of low iron dolomites: Am. Mineralogist, v. 37, p. 1–27; reprinted as Ill. Geol. Survey Rept. Investigations 161.

GRAF, D. L., AND LAMAR, J. E., 1955, Properties of calcium and magnesium carbonates and their bearing on some uses of carbonate rocks: Econ. Geology, 50th Ann. Vol., pt. II, p. 639–713.

KREY, F., AND LAMAR, J. E., 1925, Limestone resources of Illinois: Illinois Geol. Survey Bull. 46, 392 p.

KULP, J. L., KENT, P., AND KERR, P. F., 1951, Thermal study of the Ca-Mg-Fe carbonate minerals: Am. Mineralogist, v. 36, p. 643–70.

LAMAR, J. E., AND THOMSON, K. B., 1956, Sampling limestone and dolomite deposits for trace and minor elements: Illinois Geol. Survey Circular 221, 18 p.

PETTIJOHN, F. J., 1949, Sedimentary rocks. Harper and Bros., New York, 526 p.

WAKSMAN, S. A., 1936, Humus. Williams and Wilkins, Baltimore, 494 p.

WELLER, J. M., 1930, Cyclical sedimentation of the Pennsylvanian period and its significance: Jour. Geol. v. 38, p. 97–135.

JOURNAL OF SEDIMENTARY PETROLOGY, VOL. 27, NO. 1, PP. 64–79
FIGS. 1–13, MARCH, 1957

SECONDARY GYPSUM OF THE SULPHUR SERIES, SICILY, AND THE SO-CALLED INTEGRATION

LEO OGNIBEN
Montecatini S. A. (Settore Miniere), Milan, Italy

ABSTRACT

The Upper Miocene Sulphur Series of Sicily comprises four main formations, which are, in ascending order, the diatomitic Tripoli Formation, the evaporitic Basal Limestone, the Gypsum Formation, and finally the Trubi Formation, an ancient Globigerina ooze. Other less continuous units are also present. Peculiar sedimentational conditions are described in detail in a larger Italian paper.

In the Gypsum formation primary anhydrite and primary gypsum are varved rocks with inverse graded bedding of the laminae, due to chemical deposition. Secondary gypsum derives from anhydrite by paradiagenetic transformation and shows two different petrologic types. In the "sulphiferous facies" of the Gypsum Formation selenitic secondary gypsum is developed, with large size crystals and a peculiar fabric of almost free growth. In the "saliferous facies" alabastrine secondary gypsum shows structures caused by hindered growth under considerable load.

A sequence of stages in the anhydrite-gypsum transformation seem to be the following: (1) building of limpid selenite crystals; (2) ruptural deformation of their peripheral zones, giving rise to superindividual polarisation; (3) production of intergranular fine-size gypsum aggregate of mylonitic character. Ruptural deformation is originated by volume increase of the solid phase during the transformation. Residual anhydrite inclusions are present in the first two stages, absent in the last one.

The above sequence is just the reverse of that described in the studies on American and German salt domes. Goldman (1952) gives the name "integration" to a process of progressive adjustment of randomly oriented fine-size gypsum pieces to superindividuals with less dispersed optical orientation and finally to limpid selenite crystals. This process is very different from the well-known "Sammelkristallisation" and does not seem to be feasible in view of the physico-chemical forces known thus far. The little disturbed Upper Miocene Gypsum Formation is likely to give a clearer picture than the severely disturbed Paleozoic salt domes.

INTRODUCTION

Sulphur exploration in Sicily by "Montecatini," Society for Mining and Chemical Industries, from 1951 to 1954 gave rise to a body of geologic and petrologic observations which have been partly published in a geologic paper (Ogniben, 1954 a) and in a later petrologic paper now in press (Ogniben, 1956). Observations on sulphur ore deposition still await publication, only a few data having been reported in the papers mentioned above.

Observations on primary gypsum were reported in this *Journal* (Ogniben, 1955). It seems also of interest to give with the present paper some observations on secondary gypsum, since this topic has been largely touched upon by American literature on salt domes. A short exposition is premised of the petrologic characters of the whole Sulphur Series, which have been more extensively described in the Italian paper in press (Ogniben, 1956).

THE SULPHUR SERIES

The Sulphur Series comprises the deposits of Upper Miocene age with restricted environment character in the Mediterranean area (Messinian Stage of Italian literature). Deposition of its uppermost formation (Trubi) took place under almost normal marine conditions, and possibly extended into Lower Pliocene time.

The four main formations (fig. 1), all of which can be missing, are given by alternation of predominantly chemical or biogenic beds and predominantly terrigenous beds, with individual thickness in the order of magnitude of meters (m-rhythm of Sander, 1936). The Tripoli, oldest formation of the Sulphur Series, is composed of diatomitic beds about 1 m thick, alternating with diatomaceous marls about 1.5 m thick, with total thickness from zero up to 60 m. The overlying Basal Limestone Formation consists of evaporitic limestone beds averaging 2.8 m, alternating with marls about 1

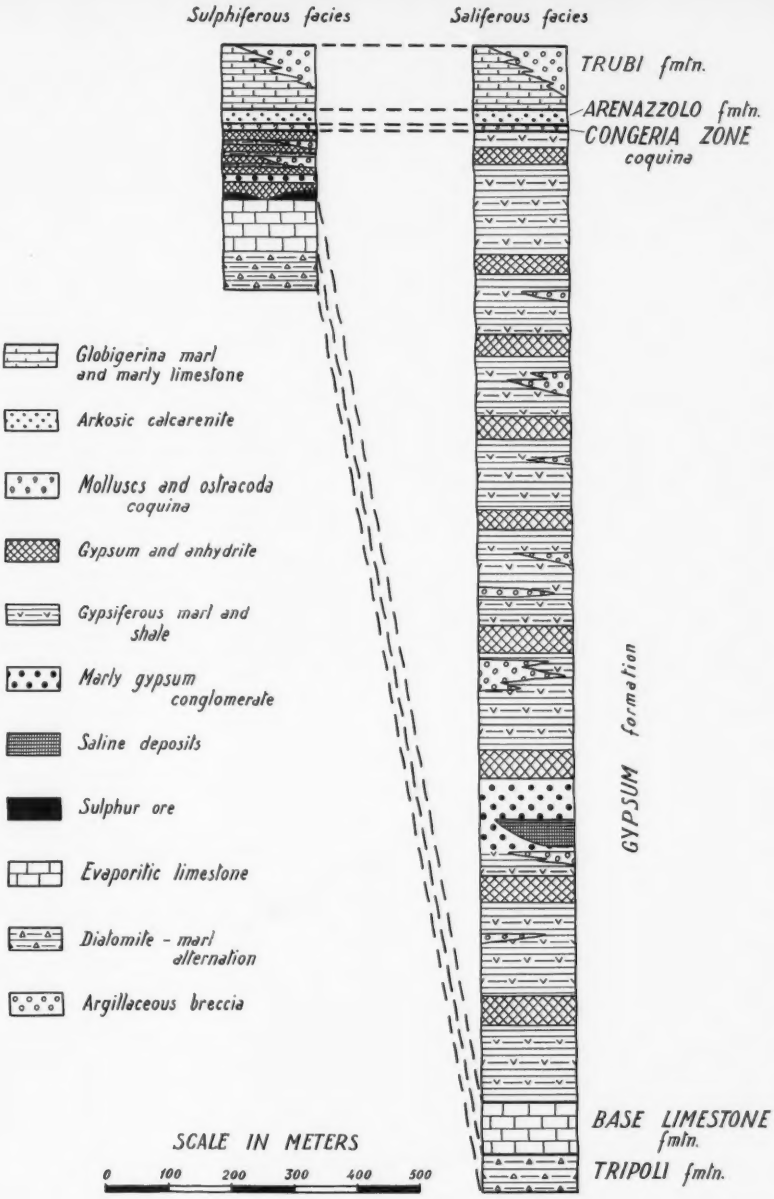

FIG. 1.—The two facies of the Sulphur Series in Sicily.

m thick, with total thickness from zero up to 80 m. The following Gypsum Formation generally comprises an alternation of gypsum and marl beds. It will be more completely described in the next section in order to give a framework for the discussion of secondary gypsum.

The uppermost formation of the series is the Trubi, consisting of Globigerina marly limestones averaging 0.33 m thickness, alternating with Globigerina marls averaging 0.22 m; total thickness varies from zero to 100 m. Two thin transition deposits, the brackish "Congeria Zone" coquinas (Molluscs, Ostracoda and Globigerinae) and the Arenazzolo Formation which is a poorly cemented arkosic calcarenite, sometimes occur between the Gypsum and Trubi.

The sedimentary column often is complicated by the presence of discontinuous bodies of "Argillaceous Breccia" (A.B.), highly variable in thickness, sometimes up to enormous amounts. This peculiar rock was described in detail in previous papers (Ogniben, 1953; 1954 a). It is composed of angular fragments of various types of clay and marl in a clayey matrix and contains characteristically mixed foraminiferal assemblages of different ages and environments. It has been interpreted as the product of erosion of diapirically uplifted clayey formations of various ages in anticlines of South Central Sicily, with short-range transportation to nearby synclines, the distances involved ranging from hundreds of meters to several kilometers. Diapiric uplifts were due to lateral folding pressure, the plastic clayey formations in anticlinal cores being able to discharge upwards through broken anticlinal axes. The chief source of the diapiric phenomena must be considered to have been a highly plastic formation, belonging to the "Argille Scagliose" of the Italian literature, or Argillaceous-Scaly complexes (A.S.). These are nappes of almost schistose, tectonized but not indurated clays, with exotic stony blocks of various ages, which slid by gravity from their sedimentational realm into more or less adjacent basins, evidently because of upward tilting or folding at their starting point.

Under the microscope almost all rocks of the Sulphur Series show varved structure, except the argillaceous breccias and some other reworked members. Varves are sedimentational laminae with thickness in the order of magnitude of millimeters (mm-rhythms of Sander, 1936) and are believed to be due to seasonal change of depositional controls. Thus, the diatomite varves result from thin opaline beds made up of diatom tests and separated by thin pelitic layers, partly terrigenous (clay) and partly due to chemical deposition (carbonate). In the Basal Limestone the varves are built up by alternating layers of pure carbonate and marl. In the Gypsum Formation similar relations are visible between gypsum and an interbedded clay-carbonate terrigenous-chemical pelite. Also in the Trubi indistinct laminae of pure calcite have been observed, separated by pelitic layers. The marly beds alternating with the chemical or biogenic ones in the order of magnitude of meters are built in the same manner, but they show thicker terrigenous layers and thinner chemical ones. From a structural point of view, the Sulphur Series rocks can thus be termed "mm-rhythmites" (Sander, 1936).

From a geological point of view the story of Messinian sedimentation shows some peculiarities. There was a restricted humid environment (Tripoli Formation) which gave way to a restricted arid one (evaporites), not because of climatic changes but probably only because of gradual increase of the salinity from mildly toxic to definitely toxic values. This intimate connection between diatomites and evaporites is reflected by a peculiar chemical trend of the Tripoli rocks. As a matter of fact, representative points of the rocks of known diatomitic formations of all the world commonly are distributed between the silica and clay apices in the carbonate-clay-silica triangular diagram. As unique among diatomitic formations thus far known to the writer, the Tripoli rocks are on the contrary scattered between the carbonate and silica apices. This fact seems due to incipient evaporative deposition of carbonate during the diatomitic sedimentation (see details in Ogniben, 1956). There are also the peculiar episodes of renewed euxinic sedimentation between the evaporitic limestone and gypsum sedimentations, which gave rise to the known sulphur ore deposits. A detailed study of these deposits is still in progress and could perhaps furnish

a key to better interpretation of the American salt dome sulphur deposits.

THE GYPSUM FORMATION

Beds of alternating gypsum and marl make up the Gypsum Formation. A characteristic polar sequence is given by the almost general bipartition of the gypsum beds in a basal thin zone of microcrystalline gypsum, with mm-rhythmic structure of sedimentational laminae about 2–3 mm thick, and in an upper thicker zone with swelling structures.

The basal zones average 1.6 m but are often less than 0.5 m thick, and have been interpreted as the product of primary chemical deposition of gypsum by evaporation. Their structure was first described in this *Journal* (Ogniben, 1955). Inverse graded bedding due to increase of grain size from bottom to top of the laminae was attributed to increase of salinity during seasonal periods of evaporative deposition.

The upper zones showing swelling structures range from a few meters to over 30 meters in thickness, with average values somewhat over 6 meters. They have been explained as secondary gypsum originated by hydration from anhydrite. Swelling structures are due to volume increase of the solid phase during the transformation (Ogniben, 1953, 1954 a, 1956).

Two different facies, charaeterized by different types of secondary gypsum, different total thickness, and association with different kinds of industrial mineral deposits, must be distinguished in the Gypsum Formation. The "sulphiferous facies" is located in North Sicily and South Sicily along the borders of the Upper Miocene basin, and shows thin intercalations of shales averaging 2 m between the gypsum beds. The total thickness of the formation ranges from zero to about 70–100 m at the outcrops. Borings for sulphur exploration in synclines, however, revealed thicknesses up to 400 m. Associated industrial mineral deposits are beds or lenses of sulphur ore developed between the Gypsum Formation and the underlying Basal Limestone, or in the lowermost Gypsum. Secondary gypsum almost exclusively is in the form of selenite aggregates with average individual grain size of several centimeters.

The "saliferous facies" is developed in a median zone of the Upper Miocene basin, trending ENE-WSW from Mt. Etna to Sciacca. It shows very thick intercalations of shales, each up to several tens of meters. Due to that and also to greater thickness of the gypsum beds, the total formation thickness reaches values of 1500 m and more. Secondary gypsum of the "saliferous facies" is mostly in form of alabastrine aggregate of saccharoidal appearance. Associated mineral deposits are lenses of halite and potassium-magnesium salts, with thicknesses up to 500 m and more. In the border zones between the two facies saline deposits can be found overlying sulphur deposits. This is the case at Bosco-Stincone, Serradifalco, Caltanissetta, now operated by "Montecatini" which discovered the potash deposit in 1952, while sulphur had been known for a long time. The relative position of the two kinds of industrial mineral deposits is of interest with respect to the Gulf Coast salt domes, where sulphur overlies the salt.

The greatest part of the formation in both facies shows a regular repetition in cyclical sequence from bottom to top, consisting of marl—primary gypsum—secondary gypsum—marl, and so on. Besides, some other less developed types of calcium sulphate rocks occur. At about the lower third of the formational column a "detrital zone" is commonly developed. This is the level of the saline lenses, and marks the time of maximum regression ending the "advancing hemicycle" before the beginning of the "retreating hemicycle" of the "major evaporitic cycle" (Sloss, 1953). Besides the saline deposits in the "saliferous facies," and without them in the "sulphiferous" one, this zone commonly contains: 1) conglomerates of gypsum fragments in a gypsiferous-shaly matrix, often very thick; 2) lenses of gypsarenites, made up of detrital gypsum of psammitic size with peculiar compaction structures due only to solution; 3) anhydrite rocks.

Most anhydrite is of the type known as "regenerated anhydrite" according to Goldman (1952), lamellar or acicular in habit, often oblique to the optical axes. It has been interpreted by Goldman as the product of transformation from gypsum by dehydration. In Sicily it is evident that dehydration

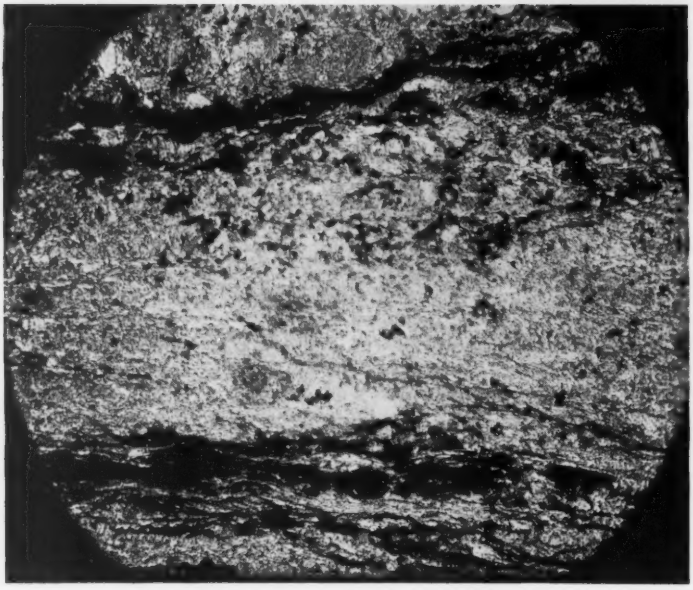

FIG. 2.—Inverse graded bedding in laminae of primary anhydrite. Mimiani N° 2 boring at 478.45 m depth, Caltanissetta. Crossed nicols, ×17.

is due to saline solutions and not to depth, since anhydrite beds are underlain by gypsum ones. Therefore, the occurrence of this anhydrite type is indicative of the close occurrence of saline deposits, sometimes as traces only. The term "regenerated anhydrite," however, implies that all gypsum from which anhydrite derives originally was of secondary character, having been produced by hydration of former anhydrite. But secondary anhydrite with the above said structure has been clearly observed to epigenize primary gypsum as well as secondary. Therefore, the more convenient name of "epigenic anhydrite" is proposed (Ogniben, 1956).

Primary anhydrite also was found as thin beds intercalated in the saline lenses. It is well characterized by the "pyle-of-brick" structure (Brown, 1931). The rock is a mm-rhythmite with varves about 2–2.5 mm thick, separated by thin layers of terrigenous and carbonatic pelite. Of interest is the inverse graded bedding of the varves (fig. 2), similar but less clearly developed than that already known in primary gypsum. This depositional feature seems, therefore, to be distinctive of evaporative chemical sedimentation. Grain size increase seems to accompany salinity increase during the evaporative season and to fall back to small sizes because of water dilution during the rainy season (Ogniben, 1955).

SELENITIC SECONDARY GYPSUM

This rock type makes up the bulk of the gypsum beds in the "sulphiferous facies" of the Gypsum Formation, generally being in each bed supported by thin basal zones of primary gypsum rhythmite. The selenite constitutes a coarse aggregate of (100) "swallow tail" twins from some millimeters to many centimeters in length, averaging about 5 centimeters. The aggregate shows a peculiar fabric with [001] of the twins perpendicular or subperpendicular to the bedding plane, the re-entrant angle of the twins facing the top and the apex facing the bottom of the beds (fig. 3). This preferred orientation has been named "Mottura's Rule" because it was first described by Mottura (1872). In fabric diagrams, [001] becomes concentrated in a maximum at 90° from the bedding plane, with dispersion not

FIG. 3.—Selenitic secondary gypsum with preferred orientation according to Mottura's Rule. Top and bottom of bedding corresponding to top and bottom respectively of the picture. Stincone mine, Serradifalco, Caltanissetta. Natural size.

FIG. 4.—Swelling structure in a bed of selenitic secondary gypsum. See hammer at left center of the picture. Grottacalda, Valguarnera, Enna.

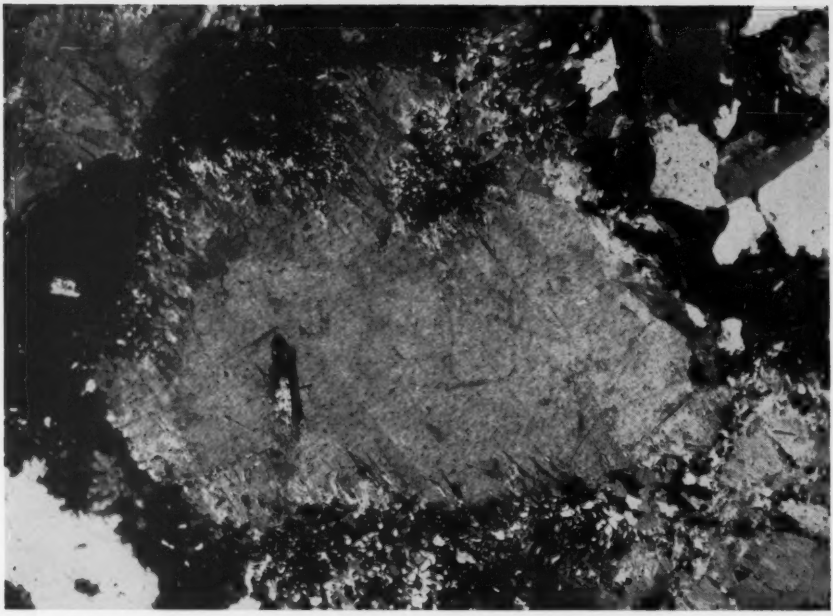

FIG. 5.—Selenitic secondary gypsum showing: (1) limpid crystalline core; (2) peripheral deformed zone with superindividual polarisation; (3) surrounding intergranular fine-size aggregate. C. Cardinale, North of Mimiani, Caltanissetta. Crossed nicols, ×50.

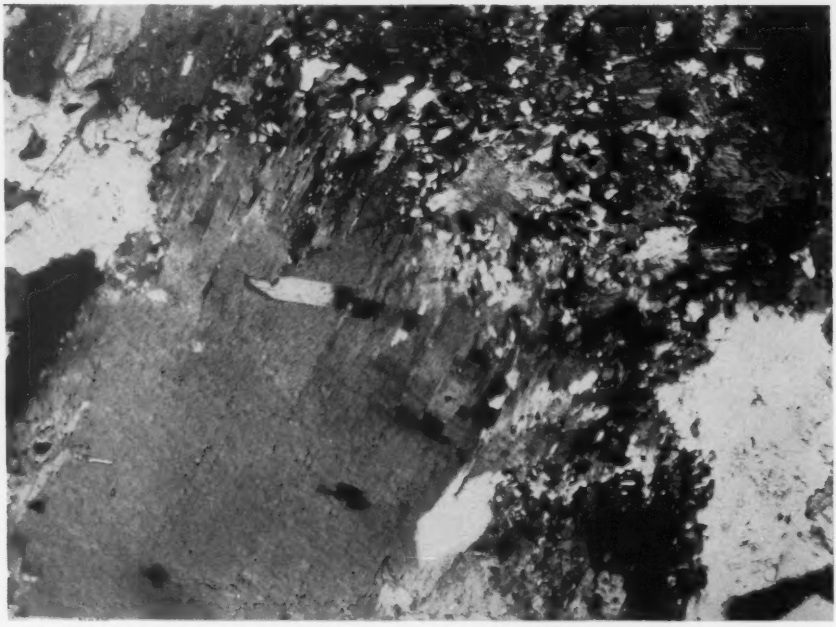

FIG. 6.—Selenitic secondary gypsum showing ruptural deformation in a peripheral zone with superindividual polarisation of the fibrous type, grading outwards in blastomylonitic fine-size aggregate. C. Cardinale, North of Mimiani, Caltanissetta. Crossed nicols, ×50.

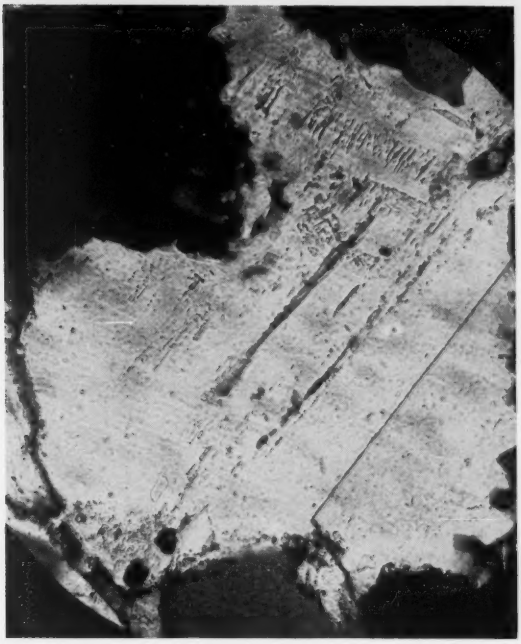

FIG. 7.—Anhydrite lamellae (high relief) arranged in gypsum cleavages. C. Cardinale, North of Mimiani, Caltanissetta. Crossed nicols, ×96.

larger than 40°–50° from the maximum pole (Ogniben, 1954 b).

The secondary origin by transformation from anhydrite is made evident megascopically by the swelling structures of the upper part of each bed (fig. 4), always showing radii of bending in an order of magnitude of several meters. The bottom of overlying gypsum beds never reflects the swellings of underlying ones. The deformation seems to be completely absorbed by the marls between the beds.

It is interesting to point out that Mottura's Rule megascopically resembles the free growth fabrics as described by Sander (1950), but the swellings at the upper surface of the beds represent a clear differential character.

Under the microscope (fig. 5) the selenite shows: (1) limpid cores constituting the bulk of the grains; (2) rupturally deformed discontinuous peripheral zones with "superindividual" polarisation, i.e. with slightly differing optical orientation of the fragments; (3) intergranular zones of fine grains, 0.05 to 0.5 mm in size, cementing the major selenite grains. Superindividual polarisation can be of a "cloudy" or cribrous type, as in figure 5, or of a fibrous one, by rupturing parallel to a cleavage, mostly (010) (fig. 6). Superindividual zones gradually pass outwards into intergranular fine-size aggregates, with a clear ruptural picture as visible in figure 6.

Most important are the anhydrite inclusions, as thin shreds or lamellae with sharp or corroded borders, mostly very small with 0.5 mm maximum length. Very often they are parallel to the gypsum cleavage planes, or ranged along them (fig. 7). There is no parallelism of optical orientation between the two minerals, and intergrowth appears to be controlled chiefly by the gypsum cleavages. Lamellae with sharp borders parallel to anhydrite cleavages are very small and clearly constitute solution residues by wearing along these cleavages. The distribution of anhydrite inclusions among the afore-

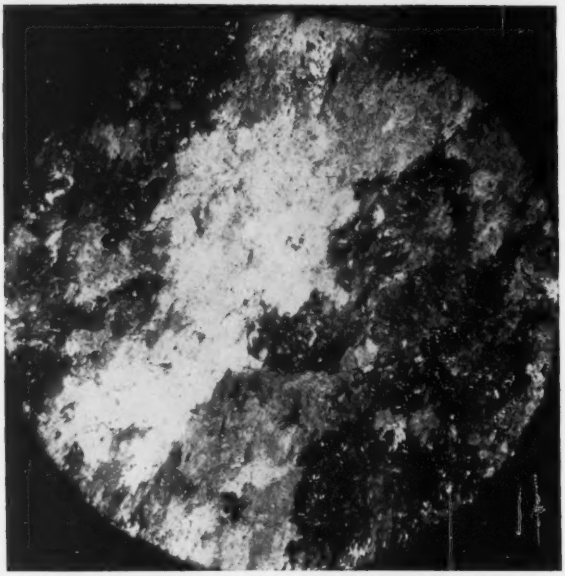

FIG. 8.—Alabastrine secondary gypsum, normal type, typical "cloudy" superindividuals. NW Sampria, Serradifalco, Caltanissetta. Crossed nicols, ×15.

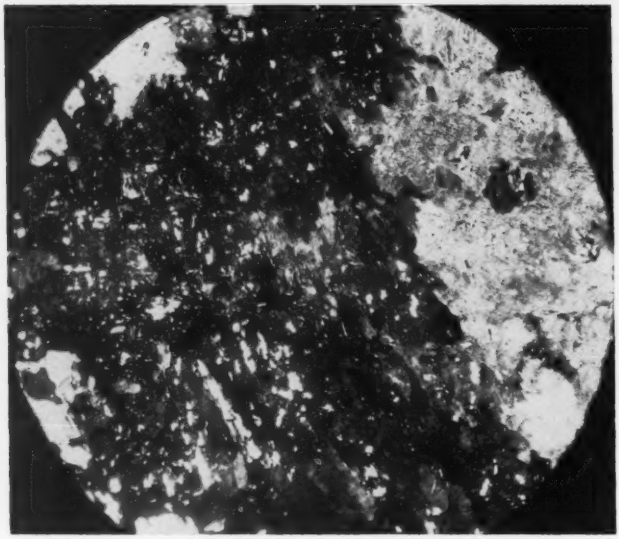

FIG. 9.—Alabastrine secondary gypsum, normal type. Enlightened anhydrite inclusions in darker gypsum superindividuals. NW Sampria, Serradifalco, Caltanissetta. Crossed nicols, ×50.

mentioned three structural elements of the secondary selenite is very significant. In limpid selenite cores anhydrite often occurs with several relatively large shreds or lamellae. In peripheral "superindividual" zones anhydrite is less abundant, with irregular boundaries and small size, and finally in intergranular aggregates it is missing.

Selenitic secondary gypsum is notably pure, inclusions other than anhydrite being only small carbonate granules (0.004–0.001 mm) often marking deformed bedding surfaces.

ALABASTRINE SECONDARY GYPSUM

In the "saliferous facies" of the Gypsum Formation a white secondary gypsum of saccharoidal appearance, or "alabastrine" gypsum, predominates. It commonly shows a coarsely knotty structure due to disordered swelling deformation from many centers during gypsification of anhydrite. When densely alternating with thin shale beds the alabastrine secondary gypsum shows the characteristic enterolithic folding. In Sicily however, it is rare to observe the well-known regularly folded "Schlangengips" ("snaky gypsum"), the occurrence of irregularly crumpled and distorted beds being the rule.

Intrastratal folding deformation by swelling becomes sometimes so tight as to produce a fibrous structure perpendicular to the bedding, because volume increase pressure chiefly acts along the bedding planes. Such petrologic types could be named "fibrous alabastrine secondary gypsum."

Under the microscope normal alabastrine gypsum shows a maximum development of superindividual polarisation zones of the "cloudy" type, already described as structural element (2) of the selenitic secondary gypsum (fig. 8). The fine-size intergranular aggregates are less important, and the limpid selenite cores are missing. There are no definite boundaries between the superindividuals, which can be considered as having lengths of several mm. They are roughly elongated perpendicular to the bedding, probably along [001]. No fabric analyses

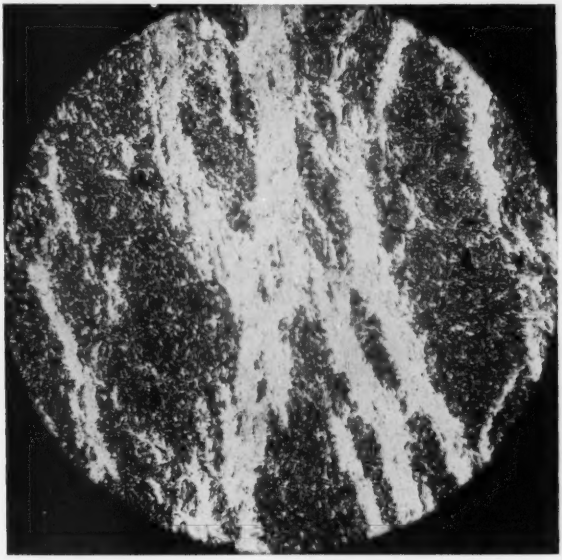

FIG. 10.—Alabastrine secondary gypsum, fibrous type. Vein-like patches belonging to one superindividual, surrounded by fine-size aggregate. SW Sampria, Serradifalco, Caltanissetta. Crossed nicols, ×15.

FIG. 11.—Alabastrine secondary gypsum, fibrous type. Enlightened anhydrite inclusions in darker gypsum superindividual, surrounded by still darker anhydrite-free fine-size aggregate. SW Sampria, Serradifalco, Caltanissetta. Crossed nicols, ×90.

have been made, however, because of the continuously varying superindividual polarisation.

Anhydrite inclusions occur in the superindividual zones and are missing in the intergranular fine-size aggregates. They are very small, averaging 0.02 mm, irregular and randomly oriented (fig. 9). The relatively regular arrangements observed in the selenitic secondary gypsum are lacking here.

The fibrous variety of alabastrine secondary gypsum under the microscope shows a framework of anastomosing vein-like gypsum patches subperpendicular to the bedding, surrounded by a homogeneous gypsum aggregate of 0.01–0.05 mm grain size (fig. 10). The vein-like patches show superindividual polarisation and nearly the same optical orientation for several neighbouring veins, over widths of one cm and more. Therefore, several veins compose an unique superindividual. The fine-size aggregate often shows fluidal structure subperpendicular to the bedding.

Residual anhydrite inclusions are to be found in the vein-like superindividuals only (fig. 11). They are very small (0.005–0.05 mm) and irregular like those already described for normal alabastrine gypsum.

Both normal and fibrous alabastrine gypsum generally lack inclusions other than anhydrite. There are only small carbonate grains ranged along strongly deformed bedding surfaces.

Summarizing, in the alabastrine gypsum only the structural elements already described for the selenitic gypsum under (2) and (3) can be found, i.e. the superindividual zones and the fine-size aggregates. In normal alabastrine type the two elements grade into each other, while there is a sharp distinction between them in the fibrous type. Residual anhydrite inclusions are exclusive of the superindividual zones, which are surrounded by anhydrite-free fine-size aggregates. The chief difference between selenitic and alabastrine secondary gypsum is that the selenitic cores of the first type are completely absorbed by the superindividual zones in the latter type.

TRANSFORMATION AND DEFORMATION FEATURES

Deformation by transformation with volume increase from anhydrite to gypsum is very evident megascopically. There are swelling structures, large and regular in selenitic secondary gypsum, smaller and irregularly arranged in the alabastrine gypsum. There is homogeneous grain size over the whole thickness of the beds, without variations due to the course of sedimentation. Also the sequence from bottom to top of shale—primary gypsum—secondary gypsum only can be explained by admitting the former deposition of anhydrite, later transformed to secondary gypsum.

Microscopically, a first symptom of the transformation is given by residual anhydrite. This is shown by microliths which are corroded and without their own formal elements. Sometimes it shows saw-like borders due to differential solution along the cleavages, and for this same reason very small anhydrite microliths can show euhedral borders, as a very advanced product of corrosion along the cleavages. Groups of anhydrite microliths sometimes outline the phantom of a substituted anhydrite crystal. There are no features to suggest gypsum substitution by anhydrite. Epigenic anhydrite on gypsum is very characteristic and already has been well described, especially by Goldman (1952) under the uncorrect name of "regenerated anhydrite."

The common elongation of anhydrite shreds along gypsum cleavages is due to the strong lattice anisotropy of the latter, which causes different growth velocities of gypsum along its different lattice directions.

Differential distribution of anhydrite inclusions is associated with differential ruptural deformation: (1) In the limpid selenite cores anhydrite inclusions are common and often regularly arranged; (2) In peripheral zones with superindividual polarisation the inclusions become smaller and disordered; (3) They disappear in the intergranular fine-size aggregates.

The ruptural character of the superindividual zones is very clear. They start in the limpid selenite cores with zones of slight distortion of the cleavages, which grade outwards into zones of "fibrous" or "cloudy" gradually variable optical orientation, like

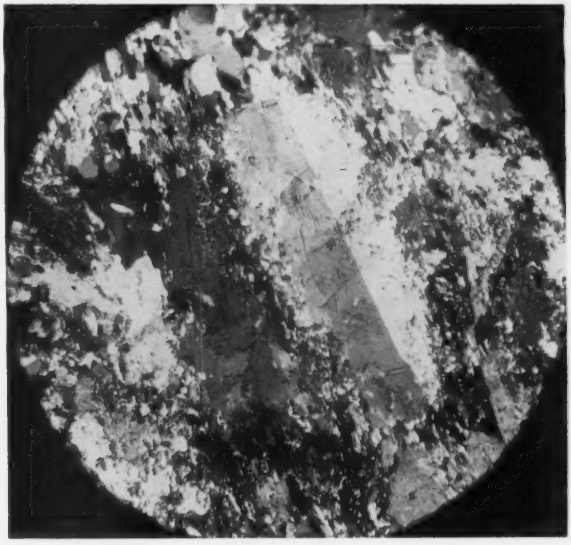

FIG. 12.—Selenitic secondary gypsum showing ruptural zones of fine-size aggregate crossing selenite crystals. C. Cardinale, North of Mimiani, Caltanissetta. Crossed nicols, ×15.

the undulatory extinction of quartz and other minerals. In gypsum such an extinction can better be termed "cloudy" than undulatory, because of its irregular variation and of the interference colours in various shades of grey, which under the microscope give a cloudy appearance (Hammerschmidt, 1883; Carozzi, 1953).

The ruptural character of the intergranular fine-size aggregates also is very evident. Towards the major crystals they grade in superindividual rupture zones (see fig. 6), and very often they occupy rupture zones going across selenite crystals (fig. 12).

Peripheral position of the mechanically deformed zones with respect to the limpid crystal cores and disappearing of residual anhydrite inclusions from the most ruptured zones suggest that deformation is due to a late stage of the gypsum growth. When volume increase of the solid phase by gypsification of anhydrite causes great pressures to act between the growing crystals, these are forced to adjust themselves in such a way as to allow the volume increase to be absorbed in the megascopic swelling structures.

The already described three structural elements of the selenitic secondary gypsum can thus be explained as the product of three successive stages in the anhydrite-gypsum transformation: (1) An initial stage of almost free growth without strong pressure produces limpid (100) twins, with much residual anhydrite left behind, chiefly along the gypsum cleavages; (2) In an intermediate stage advancing volume increase causes a pressure strong enough to deform the border zones of the growing gypsum crystals. In these zones, therefore, polarisation becomes superindividual and anhydrite inclusions become disordered and tend to disappear, being not protected against hydration by an undamaged gypsum lattice; (3) In a final stage volume increase attains its maximum value, with ensuing strong pressure and internal deformation by mutual displacement of crystals. This produces a mylonitic fine-size intergranular aggregate from which anhydrite wholly disappears, being unprotected against the absorption of water.

The best evidence of the relative time sequence of the three structural elements of secondary gypsum seem, therefore, to be given by the distribution of residual anhydrite among them, since anhydrite must disappear as gypsification advances.

Due to strong solubility and ionic mobility of gypsum, the mylonitic fine-size aggregate undergoes slight recrystallisation almost at the same time with the ruptural phenomena, getting a crystalloblastic character without greatly increasing in size. This seems to be the reason why Von Gaertner (1932), Goldman (1952), and Carozzi (1953) deny the occurrence of mylonitic gypsum, although they describe aggregates very similar to those now in question. Goldman even recognizes that in gypsum "reintegration takes place almost as fast as crushing" due to great ionic mobility, in order to explain the absence of mylonitic gypsum. Pointing out its crystalloblastic character, the fine-size aggregate could be qualified as "blasto-mylonitic," borrowing a word which Sander (1912) coined for recrystallized silicate mylonites.

The alabastrine secondary gypsum differs from the selenitic one because lacking the stage (1) of undeformed crystallization. It appears to have been deformed from the very beginning of transformation, with resulting large "cloudy" superindividuals surrounded by minor blastomylonitic aggregate. The latter attains its maximum development in the fibrous variety of alabastrine gypsum, where the superindividual cores are reduced to vein-like elongated shreds. The most probable clue from the absence of limpid crystal cores is that transformation took place under pressure from the very beginning.

THE SO-CALLED "INTEGRATION" OF GYPSUM

Von Gaertner (1932) and especially Goldman (1952) describe pictures very similar to those of the secondary gypsum now in question. From such factual data these authors, and Carozzi (1953) who largely summarizes their papers, come to conclusions quite opposite to those reached in the present paper. A fine-size aggregate should be the initial stage of anhydrite-gypsum transformation. From this stage a progressive isorientation of the discrete gypsum pieces would lead to an intermediate superindivid-

ual stage, and finally to limpid selenite crystals.

On the contrary, direct transformation from anhydrite to selenite crystals is admitted by Brown (1931), but he gives no details.

The building of greater size crystals from finer size ones is known as "Sammelkristallisation" as defined by Rinne (1923), and could be translated with "syncrystallization" (=crystallizing together). It takes place through progressive solution of finer size crystals and corresponding accretion of a smaller number of greater size ones, according to Riecke's principle and anisotropy of growth velocity. Such a phenomenon does not allow an intermediate superindividual stage.

In known occurrences, superindividuals are originated by destructive mechanical deformation of crystals, with or without recrystallization, and sometimes would result as a final stage from constructive preferred orientation in tectonites (Sander 1930). Between major crystals and fine-size aggregates, superindividuals can play an intermediate role only in the destructive sense.

According to Goldman (1952), progressive isorientation of discrete fine-size gypsum particles up to ever-larger superindividuals with increasing common optical orientation, and finally to large true crystals, probably is allowed by the presence of abundant crystallization water in gypsum. The water would "act as a medium in which the lattice of gypsum crystals is unstable or mobile, so that one crystal can exert an orienting effect on the lattice of others. Under the influence of several adjacent crystals a lattice might assume an intermediate orientation." This phenomenon he calls "integration." However, no such forces are as yet known in the physico-chemical realm as to originate such a progressive orientation of discrete mineral particles, nor as to allow "some growing crystals to influence and reorient the lattice of other crystals at a distance" in order to give true larger crystalline individuals, except through solution and redeposition. In tectonitic fabrics the strongest preferred orientation never produces large crystalline individuals from many smaller sized ones but, at the most, superindividual zones of many individuals with limited diversity of orientation.

The time sequence of the various structural elements in Sicilian secondary gypsum, as recognized from deformational relationships and from distribution of residual anhydrite microliths, is the reverse of that admitted by Goldman. Since limpid crystals, superindividuals and fine-size aggregates have been seen as successive deformational stages in the destructive sense, there is agreement with the more general observations of Sander (1930), and with the theoretic principles enumerated just above.

Moreover, Von Gaertner and Goldman, having not recognized the occurrence of deformational structures, could conceive anhydrite gypsification as a metasomatic process without volume change and with escape of excess calcium sulphate in solution. The fine-size gypsum, that is a final mechanical product, could in this manner be considered an initial hydration product. Since the factual data described by said authors do not fundamentally differ from those observed in the Sicilian rocks, it must be admitted, however, that also in American and German gypsum rocks the anhydrite-gypsum transformation took place with strong volume increase of the solid phase and with joint internal deformation. In Sicilian rocks, postdiagenetic epigenic anhydrite has been observed to hydrate to recent gypsum down to 514 m depth, with strong deformation by volume increase (*fig.* 13). The pictures of incomplete transformation are very like those of complete transformation already seen in secondary gypsum. The above given depth is about the maximum at which anhydrite gypsification can be expected, according to the theoretical figures of Macdonald (1953), and it takes place with strong volume increase and not metasomatically (see also Ogniben, 1956). With greater reason this must have happened for paradiagenetic secondary gypsum.

Sicilian gypsum rocks are Upper Miocene in age and little disturbed, while those studied by Von Gaertner and by Goldman were Paleozoic and belonged to severely disturbed salt domes. Therefore, the picture gained from the Sicilian rocks should seem to be much clearer and more easily explained, and thus more reliable.

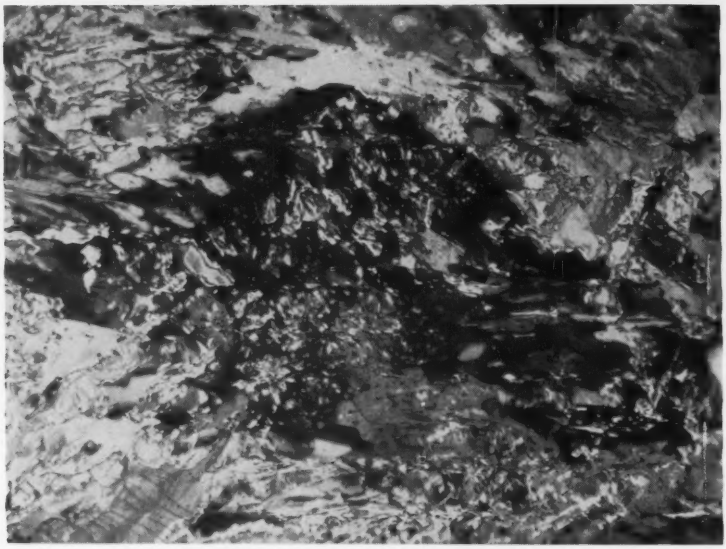

FIG. 13.—Helicitic structure of residual anhydrite in crystalloblastic gypsum, due to swelling by recent transformation. Passarello N° 1 boring at m 402 depth, Licata, Agrigento. Crossed nicols, ×85.

SIGNIFICANCE OF THE VARIOUS TYPES OF SECONDARY GYPSUM

From a megascopic point of view, anhydrite transformation in selenitic secondary gypsum can be considered to be of paradiagenetic age. As a matter of fact: (1) Deformation of overlying shales indicates the presence of at least a small load of sediments over the bed in transformation; (2) The arising fabric strongly resembles those of free growth described by Sander (1950), thus showing that superincumbent load was very little; (3) Grain size, fabric, and swelling structures are homogeneous throughout the whole bed, showing that transformation took place as an unique act for the whole bed after its deposition.

From a microscopic point of view, the undeformed selenite cores prove that initial pressure, i.e. load pressure, was very small or nil. Deformation taking place in advanced stages of the transformation must be attributed not to load pressure, but to volume increase pressure which clearly reached considerable values only with advanced progress of the transformation. Absence, or near absence of load caused initial selenite to grow upwards in wedge-shaped crystals, like the comb structures of hydrothermal veins. Late-stage pressure by volume increase caused the beds to swell upwards at their upper surface, through mutual displacement of crystals with rupturing and mylonization phenomena. These are not related to definite shear planes as in tectonites, but are localized peripherically around every single crystal.

Because it depended on water circulation in the calcium sulphate rock, the course of transformation was relatively slow, so as to allow the development of large size crystals and of strong preferred orientation. Probably the greatest part of the hydration water did not percolate from the above basin, where salinity varied strongly and periodically reached values beyond the stability field of gypsum. Smaller salinity can be assumed for the compaction water rising upward from the underlying sediments, chiefly shales. This water probably hindered downwards percolation of strong saline water from above, and made a slow gypsification possible. Since the greatest part of compaction water is driven out from shales before

reaching 150 m depth (Hedberg 1936), by this way a paradiagenetic age of transformation seems to be confirmed. Another proof is the occurrence of selenitic secondary gypsum as a detrital element in intraformational gypsarenites and conglomerates.

In alabastrine secondary gypsum there are no limpid selenite cores, but only rupturally deformed cores showing superindividual "cloudy" polarisation. From the lack of an initial free growth stage, the presence of considerable load at the very beginning of gypsification can be inferred. This hypothesis is in agreement with the strong thickness figures observed in the "saliferous" facies, of which alabastrine gypsum is typical. A sedimentation rate 10 to 20 times greater than that of the "sulphiferous" facies gave rise to high values of the superincumbent load, already in early paradiagenetic stages. Higher salinity in the above lying basins possibly contributed to delay gypsification, which probably was accomplished by the upwards rising compaction water.

Both selenitic and alabastrine secondary gypsum have been found substituted by postdiagenetic epigenic anhydrite near saline deposits. This fact excludes the possibility of a recent age of anhydrite transformation into these gypsum rocks. Before this finding, alabastrine secondary gypsum was tentatively attributed by the writer (Ogniben, 1955) to recent transformation.

Summarizing, anhydrite transformation into the secondary gypsum rocks described here seems to be of paradiagenetic age. An early paradiagenetic phase can be inferred for selenitic gypsum in the "sulphiferous" facies of the Gypsum Formation, under load very small to nil. Alabastrine gypsum, on the contrary, was formed under considerable load due to a much greater sedimentation rate in the "saliferous" facies, and perhaps to a later phase of diagenesis.

REFERENCES

Brown, L. S., 1931, Cap-rock petrography: Am. Assoc. Petroleum Geologists Bull., v. 15, p. 509–529.

Carozzi, A., 1953, Pétrographie des roches sédimentaires: Librairie de l'Université, Lausanne.

Goldman, M. I., 1952, Deformation, metamorphism, and mineralization in gypsum-anhydrite caprock, Sulphur Salt Dome, Louisiana: Geol. Soc. America Memoir 50, 169 p.

Hammerschmidt, F., 1883, Beiträge zur Kenntnis des Gips- und Anhydritgesteines: Tschermaks Min. u. Petr. Mittheil., N. F., Bd. 5, p. 245–285.

Hedberg, H. D., 1936, Gravitational compaction of clays and shales: Am. Jour. Sci., v. 231, p. 241–287.

MacDonald, G. J. F., 1953, Anhydrite-gypsum equilibrium relations: Am. Jour. Sci., v. 251, p. 884–898.

Mottura, S., 1872, Sulla formazione terziaria nella zona solfifera della Sicilia. Appendice: Caltanissetta 1910.

Ogniben, L., 1953, "Argille scagliose" ed "Argille brecciate" in Sicilia: Boll. Serv. Geol. d'Italia, v. LXXV, p. 281–289.

———, 1954 a, Le "argille brecciate" siciliane: Mem. Ist. Geol. e Min. Univ. Padova, v. XVIII, 92 p.

———, 1954 b, La "Regola di Mottura" di orientazione del gesso: Period. Mineral., Anno XXIII, p. 53–72.

———, 1955, Inverse graded bedding in primary gypsum of chemical deposition: Jour. Sedimentary Petrology, v. 25, p. 273–281.

———, 1956, Petrografia della serie Solfifera siciliana e considerazioni geologiche relative: Mem. descr. Carta Geol. d'Italia, v. XXXIII, 275 p.

Rinne, F., 1923, Gesteinskunde: 8/9 Aufl., Jänecke, Leipzig.

Sander, B., 1912, Ueber tektonische Gesteinfazies: Verh. k. k. geol. Reichsanst., n. 10, p. 249–257.

———, 1930, Gefügekunde der Gesteine mit besonderer Berücksichtigung der Tektonite: Springer, Wien.

———, 1936, Beiträge zur Kenntnis der Anlagerungsgefüge (Rhythmische Kalke und Dolomite aus der Trias): Zeitschr. f. Krist. Min. u. Petr. Abt. B, Min. u. Petr. Mitt., N.F., Bd. 48, p. 27–139 and 141–209.

———, 1950, Einführung in die Gefügekunde der geologischen Körper. II. Die Korngefüge: Springer, Wien.

Sloss, L. L., 1953, The significance of evaporites: Jour. Sedimentary Petrology, v. 23, p. 143–161.

Von Gaertner, H. R., 1932, Petrographie und paläogeographische Stellung der Gipse vom Südrande des Harzes: Jb. Preuss. Geol. Landesanst. zu Berlin, Bd. 53, p. 655–694.

JOURNAL OF SEDIMENTARY PETROLOGY, VOL. 27, NO. 1, PP. 80–88
FIGS. 1–7, MARCH, 1957

DIFFERENTIAL COMPACTION OF PENNSYLVANIAN SEDIMENTS IN RELATION TO SAND-SHALE RATIOS, JEFFERSON COUNTY, ILLINOIS

JOSEPH C. MUELLER AND HAROLD R. WANLESS
Continental Oil Company, Wichita, Kansas and University of Illinois, Urbana, Illinois

ABSTRACT

In Jefferson County, in the Illinois coal basin, southern Illinois, the Pennsylvanian column between the Shoal Creek and Stonefort Limestones, an interval of about 900 feet, was divided into seven intervals separated by widespread coals or limestones readily recognized on electric logs, namely the Shoal Creek Limestone, coal No. 8, West Franklin Limestone, coal No. 7, coal No. 5, coal No. 4, coal No. 2, and the Stonefort Limestone listed in descending order. These intervals were determined from 578 electric logs in the county, an average of about one per square mile. Sand-shale ratios were determined for each interval and it was found than a "channel" sandstone of one age occurs in each interval except between the Shoal Creek Limestone and coal No. 8. Two ages of channels occur in one interval. Sandstone percentage maps were made of each interval. Thicknesses of each interval were compared in the "channel" areas and nearby, outside the channel, to avoid regional variations in thickness. Assuming that the coals and limestones were laid down nearly parallel to each other, variations in interval result from greater compaction of the shales than of the sandstones. Results show the following percentages of differential compaction for the six intervals with channels listed in descending order: 21, 34, 29, 35, 42 and 54 percent.

It is well known that clays and shales are reduced in thickness during consolidation to a greater degree than sands and sandstones. The rocks considered in this paper seem particularly well suited for throwing light on the quantitative aspects of greater differential compaction of shales than of adjacent sandstones.

Jefferson County is in southern Illinois in the deeper part of the Eastern Interior basin, with an area of 576 square miles. Electric logs of 578 oil test borings penetrating the entire Pennsylvanian are available in all parts of the county and such logs were studied in the course of the present investigation by the first named author.

The Pennsylvanian system in Jefferson County is represented by from 1200 to 1800 feet of strata. It has been divided into Caseyville, Tradewater, Carbondale, and McLeansboro Groups. At the base of the Pennsylvanian a series of valleys excavated into underlying strata of the Chester Series, Mississipian, has been described by Siever (1951). Strata of the Caseyville and lower Tradewater Groups show marked local variability in lithology and sequence, no doubt reflecting the uneven surface at the beginning of the Pennsylvanian. Much greater uniformity existed in conditions of sedimentation during the later Tradewater, Carbondale, and McLeansboro so that many thin coals, limestones, and underclays are readily traceable throughout the county. The rock types in this part of the column have the following order of abundance: shale and clay, sandstone, coal, limestone. Sedimentation is of the cyclic type as described by Weller (1930). Sandstones are variable in thickness and are commonly of the "channel" type, occupying erosional valleys cut into underlying strata and individual sandstones vary from a few feet to more than 100 feet in thickness within the county. The erosional "valleys" seem largely to have filled with sandstone during each cycle as two or three feet of underclay overlain by a widespread coal bed, a marine black shale, and limestone generally lie between the top of a sandstone and the base of a moderately thick shale underlying the next higher sandstone. The under clay represents a level plain supporting vegetation, changed to a marsh by rising water table and then inundated by marine waters, first perhaps as a lagoon (black shale) and then as a relatively clear well-ventilated shallow sea. The essential flatness of the depositional surface is shown by the fact that the underclays, coals, black shales, and lime-

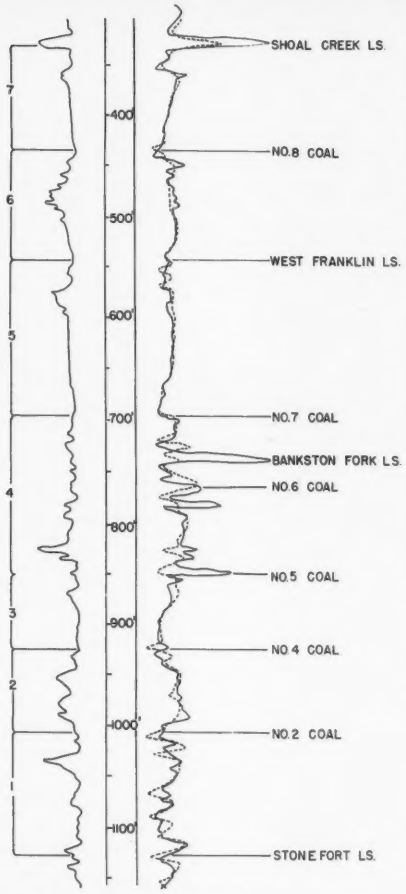

FIG. 1.—Representative electric log from Jefferson County, Illinois, showing division of the interval between the Stonefort and Shoal Creek Limestones into the 7 intervals whose variation in thickness and sandstone percentage were separately mapped.

stones are virtually continuous sheets, not only in Jefferson County, but through a much larger region in the Eastern Interior basin. Regional variations in intervals between these thin persistent "key beds" reflect differences in rates of downwarping. In Jefferson County most intervals are smaller in the northwestern part of the county and greater toward the southeast due to this cause.

A second cause of variation in interval between key beds is the degree to which each interval has been thinned by post-depositional compaction. This, in the Pennsylvanian of Jefferson County, is largely influenced by the relative proportions of shale and sandstone at different places, the sandstone being relatively incompactible. If the coals and limestones varied markedly in thickness within the county the relative amounts of their compaction would be important, but each of the coals and limestones in the interval treated in this study is relatively uniform in thickness throughout the county. It was decided that the study of the Pennsylvanian column, split into a series of relatively small intervals by widespread key beds recognizable in electric logs would show (1) the positions of "channel" sandstones in each interval, (2) the variation in total sandstone percentage (or sand-shale ratio) for each interval within the county, (3) the variation in thickness of each interval within the county (isopach map) and (4) by comparisons of thickness in "channel" areas and just outside them, to determine the relative compactional thinning of the shales and sandstones.

The Lower Tradewater and Caseyville were not studied because of the general lack of key beds easily recognizable in electric logs. For the remainder of the column the following key beds were at first selected to divide the column into segments for study (fig. 1).

McLeansboro group
- Shoal Creek Limestone
- No. 8 Coal (and Trivoli Limestone)
- West Franklin Limestone
- No. 7 Coal
- Bankston Fork Limestone

Carbondale group
- No. 6 Coal
- No. 5 Coal
- No. 4 Coal
- No. 2 Coal

Tradewater group
- Stonefort Limestone

The Shoal Creek Limestone is the highest key bed throughout Jefferson County,

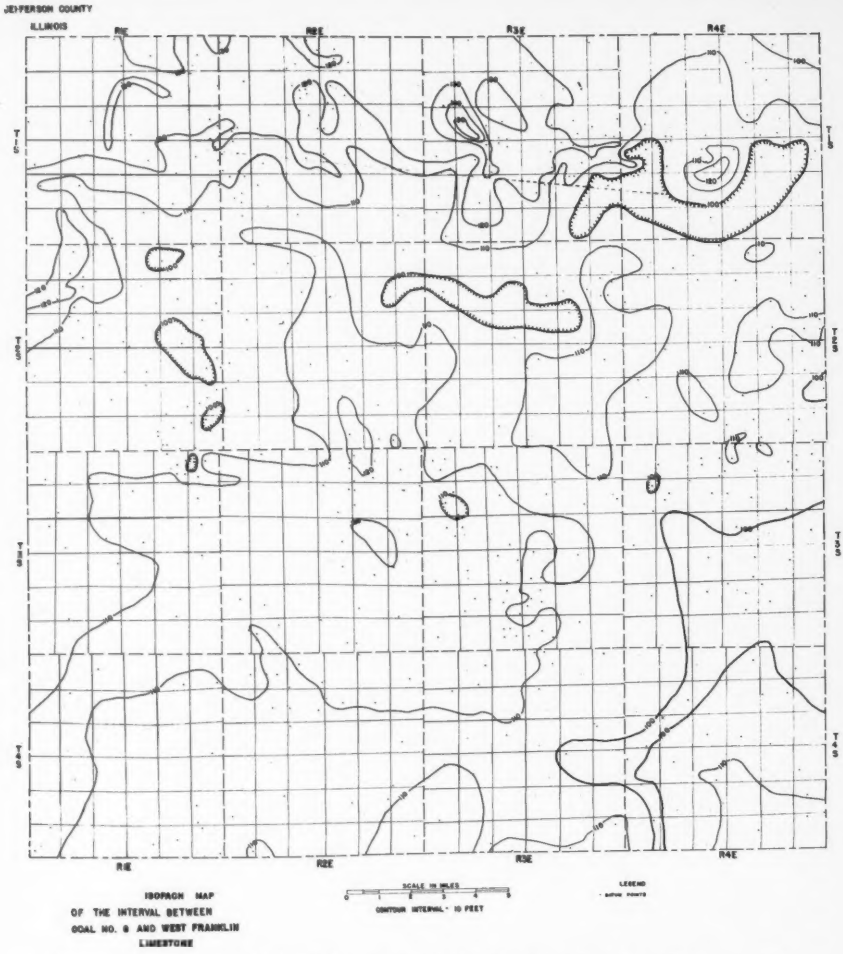

FIG. 2.—Isopach map of interval between Coal No. 8 and the West Franklin limestone in Jefferson County, Illinois. Wells used in the study are shown by dots.

though younger Pennsylvanian strata are present in the northern part of the county. As the study progressed it was found that the No. 6 Coal was absent in parts of the county where it was cut out by the overlying Anvil Rock Sandstone. The Bankston Fork Limestone was also found to be absent in substantial parts of the county, so these two key beds were dropped and the following seven intervals were studied:

Shoal Creek Limestone-No. 8 Coal
No. 8 Coal-West Franklin Limestone
West Franklin Limestone-No. 7 coal
No. 7 Coal-No. 5 Coal
No. 5 Coal-No. 4 Coal
No. 4 Coal-No. 2 Coal
No. 2 Coal-Stonefort Limestone

It was decided that the prominence of sandstone in an interval could be better characterized by a sandstone percentage (sandstone thickness/total thickness), than

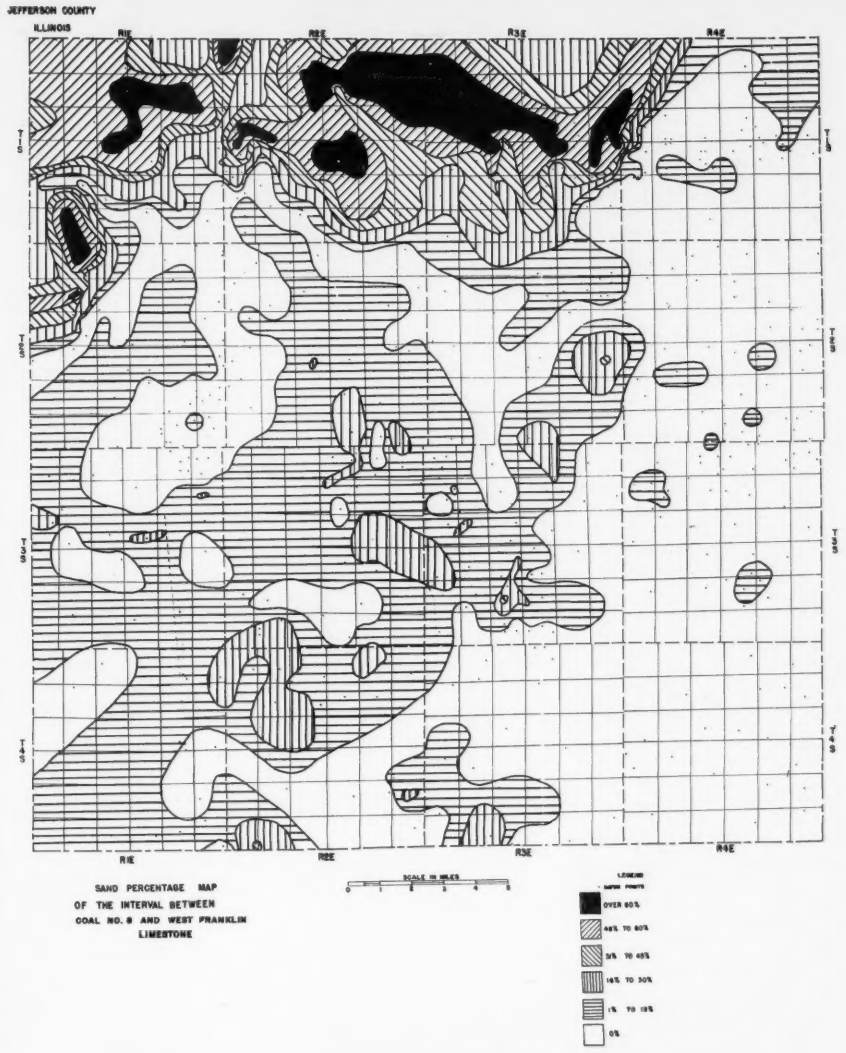

FIG. 3.—Sandstone percentage map of interval between Coal No. 8 and the West Franklin limestone in Jefferson County, Illinois.

by sand-shale ratio (sandstone thickness/shale thickness). In studying the electric logs the total thickness in each interval and the amount of sandstone, as indicated by the self potential curve, were recorded. Maps were prepared of the total thickness and sandstone percentage for each interval (figs. 2–5). It was found that there is no channel sandstone in the Shoal Creek-No. 8 Coal interval in Jefferson County, and that there are two systems of channel sandstone between Coals 5 and 7, the Anvil Rock Sand-

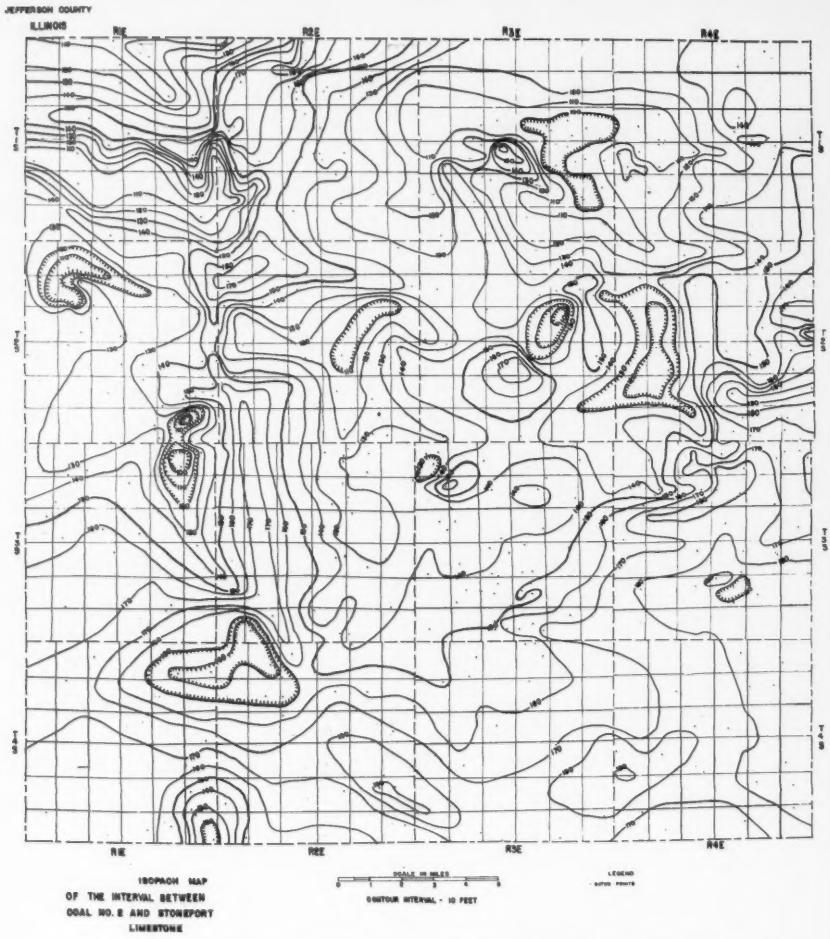

FIG, 4.—Isopach map of interval between Coal No. 2 and the Stonefort Limestone in Jefferson County, Illinois.

stone between Coals 6 and 7 and the Cuba Sandstone (a western Illinois term) between Coals 5 and 6. In the five other intervals there is one system of channels in each interval, as follows:

No. 8 Coal-West Franklin Limestone	Trivoli Sandstone
West Franklin Limestone-No. 7 Coal	Gimlet Sandstone
No. 5 Coal-No. 4 Coal	St. David Sandstone
No. 4 Coal-No. 2 Coal	Pleasantview Sandstone
No. 2 Coal-Stonefort Limestone	Palzo Sandstone

All of the sandstone names except the Palzo are derived from western Illinois nomenclature.

A map was prepared showing the superposed patterns of channel systems of the seven different sandstones recognized in the county (fig. 7). This map shows a common lack of superposition of one channel sandstone over another except in small areas.

In order to avoid confusing regional changes in interval due to differential downwarping with the effects of compaction,

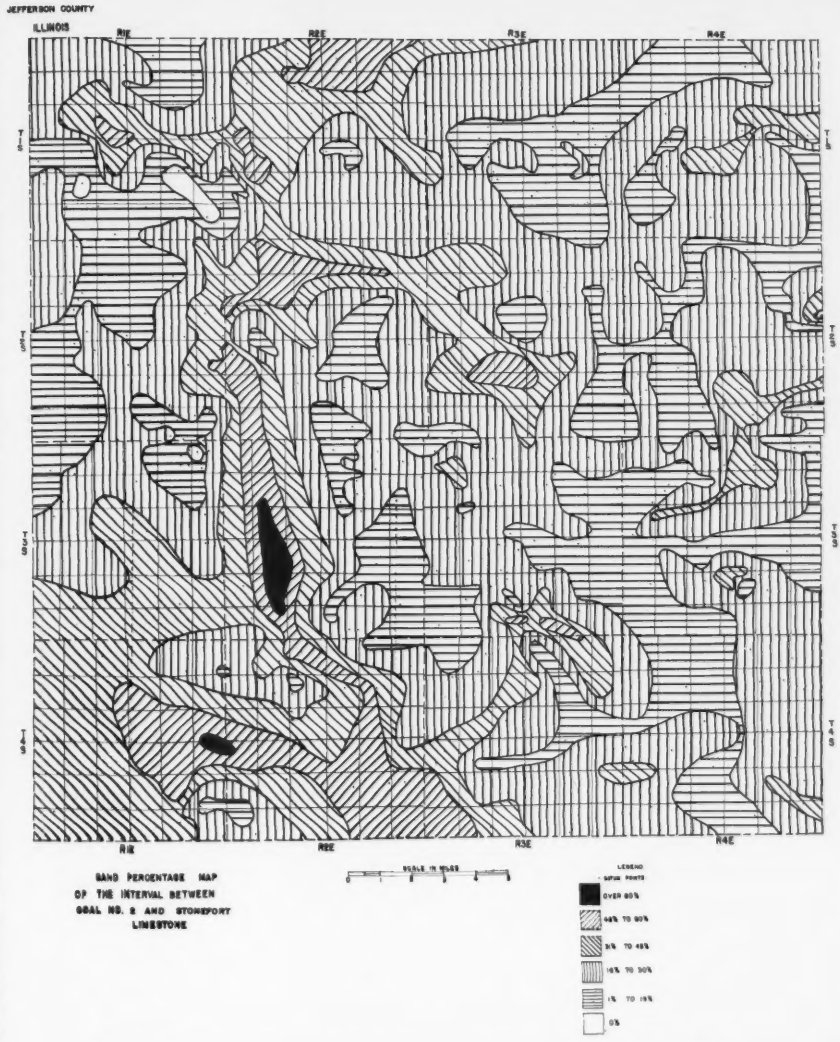

FIG. 5.—Sandstone percentage map of interval between Coal No. 2 and the Stonefort limestone in Jefferson County, Illinois.

comparison of interval was made between several thicknesses in a channel area and several thicknesses just a little outside the channel area. The differences were averaged to obtain an average compaction percentage for each interval. It should be noted that outside a "channel" area there may be a widespread thin fine-grained "non-channel" sandstone. Thus, areas outside the channels may contain as much sandstone as 25% in the total thickness, with more than 60% in the "channel" areas. Figure 6 is an electric log cross section to illustrate a representative cross section of a channel and adjoining non-

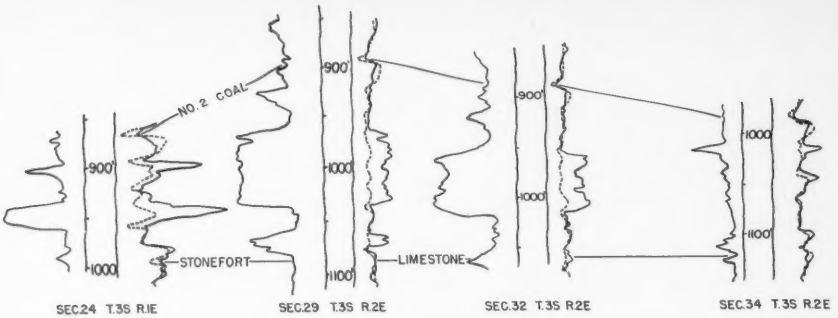

FIG. 6.—Cross-section through lenticular sandstone between Coal No. 2 and Stonefort Limestone, Jefferson County, Illinois.

channel areas between No. 2 Coal and the Stonefort Limestone beds.

The average percentages of compactional thinning of shaly sections outside channels for the six intervals in which channel deposits were found are as follows:

No. 8 Coal to West Franklin Limestone	21%
West Franklin Limestone to No. 7 Coal	34%
No. 7 Coal to No. 5 Coal (two systems of channels)	29%
No. 5 Coal to No. 4 Coal	35%
No. 4 Coal to No. 2 Coal	42%
No. 2 Coal to Stonefort Limestone	54%

One must exercise caution in drawing general conclusions from these percentages for several reasons: (1) Sandstones vary in coarseness and in the amount of interstitial clay, so some sandstones are appreciably compactible while others are relatively incompactible. (2) In some cases 20 to 70 feet of shale had accumulated before the erosional interval involved in channel cutting. The lower layers of shale in such cases were already somewhat thinned by compaction due to the weight of column on them even before the erosional interval. (3) In some cases the channels may not have filled completely with sandstone but may have filled in the later stages with shale or even local basins of coal, as in the outcrop area of western Illinois. (4) Some errors may have been made in identification of limiting key beds on electric logs or in determining the amount of sandstone in each interval.

A general inspection of the percentages of compaction above suggests that the shales deeper in the Pennsylvanian Column of Jefferson County show a larger percentage of compaction than the more shallow intervals not now so deeply buried.

One may question whether compaction had taken place so soon after deposition as to produce topographic relief influencing sedimentation in the next coal-black shale-limestone sequence above the sandstone. Studies currently in progress by M. E. Hopkins of the Anvil Rock Sandstone have shown that while the Bankston Fork Limestone is commonly several feet above the Anvil Rock Sandstone, it may immediately overlie the sandstone above some of the thicker sand deposits and at some localities it has been found to wedge out over the thick sandstone. In the same way Coal No. 2 thins from a regional thickness of 30 inches to 12 inches above a channel deposit of the Browning Sandstone in Schuyler County, western Illinois. These observations suggest that the thicker sand bodies, though level with surrounding shale areas at the end of deposition, stood slightly above the level surface so that they tended to inhibit marsh sedimentation or marine inundation just a short while after the end of channel filling. The

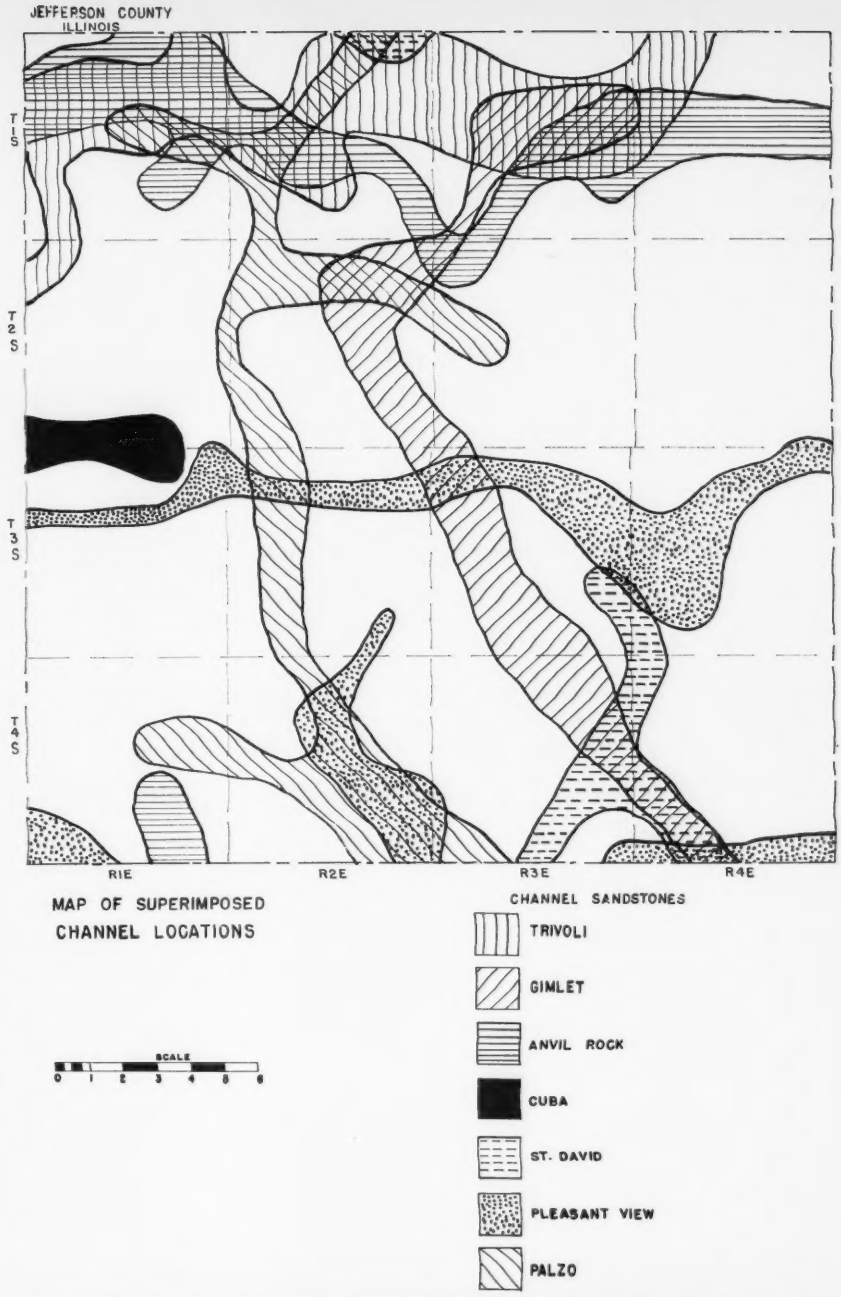

FIG. 7.—Map of superposed channel sandstones in Jefferson County, Illinois.

tendency of successive channel sandstones not to be superposed one above another (fig. 7) shows that continued compaction of the shales after their burial produce lower topographic surfaces. Later valleys are more likely to be located in such lowlands than over buried older channel deposits which would tend to stand a little higher.

REFERENCES

SIEVER, R. A., 1951, The Mississippian-Pennsylvanian unconformity in southern Illinois: Am. Assoc. Petroleum Geologists Bull., v. 35, p. 542–581.

WELLER, J. M., 1930, Cyclical sedimentation of the Pennsylvanian Period and its significance: Jour. Geology, v. 38, p. 96–135.

JOURNAL OF SEDIMENTARY PETROLOGY, VOL. 27, NO. 1, PP. 89–90
MARCH, 1957

SOCIETY OF ECONOMIC PALEONTOLOGISTS AND MINERALOGISTS

PROGRAM FOR S.E.P.M., ST. LOUIS MEETING (Kiel Auditorium)

Richard V. Hollingsworth, Technical Program Chairman

TUESDAY, APRIL 2 — 1:30 P.M.

Assembly Hall No. 1, Kiel Auditorium

RESEARCH COMMITTEE SYMPOSIUM: BIOSTRATIGRAPHY

1. INTRODUCTION, Curt Teichert, U. S. Geological Survey, Denver, Colorado, and Alfred A. Loeblich, Jr., U. S. National Museum, Washington, D. C.
2. *PRIMARY FACTORS IN BIOSTRATIGRAPHY*, V. Standish Mallory and Harry E. Wheeler, University of Washington, Seattle, Washington
3. CAMBRIAN BIOSTRATIGRAPHY IN NORTH AMERICA, Christina Lochman-Balk, New Mexico Bureau of Mines and Mineral Resources, Socorro, New Mexico, and James Lee Wilson, Shell Development Company, Houston, Texas
4. *THE SILURIAN-DEVONIAN BOUNDARY IN THE ARBUCKLE REGION, OKLAHOMA*, Thomas W. Amsden, Oklahoma Geological Survey, Norman, Oklahoma
5. EVOLUTION AND STRATIGRAPHIC USE OF BRYOZOANS, M. K. Elias, Nebraska Geological Survey, Lincoln, Nebraska
6. STRATIGRAPHIC DISTRIBUTION OF SOME UPPER PENNSYLVANIAN FUSULINIDS FROM CENTRAL TEXAS, Donald A. Myers, U. S. Geological Survey, Denver, Colorado
7. PLANT MICROFOSSILS IN THE CABANISS COALS OF OKLAHOMA AND KANSAS, L. R. Wilson, New York University, New York, New York, and William S. Hoffmeister, Carter Oil Company, Tulsa, Oklahoma
8. CORRELATION OF THE GULF AND ATLANTIC COASTAL PLAIN PALEOCENE-LOWER EOCENE BY MEANS OF PLANKTONIC FORAMINIFERA, Alfred R. Loeblich, Jr., and Helen Tappan Loeblich, U. S. National Museum, Washington, D. C.

WEDNESDAY, APRIL 3 — 9:00 A.M.

Assembly Hall No. 1, Kiel Auditorium

SEDIMENTARY MINERALOGY, PETROLOGY, AND SEDIMENTOLOGY

1. SURF-STRENGTH FACTORS IN REEF GROWTH AND DEVELOPMENT, Robert J. Burnside, U. S. Geological Survey, Denver, Colorado
2. *ORIGIN OF BAHAMIAN OOLITE*, Norman D. Newell, Edward G. Purdy, and David L. Thurber, Columbia University, New York, New York
3. BEACH SANDS FROM THE NORTHERN MARSHALL ISLANDS, Dorothy Carroll, U. S. Geological Survey, Washington, D. C.
4. CALCIUM CARBONATE DEPOSITION WEST OF ANDROS ISLAND BAHAMAS, Preston E. Cloud, Jr., Paul D. Blackmon, and Frederick D. Sisler, U. S. Geological Survey, Washington, D. C.
5. PALEOECOLOGY OF THE NODULOSE ZONE AT THE TOP OF THE HASKELL LIMESTONE (UPPER PENNSYLVANIAN) IN KANSAS, Halsey W. Miller and Ada Swineford, Kansas Geological Survey, Lawrence, Kansas
6. *PRACTICAL PETROGRAPHIC CLASSIFICATION OF LIMESTONES*, Robert L. Folk, University of Texas, Austin, Texas

WEDNESDAY, APRIL 3 — 2:00 P.M.

Assembly Hall No. 1, Kiel Auditorium

SYMPOSIUM ON GEOCHEMISTRY OF SEDIMENTARY MATERIALS

1. INTRODUCTION, W. J. Plumley, California Research Corporation, La Habra, California
2. CERTAIN ASPECTS OF THE THERMOCHEMISTRY OF CHEMICAL SEDIMENTATION, Gordon J. F. MacDonald, U. S. Geological Survey, Denver, Colorado
3. THE OCCURRENCE OF ALKALI METALS IN SOME GULF OF MEXICO SEDIMENTS, Charles W. Welby, Middlebury College, Middlebury, Vermont
4. BIOGEOCHEMISTRY OF CALCIUM CARBONATE PRECIPITATED BY MARINE ORGANISMS, Heinz A. Lowenstam, California Institute of Technology, Pasadena, California

5. CHEMICAL FACIES IN THE FIORENA SHALE (PERMIAN) OF NEBRASKA, KANSAS, AND OKLAHOMA, John Imbrie, Columbia University, New York, New York
6. SOME VIEWS AND EXPERIMENTS ON THE CRYSTALLIZATION OF DOLOMITE, Julian R. Goldsmith, University of Chicago, Chicago, Illinois
7. THORIUM TO URANIUM RATIOS AS INDICATORS OF SEDIMENTARY PROCESS, THE CONCEPT OF GEOCHEMICAL FACIES, John A. S. Adams, The Rice Institute, Houston, Texas, and Charles E. Weaver, Shell Oil Company, Houston, Texas

THURSDAY, APRIL 4 9:00 A.M.

Assembly Hall No. 1, Kiel Auditorium

PALEONTOLOGY AND STRATIGRAPHY

1. BITHECAE AND NEMATOTHECAE ON SPECIES OF GRAPTOLOIDEA, Charles E. Decker, University of Oklahoma, Norman, Oklahoma
2. MIOGYPSINIDS, PLANKTONIC FORAMINIFERA, AND GULF COAST OLIGOCENE-MIOCENE CORRELATIONS, W. H. Akers, The California Company, New Orleans, Louisiana, and C. W. Drooger, Geologische Institut, Universiteit Utrecht, Utrecht, Netherlands
3. METHODS OF CORRELATION IN SOUTHERN CALIFORNIA, W. T. Rothwell, Richfield Oil Corporation, Long Beach, California
4. THE RELATION BETWEEN CHAROPHYTE EVOLUTION AND STRATIGRAPHIC CORRELATION IN THE MORRISON FORMATION, Charles A. Ross, Yale University, New Haven, Connecticut
5. CONODONTS FROM THE GLEN DEAN FORMATION IN ILLINOIS, INDIANA, AND WESTERN KENTUCKY, Carl B. Rexroad, Texas Technological College, Lubbock, Texas
6. PALYNOLOGY OF RECENT ORINOCO DELTA AND SHELF SEDIMENTS, J. Miller, Compania Shell de Venezuela, Maracaibo, Venezuela
7. DISPLACEMENT OF MICROFOSSILS—A REVIEW, Daniel J. Jones, University of Utah, Salt Lake City, Utah

THURSDAY, APRIL 4 2:00 P.M.

Assembly Hall No. 1, Kiel Auditorium

SEDIMENTARY MINERALOGY, PETROLOGY, AND SEDIMENTOLOGY

1. CARBONATE REPLACEMENT OF QUARTZ AND FELDSPAR AS A SOURCE OF SILICA IN CHERTIFIED SEDIMENTS, Theodore R. Walker, University of Colorado, Boulder, Colorado
2. USE OF THE CURVED-CRYSTAL SPECTROMETER FOR MINERALOGICAL INVESTIGATIONS, I. Adler and J. M. Axelrod, U. S. Geological Survey, Washington, D. C.
3. AGE DETERMINATIONS ON ZIRCON, A POSSIBLE AID IN PROVENANCE STUDIES, Howard W. Jaffe, David Gottfried, and Claude L. Waring, U. S. Geological Survey, Washington, D. C.
4. PETROLOGY OF THE CRETACEOUS WOODBINE SAND IN NORTHEAST TEXAS, Augustus S. Cotera, Jr., Liberal, Kansas
5. STRATIGRAPHIC AND STRUCTURAL UTILITY OF LAYERED VOLCANIC ROCKS, E. F. Cook, University of Idaho, Moscow, Idaho

MEMBERSHIP LIST

The Society of Economic Paleontologists and Mineralogists' Membership List may be obtained by S.E.P.M. members who regularly subscribe to the Journal of Sedimentary Petrology by writing to S.E.P.M., Box 979, Tulsa 1, Oklahoma.

INSIST ON THE . . .
HUBCO
PROTEXO BAG
with the Guaranteed
"MAGIC-MARK"
TAG!
for your . . .
. . . sand samples!
PROTEXO BAGS . . .
• Strong
• Sift-Proof
• Geologist Designed
• Highest-Quality Cambric Cloth
MAGIC-MARK TAGS . . .
• Water-Insect- and Mildew-Proof
• Guaranteed to Keep Even Ordinary Pencil Markings Legible
HUBCO PROTEXO BAG
Sold by oil field supply jobbers & dealers. Write for FREE sample, price list & your dealer's name.
HUTCHINSON BAG CORP. Hutchinson, Kan.

HARPER

TEXTS IN THE GEOSCIENCE SERIES

Under the editorship of Carey Croneis

A New Revised Edition of:

"The best single-volume text on sedimentary rocks on the market at this time."
Walter H. Schoewe, *University of Kansas*

SEDIMENTARY ROCKS

F. J. Pettijohn, Johns Hopkins University

This revision of the most widely used textbook in its field is completely rewritten and expanded by about 30%. Illustrations greatly expanded—77 of 173 line drawings are new, and there are 40 plates including over 100 photomicrographs. The most useful single-volume guide to the observation, classification, and interpretation of the basic phenomena in geology.

Still the only general work available on micropaleontology:

"This book should become the standard reference source to the study of microfossils. It is a major contribution to the field of petroleum geology."
E. Willard Miller, *Pennsylvania State University.*

INTRODUCTION TO MICROFOSSILS

Daniel J. Jones, University of Utah

Describes methods of collecting, separating, and mounting microfossils and micropaleontological objects representing all major groups of the plant and animal kingdom. Special attention to plant microfossils and full discussions of the environmental significance of various microfossils and the applications of micropaleontological data to practical problems in economics and geology. Text thoroughly documented and lavish illustrations outstanding.

HARPER & BROTHERS PUBLISHERS

49 East 33d Street, New York 16, New York

Please mention the *Journal of Sedimentary Petrology when writing to advertisers.*

sees more—tells more

ANOTHER NEW SERVICE DEVELOPED BY SCHLUMBERGER —THE COMBINATION INDUCTION-ELECTRICAL LOG

This new service incorporates advantages given only by the Induction Log while retaining important features of the Electrical Log.

The Induction Log . . .

- has none of the lags, shadow zones and reflection peaks associated with the long normal and lateral curves
- gives more detail on thin beds
- is less influenced by the mud column
- is less influenced by the invaded zone
- gives greater accuracy in low resistivities and in true resistivity determinations
- provides more accurate determination of oil water contacts

This New Service Combines These Curves:

Electrical Log
Spontaneous Potential
16" Short Normal
16" Amplified Normal

Induction Log
40" Resistivity
40" Conductivity

The combination is a more easily used log for quick analysis or detailed study — and with fewer resistivity spacings.

SCHLUMBERGER WELL SURVEYING CORPORATION — THE EYES OF THE OIL INDUSTRY

Please mention the *Journal of Sedimentary Petrology when writing to advertisers.*

SOCIETY OF ECONOMIC PALEONTOLOGISTS AND MINERALOGISTS

SOCIETY OFFICERS (MARCH 1957-MARCH 1958)

President: RICHARD V. HOLLINGSWORTH, Midland, Texas
First Past-President: ROBERT R. SHROCK, Cambridge, Massachusetts
Vice-President: STUART A. LEVINSON, Houston, Texas
Secretary-Treasurer: SAMUEL P. ELLISON, JR., Austin, Texas
Editor, Journal of Sedimentary Petrology: JACK L. HOUGH, Urbana, Illinois
Editor, Journal of Paleontology: W. M. FURNISH, Iowa City, Iowa

PACIFIC SECTION OFFICERS (1955-1956)

President: WILLIAM H. EASTON, Los Angeles, California
Secretary-Treasurer: RICHARD L. PIERCE, Long Beach, California

GULF COAST SECTION OFFICERS (1956-1957)

President: LLOYD M. PYEATT, Houston, Texas
Vice-President: J. O. COLLE, Houston, Texas
Secretary: HERVIE DILLINGHAM, JR., Houston, Texas
Treasurer: MISS ELEANOR CALDWELL, Tallahassee, Florida

THE AMERICAN ASSOCIATION OF PETROLEUM GEOLOGISTS

ASSOCIATION OFFICERS (APRIL 1956-MARCH 1957)

President: THEO. A. LINK, Toronto, Ontario.
Past-President: G. M. KNEBEL, New York, N.Y.
Vice-President: BEN H. PARKER, Denver, Colorado
Secretary-Treasurer: W. A. WALDSCHMIDT, Midland, Texas
Editor: W. C. KRUMBEIN, Evanston, Illinois

GEORGE BANTA COMPANY, INC., MENASHA, WISCONSIN